Universal Physics-based Rate of Penetration Prediction Model for Rotary Drilling

by

© Jeronimo de Moura Junior

A Dissertation submitted to the

School of Graduate Studies

In partial fulfillment of the requirements of the degree of

Doctor of Philosophy

Faculty of Engineering and Applied Science

Memorial University of Newfoundland

May 2021

St. John’s Newfoundland and Labrador

Abstract

The drilling process is one of the most important and expensive aspects of the oil and gas industry. Drilling is required during mining for different ore production processes such as blasting and large drilling operations. Overall, it contributes significantly to the total cost of mining. As a result, an accurate prediction of the rate of penetration (ROP) is crucial for drilling performance optimization and contributes directly to reducing drilling costs. Knowledge of drilling performance is a powerful tool to aid in the development of a consistent drilling plan as well as to anticipate issues that may arise during drilling operations. Several approaches, with varying degrees of complexity and accuracy, have been tested to predict drilling performance, but all have shown several limitation to predict the complete drilling performance curve including locate the founder point. This limitation can be extended to their capacity of covering different drilling scenarios with high accuracy. In this thesis (manuscript style) a review of the history of drilling performance prediction is conducted with emphasis on the rotary drilling of small and large diameters. The approaches are grouped into two categories: physics-based models and data-driven models. Due to the low complexity of the physics-based models and the scarcity of drilling performance prediction research that reports the founder point location, a novel physics-based ROP prediction model for rotary drilling that includes the founder point location is presented. This model presents high accuracy to predict the drilling performance for fixed cutter drill bit, roller-cone drill bit, and large diameter drilling operations. The behaviors of the new model constants (drillability coefficient and drillability constant term) are discussed when analyzed in relation to the unconfined compressive strength (UCS), bit diameter, and rotary speed. Additionally, a new experimental setup approach was developed based on the circular movement of the full-scale disc cutter that are normally used in raise boring and

tunnel boring machines. This setup will permit to simulate the large diameter drilling operations in laboratory scale aiming the understanding of the fragmentation process and application of optimization to this scenario.

Acknowledgments

I would like to express my gratefulness to my wife Wanderléia Fanticelli de Moura, my daughter Brunna Fanticelli de Moura and my son Eduardo Fanticelli de Moura who supported and encouraged me with their patience and love, being my foundation and my inspiration.

I would like to express my immense gratitude to my supervisor Dr. Stephen D. Butt and my co-supervisor Dr. Jianming Yang, as well as to Dr. Syed Imtiaz who was a part of my supervisory committee, for their patience, technical support and guidance during my research work.

I am grateful to Novamera Inc., Memorial University of Newfoundland, and MITACs through the Sustainable Mining by Drilling (SMD) project's technical and financial support, which made the results of this research possible.

I would like to express my appreciation to all the group members of Drilling Technology Laboratory, which supported me in several activities such as drilling experiments, field trials, and literature reviews; always acting with a great sense of partnership.

Last but not least, I would like to dedicate this work to my mother Maria da Penha Leite de Moura (*in Memoriam*), my sister Jaqueline Aparecida de Moura (*in Memoriam*), my father Jeronimo Jose de Moura, my brother Alex Sander de Moura, and my parents-in-law Edson Fanticelli (*in Memoriam*), and Tercia Rossini Fanticelli (*in Memoriam*).

Contents

List of Tables

List of Figures

Abbreviations

a	Drillability Coefficient
ADCM	Adjustable Disc Cutter Mounting
ANN	Artificial Neural Network
ASME	American Society of Mechanical Engineers
b	Drillability Constant Term
BA	Bat Algorithm
BHA	Bottom Hole Assembly
BI	Intact Rock Brittleness
BP	Back Propagation
BTS	Brazilian Tensile Strength
CCS	Confined Compressive Strength
CSM	Colorado School of Mines
D	Drill Bit Diameter
DIC	Deviance Information Criterion
DOT	Drill-Off Test
DPW	Distance Between Planes of Weakness
DTL	Drilling Technology Laboratory
ELM	Extreme Learning Machines
FPI	Field Penetration Index
GSI	Geological Strength Index
IADC	International Association of Drilling Contractors

ID	Inner diameter
k	Drillability Constant (Maurer Model)
K	Drillability Linear Equation
LDS	Large Drilling Simulator
MCMC	Markov Chain Monte Carlo
MSE	Mechanical Specific Energy
MUN	Memorial University of Newfoundland
N	Rotary Speed
OD	Outer Diameter
PDC	Polycrystalline Diamond Compact
PDM	Positive Displacement Motor
pVARD	Passive Vibration Assisted Rotational Drilling
r	Repeatability Limit
R	Rate of Penetration
R_{fp}	ROP Correspondent to the Founder Point
Ra	Radial Adjustment
RBF	Radial Basis Function Network
RBM	Raise Boring Machine
RMR	Rock Mass Rating
ROP	Rate of Penetration
rpm	Revolutions Per Minute
RSM	Response Surface Methodology
R^2	Coefficient of Determination

S	Rock Strength
SDS	Small Drilling Simulator
$S_{y,x}$	Standard Error of Estimate
s_r	Repeatability Standard Deviation
$SR_{y,x}$	Relative Standard Error of Estimate
TBM	Tunnel Boring Machine
TCI	Tungsten Carbide Insert
TOB	Torque on Bit
TSP	Thermally Stable Polycrystalline
UCS	Unconfined Compressive Strength
VARD	Vibration Assisted Rotary Drilling
W	Weight on Bit
W_{fp}	WOB Correspondent to the Founder Point
WOB	Weight on Bit
W_0	Threshold WOB Before Cratering
x	Predicted ROP
y	Real ROP
α	Slope of Least-Squares Linear Fit Curve with Origin Fixed at (0,0)
β	Constant Term of Least-Squares Linear Fit
γ	Constant Coefficient of Least-Squares Linear Fit
θ	Offset Angle
ϕ	Journal angle

Appendices

Chapter 1 Introduction and Overview

1.1 Introduction

In the oil and gas industry, as well as in mining and construction areas, the drilling process is challenging because of the complexity of the operations involved and its consecutive impact in economic feasibility of drilling projects. Due to the explained before, it is crucial that each process involved in a drilling operation is fully understood. To have a successful drilling project, the rate of penetration (ROP) prediction is a crucial factor that provides the capability to predict the drilling problems and inefficiencies of a drilling operation.

One of the most famous models for drilling performance prediction was developed by Maurer. This model as well as the other available prediction models are limited to predict a completed drilling performance curve including the founder point location (local maximum of this curve). Additionally, the vast majority of these models are restricted to a specific drilling scenario (a specific type of drill bit, rock properties, drilling fluid rheology, rotary speed, etc.) and their generalized application in a way implies to inaccurate prediction values. A detailed discussion of these models including the Maurer model is present in Chapter 2.

This thesis explores the linear relationship between the drillability constant (Maurer model) and weight on bit (WOB). This relationship was identified in the present research and allowed for a new correlation to be developed that is able to predict the complete drilling performance curve including the founder point location. Additionally, the new model was applied in three different drilling scenarios, fixed cutter drill bits, roller-cone bits, and large diameter drilling, which are

differentiated by the drilling mechanics involved in their respective drilling process. This model proves to be a powerful tool since its accuracy remains highly independent of the drilling scenario that it is applied to.

1.2 Statement of the Problem

For decades, many research projects were conducted to determine an accuracy correlation to predict the drilling performance. Normally, these correlations are very specific and their predictions become increasingly inaccurate as their application is extended beyond those drilling scenarios (see Chapter 2 for more details). More recent studies about ROP prediction focus on bit-rock interaction and cutting subject to a high confining pressure. These studies use the finite element to model the drilling scenario. One of the main points for the ROP prediction is the identification of the maximum WOB that results in a maximum ROP, called founder point. There is limited research that tries to predict the founder point location. The research is focused on predicting the drilling performance before the founder point, limiting comparison between different drilling scenarios and application of the optimization techniques. Therefore, this investigation is required to develop a universal drilling performance prediction model for the rotary drilling that includes the founder point location.

1.3 Research Plan and Objectives

The objective of this thesis is to develop a new model to predict drilling performance, including the founder point location, for rotary drilling. The objective of this study is to be able to predict the ROP for small and large diameter drilling for different types of drill bits and rock formations. In this way, drilling performance for different drilling scenarios are evaluated from

drill-off tests (DOTs) or field drilling operations previously conducted in other studies or performed in a laboratory as part of the current study. This research is divided into the three projects.

1.3.1 A New Model to Predict the Drilling Performance for Fixed Cutter Drill Bits

This project aimed to develop a new model to predict the drilling performance, including the founder point location for fixed cutter drill bits, based on limitations of models that are available in literature to predict the complete drilling performance curve including the founder point location. To measure the efficiency and accuracy of the new model, DOTs and field drilling operations available in literature as well as the data obtained from laboratory experiments conducted in this study were analyzed. In Drilling Technology Laboratory, DOTs are performed using a drilling simulator that simulates a drilling operation with different drill bits, different rock specimens, and in different drilling conditions. DOTs are used to establish a relationship between the WOB and ROP for a specific drilling scenario and are a base for the development of drilling performance models. Initially in this study, a DOT was performed with coring bit due the ease to generate a complete drilling performance curve including the founder point location, which was used to develop a new model. Finally, the effectiveness and accuracy of the new model was evaluated based on different scenarios of fixed cutter drill bits.

1.3.2 Extension of the New Model to Predict the Drilling Performance Including the Founder Point Location for Roller-Cone Drill Bits

This project studied the possibilities of an extension of the new drilling performance prediction model developed for fixed cutter drill bits for roller-cone drill bits. The need of this

analysis is based on the difference between the rock fragmentation mechanisms of these bit types. In the fixed cutter drill bit operation, a dragging-scraping (shearing) process is present. In the roller-cone drill bit operation, a gouging-scraping or chipping-crushing process is present. During this project, DOTs in Drilling Technology Laboratory was performed and analyzed. Additionally, DOTs and field drilling operations previously conducted in other studies as well as the data obtained from laboratory experiments conducted in this study were analyzed. Similar to the previous project, the effectiveness and accuracy of the new model was proven during analysis of different roller-cone drill bit operations.

1.3.3 Extension of the New Model to Predict the Drilling Performance Including the Founder Point Location for Large Diameter Drill Bits (RBM and TBM)

This project was a comprehensive evaluation of the new model in a drilling scenario, outside the normal oil and gas application. This drilling scenario covers raise boring machine (RBM) and tunnel boring machine (TBM) applications where the main factor that differs from the application of fixed cutter and roller-cone drill bits analyzed in the two previous projects is the scale of the bit diameter. In the first two drill bit types, the drill diameter is in the order of inches, while in the large diameter the drilling is in the order of meters. In small diameter drilling it is assumed that only the intact properties of the rock affects the drilling performance. While in large diameter drilling, the property of the rock mass, which consists of the rock material and discontinuities, affects the drilling performance considerably. In this project, a comparative analysis of the Colorado School of Mines (CSM), Gehring, and de Moura and Butt models were performed and the founder point existence in large drilling operations is discussed (see Chapter 5 for more details).

Chapter 2 Literature Review

2.1 Rotary drilling

Rotary drilling is the most widely used worldwide drilling method for oil and gas drilling. Regardless of the drill rig, the basic rotary-drilling equipment is as shown in Figure 2-1 [1].

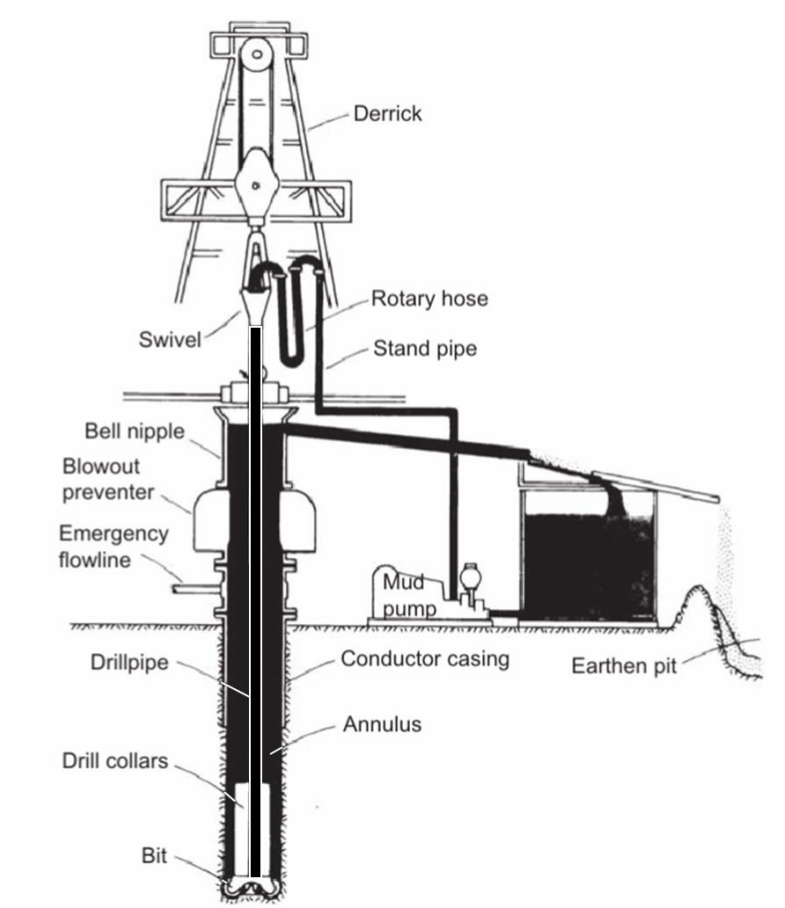

Figure 2-1 The rotary drilling process [1].

In order to drill a well, it is necessary that a bit, under a downward force and torque, will produce fractures in the rock and will break it consecutively. The downward force, weight on bit (WOB) is provided by the weight of the drillstring and, in specific cases, a hydraulic system on the surface. The torque is transmitted from surface equipment to the drill bit through the drillstring.

After the fragmentation of the rock, the cuttings are transported to the surface by the drilling fluid that is constantly pumped inside the drillstring (direct circulation) which returns to the surface carrying the cuttings through the annular space between the borehole wall and the drillstring. On the surface, the cuttings and drilling fluid pass to a separation process for drilling fluid reuse [1].

There are many different types of drill bits whose main difference is in rock cutting mechanics [2] (see Figure 2-2).

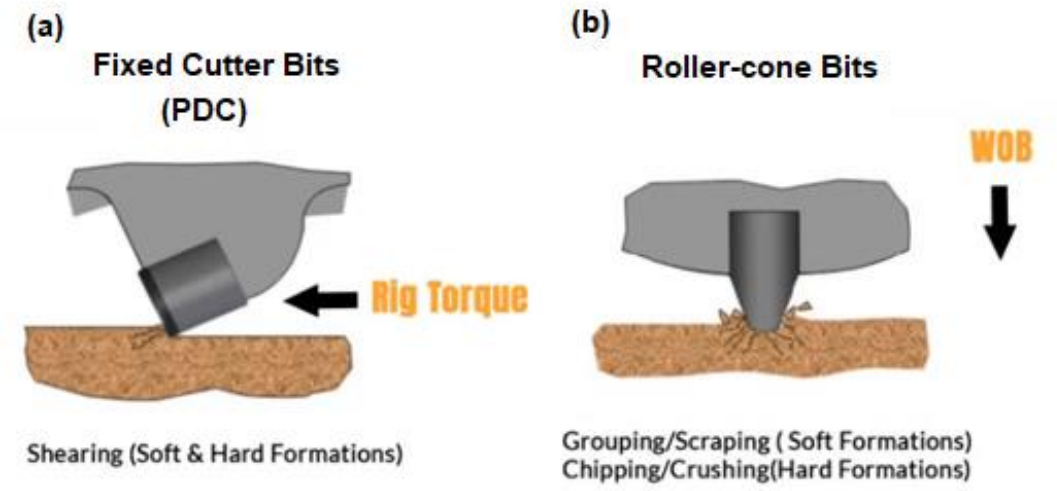

Figure 2-2 Rock fragmentation mechanism– (a) Fixed Cutter Bits (polycrystalline diamond compact (PDC)), (b) Roller-cone Bits. Adapted from [3].

In the next sections, the difference between three distinct drilling scenarios will be discussed: drilling with fixed cutter bits, drilling with roller-cone bits, and large diameter drilling.

2.1.1 Fixed Cutter Drill Bits

In fixed cutter drill bits, the cutter has continuous contact with rock, moving parallel to the rock surface, and it is characterized by a shearing action during the rock fragmentation process (see Figure 2-3) [2].

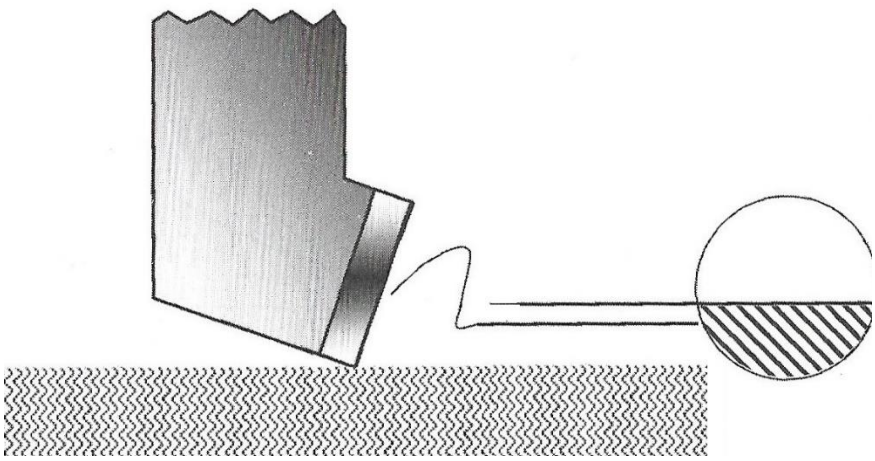

Figure 2-3 PDC cutter engaged in rock. Adapted from [2].

Drag bits were the first version of fixed cutter drill bits that were introduced in very soft rock formation drilling operations in the early 1900s. Traditionally, they were made of steel and had two blades that were covered with harder alloy coatings (see Figure 2-4) [1].

The fixed cutter drill bits can be divided into three groups: PDC, Thermally Stable Polycrystalline (TSP), and diamond matrix bits. Each group has its own specific design features and rock fragmentation mechanisms [2].

Bits that used diamond as their cutting elements were first used in the 1940s and TSP and PDC technology was developed in the late 1970s (see Figure 2-5). In the 1970s, General Electric developed the concept of PDC and University of Tulsa Drilling Research Projects, as subcontractors of the United States Department of Energy, worked on the engineering design development and testing [2].

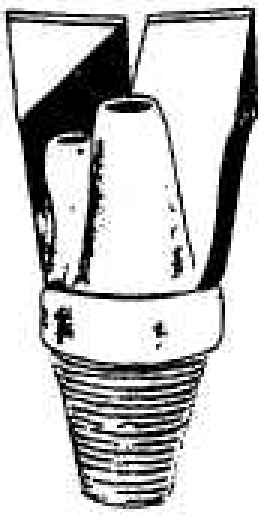

Figure 2-4 Drag bits with two blades. Adapted from [4].

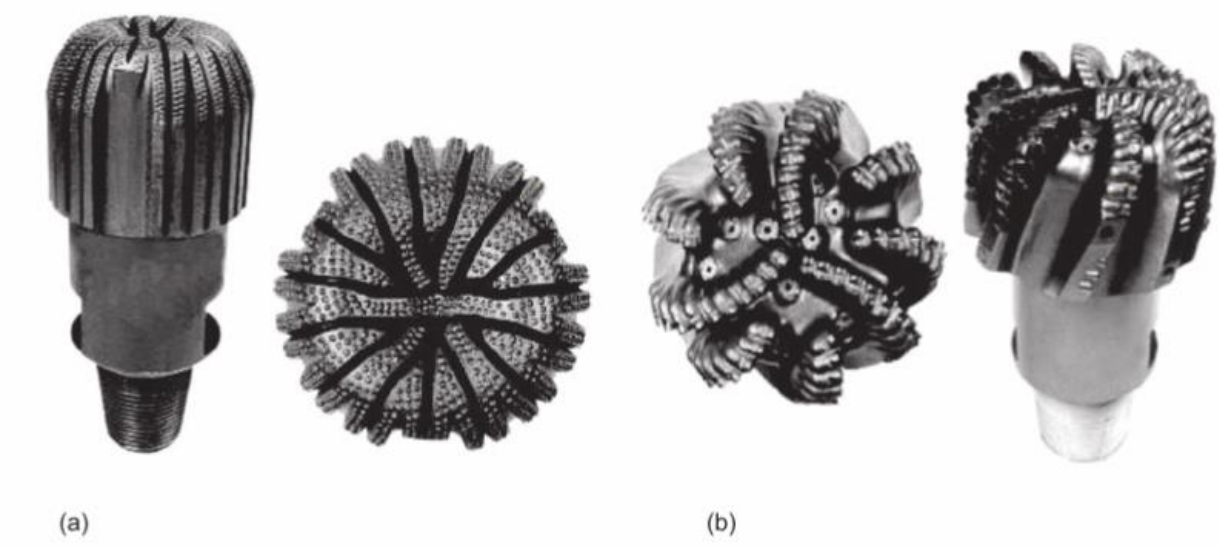

Figure 2-5 (a) Diamond bits; (b) PDC bits [1].

The PDC is a 1/32 inches thick polycrystalline layer applied on a tungsten carbide material that is installed into a hole in the bit body [2]. TSP bits were the first bit with synthetic diamond elements used by the drilling industry and are an evolutionary milestone to the modern PDC bits [1]. In the PDC and TSP bits, small synthetic diamond disks provide the scraping/cutting surface.

The rock fragmentation mechanism of these bits is primarily by shearing where the cutters have enough axial force to penetrate into rock and torque for its rotation [1].

Diamond matrix bits use a PDC matrix material and natural or synthetic diamonds. Normally, this type of bit runs with turbo drills and Positive Displacement Motor (PDM). Its cutting action is scraping where the drill uses a high-speed plowing action that breaks the cementation that holds the rock grains together [1].

2.1.2 Roller-cone Drill Bits

In 1909, Howard Hughes invented the first roller-cone bits with two cones. The tricone bits were introduced in the early 1930s for application in hard and soft formations. Initially, the roller-cone bits had milled-teeth but in the late 1940s, with the deep drilling events that meant harder rock formations, the Hughes Tool Company introduced the first tungsten carbide insert tricone bits [1].

The roller-cone bits are categorized into two groups (see Figure 2-6): milled tooth (or steel tooth) bits typically used for drilling relatively soft formations; and tungsten carbide insert (TCI) tooth bits (button bit) – it has wide application including the hard and abrasive formations. The rock-cutting mechanisms of the milled tooth bits are gauging, scraping, and chiseling and the failure mechanisms are tooth wearing, bearing failure, or both. In the case of the TCI bits, the rock-cutting mechanisms are chipping and crushing and the failure mechanism is bearing failure [1], [2].

Figure 2-6 (a) Roller-cone milled-tooth and (b) Tungsten carbide insert bits [2].

In 1965, Maurer performed laboratory experiments with an original setup of single tooth bits impacting or indenting a rock specimen surface simulating the real field borehole conditions (see section 2.2.1 for more details). He observed that the crater mechanism is related to the pressure differential between the rock-pore pressure and the borehole. Figure 2-7 shows the crater mechanism for low differential fluid pressure. This enables the ejection of the cutting from the crater almost completely. High differential fluid pressure hampered the cuttings and prevented their ejection from the crater because of the chip hold-down effect [1].

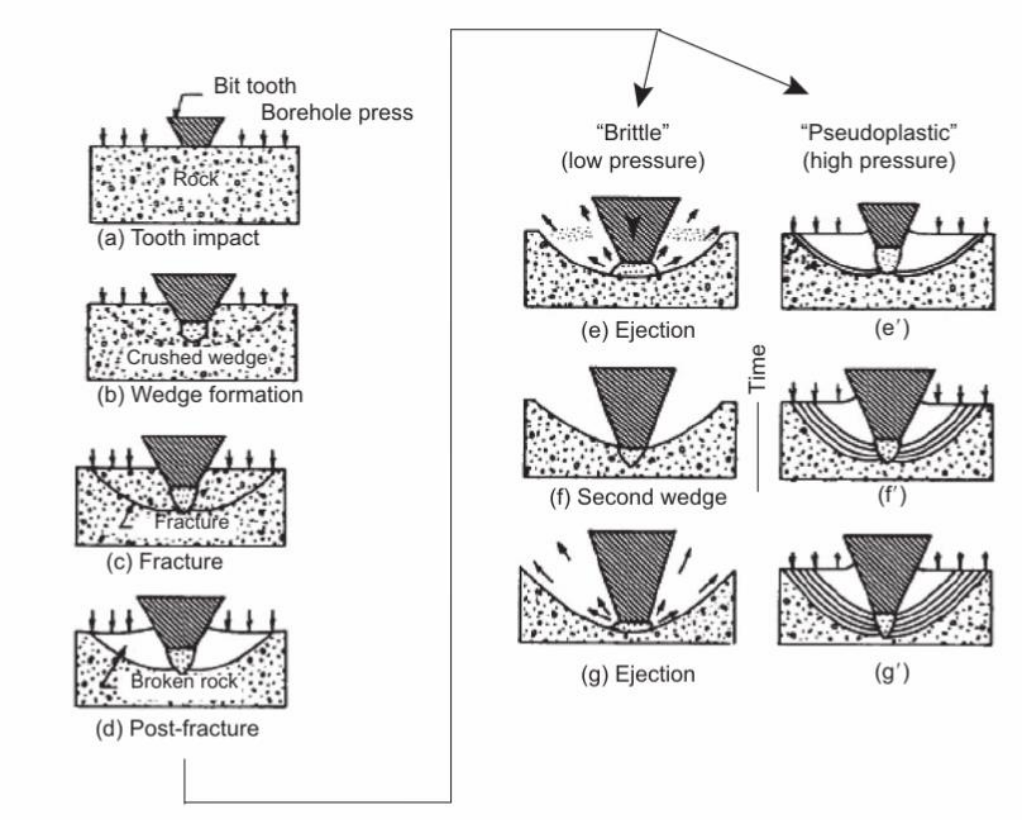

Figure 2-7 Crater mechanism beneath a bit tooth [1].

2.1.3 RBM and TBM

In mining and construction projects, the proper selection of an excavation machine and an accurate prediction of its performance are crucial to cost estimates and planning. Currently, mechanical excavation is a strong alternative to conventional drill and blasting in tunneling and mining projects. The most used excavation machines in these types of projects are TBM and RBM.

TBMs are applied in tunnel construction for traffic, hydropower, sewerage and water, underground storage, and mining. Currently, there are a wide variety of TBMs available in the marketplace including machines with different diameters and adapted to different formation conditions [5]. TBMs present considerable advantages over drill and blast in favourable ground

conditions due to their normally high advance rates and lower risk levels, but in adverse ground conditions these machines present a significant increase in cost and decrease in safety [6].

Basically, the main parameters of a TBM are the thrust and torque. A motor rotates the cutterhead and the thrust is provided by cylinders that push the cutterhead against the precast segmental lining (Figure 2-8) [7].

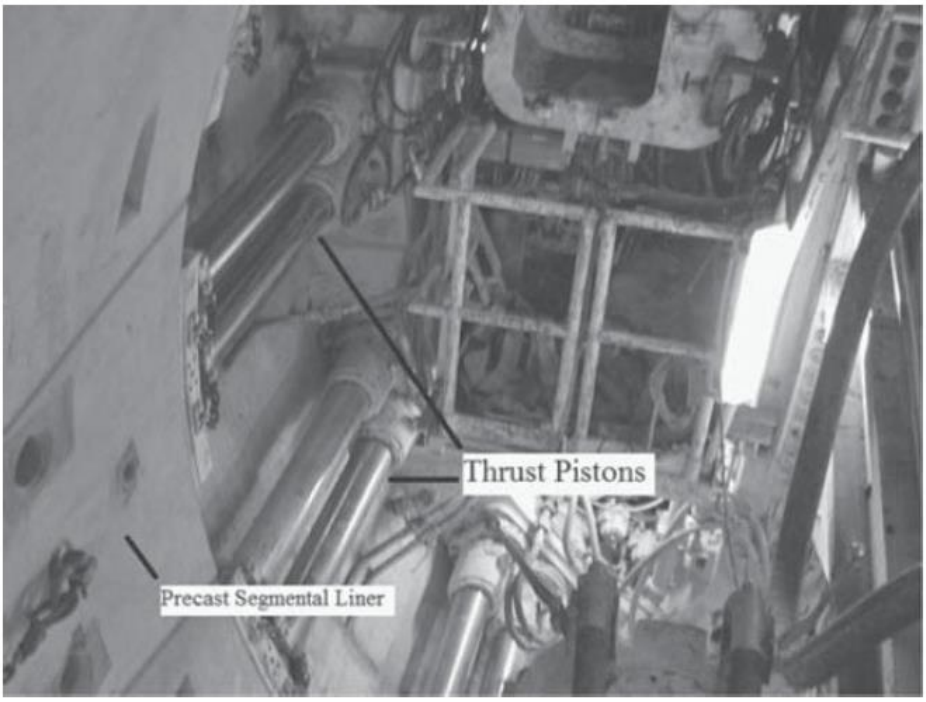

Figure 2-8 TBM Push Cylinders [7].

Figure 2-9 shows a schematic of a TBM. From the Figure, four systems can be identified: (1) Boring system, including the cutterhead and disc cutters; (2) Thrust and clamping system, including the thrust cylinders, gripper shoes, front shoe, side-steering shoe, and supporting invert shoe; (3) Muck removal system, including the conveyor; and (4) Support system, including the roof shield and drills [7].

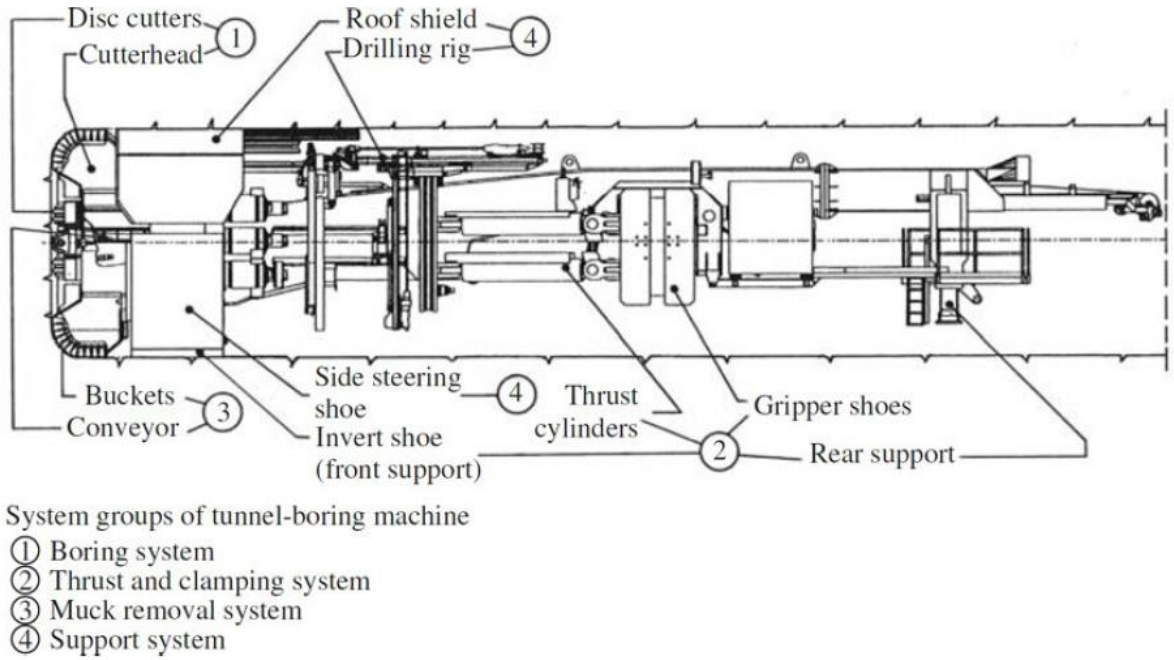

Figure 2-9 TBM Schematic [7].

The standard TBM cutter consists of steel alloy discs with a tapered edge. The cutter has a bearing and is mounted on the cutterhead. The bearing has extreme importance for the excavation process because of the magnitude of the thrust and drag forces that are observed during the drilling process. The cutter can have single or multiedge discs (see Figure 2-10) and have TCI elements [7].

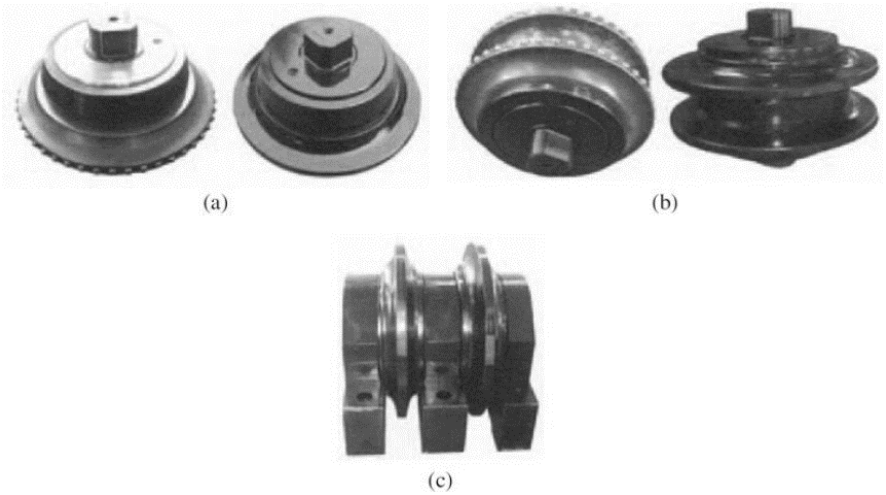

Figure 2-10 Disc Cutters: (a) Single-Disc Cutters, (b) Twin-Disc Cutters, and (c) Center-Disc Cutters [7].

Figure 2-11 shows the disc cutter chipping process, called Kerf principle. According to this principle, the cutters are pushed against the rock face then the discs will penetrate in the rock creating craters and cracks. The debris is expelled by the shear and tensile stress caused by the penetration mechanism. Generally, a penetration between 4 mm and 15mm in hard rock and up to 20 mm in softer rock are considered a good assumption [7].

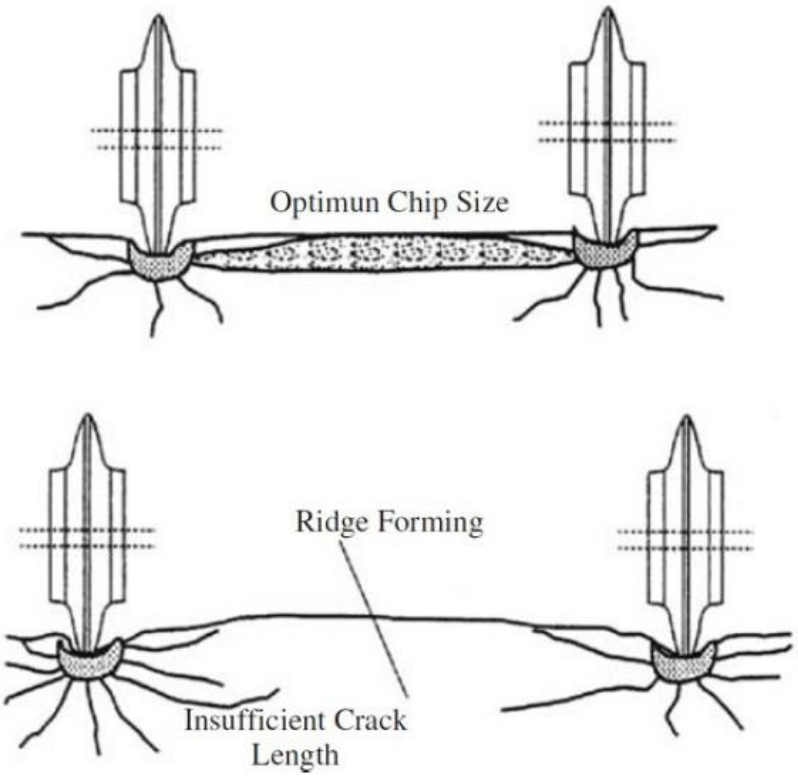

Figure 2-11 Disc Cutter Chipping Process [7].

The TBM drilling performance is influenced by several factors such as geology, rock properties, water, and tunnel design. The rock discontinuities (joints or other cracks) are factors that needs to be highlighted in the TBM drilling process. Its effects on TBM drilling are based on the type of discontinuity, frequency, and orientation [7]. Additionally, the rock mass heterogeneity has considerable impact on the TBM performance. Normally, the geology-related problems are responsible for over 70% of TBM failures in mines [5].

RBMs are used in mining and construction projects to excavate shafts and other vertical structures. Initially, a pilot hole of a 230-350 mm diameter is drilled down. Next, the drill bit used during the pilot hole drilling is changed to a large diameter reamer, and it is pulled back up to the upper level (Figure 2-12). An RBM has the flexibility to work with different dip angles and bit diameters [8].

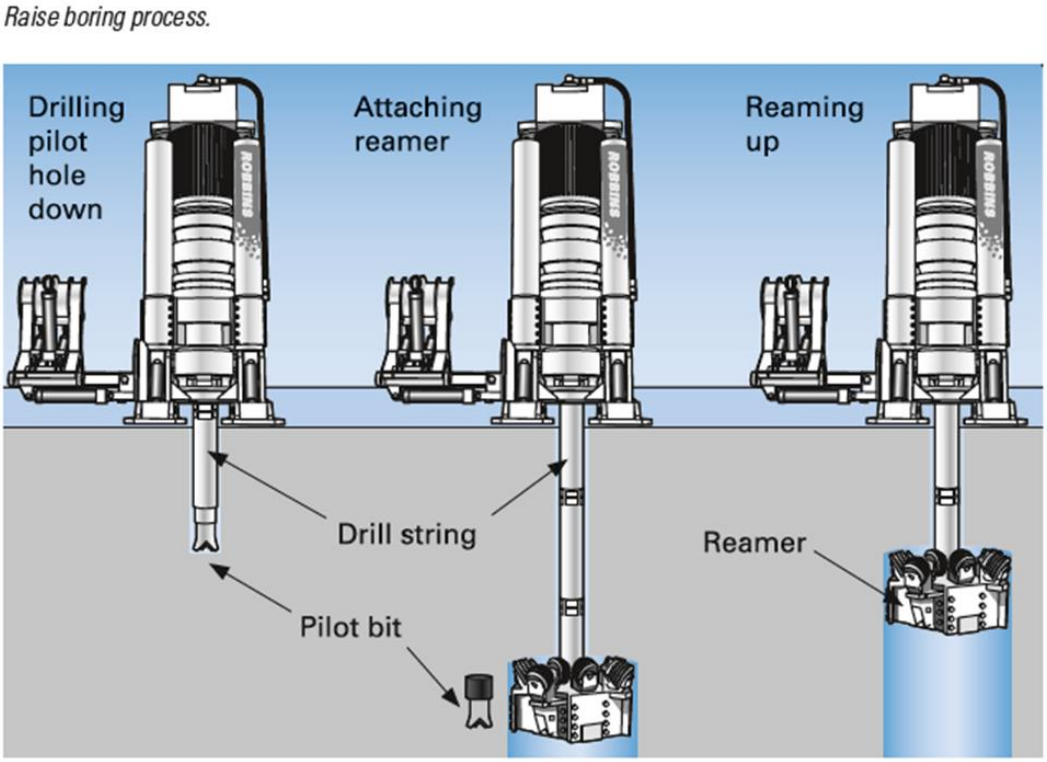

Figure 2-12 Raise Boring Process [9].

Additionally, where the upper level access is limited, a RBM can be used to drill on upward direction. In this application, called boxhole boring method, the RBM is installed on the lower level and, with or without a pilot hole, a reamer or full face bit is used to drill the hole upward adding stabilizers to the drillstring to minimize the vibrations and bending stresses. In the boxhole boring method, the cuttings fall down (gravity effect) and are collected above the RBM by a muck collector and a muck chute (see Figure 2-13) [9].

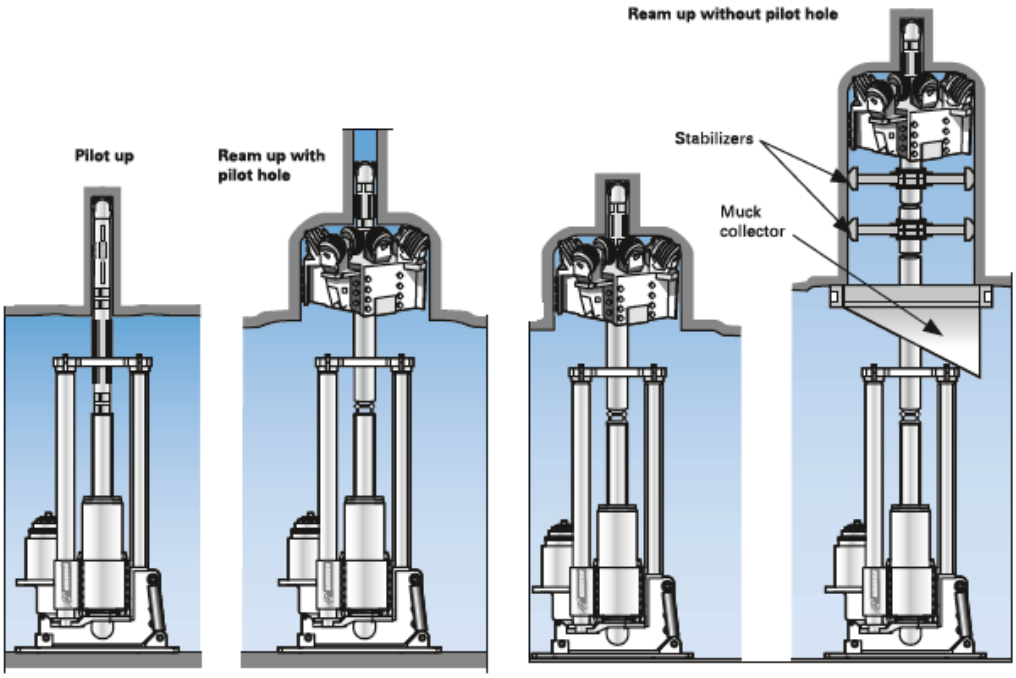

Figure 2-13 Boxhole boring method [9].

With respect to the drilling mechanics, the RBM is very similar to the TBM. Due to its large diameter, the rock discontinuities and heterogeneity have considerable impact on its drilling performance.

2.2 Drilling Performance Prediction Modelling

The ROP prediction models can be divided into two major approaches: physics-based and data-driven prediction models. Physics-based prediction models or traditional models are based on laboratory experiments, being empirical models designed for specific types of drilling parameters. Data-driven models are based purely on data, incorporating machine learning and/or implementing neural networks to the ROP prediction [10].

With for a few rare exceptions, both major approaches need calibration with real drilling data-set. Normally, the prediction models that do not need calibration present low accuracy to

embrace a different drilling scenario. Additionally, research on prediction of the drilling performance including the founder point location is scarce.

2.2.1 Physics-based Models

Maurer (1962) presented a model to predict the drilling performance for roller-cone bits, which is derived from rock cratering mechanisms. This model is called "perfect cleaning" because it assumes that all of the rock debris is removed during the drilling operation. His work was compared with experimental data where full-scale W7R bits were applied to drill in impermeable Beekmantown dolomite rocks using water as the drilling fluid under near "perfect cleaning" conditions [11].

Equation (3-1) presents Maurer's correlation [11].

$$R = k\left(\frac{N(W - W_0)^2}{60D^2S^2}\right) \; for \; W > W_0 \tag{2-1}$$

Where *k* is called "drillability constant", *N* is the rotary speed (rpm), *W* is the WOB (kN), W_0 is the threshold WOB before cratering is initiated (kN), *D* is the bit diameter (mm), *S* is the rock strength (MPa), and *R* is the ROP (m/h).

Due to the high WOB involved in the drilling operations, normally it is assumed that $W \gg W_0$, which reduces Eqn. (3-1) to Eqn.(*3-2*).

$$R = k\left(\frac{NW^2}{60D^2S^2}\right) \tag{2-2}$$

Despite the high accuracy to predict the drilling performance, Maurer's correlation is limited to the values before the founder point. This limitation is due to the squared defence of the ROP to the WOB, which is evidence of the nonexistence of a local maximum point in the curve generated by Maurer's correlation.

Bauer and Calder (1967) used previously published field data to develop an empirical equation to predict the rotary drilling performance which relates the ROP to the rock strength, WOB, rotary speed and hole diameter. To validate the field data used in their formulations, they conducted laboratory indenter tests to study rock failure in hard rock. Their results provide a method to describe and predict the ROP through indenter penetration and sub-surface fracturing [12].

Equation (2-3) presents the Bauer and Calder's correlation.

$$R = [61 - 28\log_{10}(S)]\frac{W}{D}\frac{N}{300} \tag{2-3}$$

Where N is the rotary speed (rpm), W is the WOB (lbf), D is the bit diameter (inch), S is the rock strength (psi), and R is the ROP (ft/h).

Bauer and Calder's correlation presents high accuracy in hard iron ores but presents considerable inaccuracy when the iron ores have low rock strength [13]. Due to the linear relationship between the ROP and WOB presented by Bauer and Calder's correlation (Eqn. (2-3)), its accuracy in predicting the drilling performance curve is very limited as well as the impossibility to locate the founder point.

In 1971, Bauer presented methodologies to both estimate drill requirements and optimize the drilling process and blasting costs in a given context. He discussed the rotary drill performance based on Bauer and Calder's equation [14] that included recommended pull-down weight, ROP versus confined compressive strength (CCS), bit life versus rock strengths, and drilling costs [15].

Warren (1979) presented a drilling prediction model for full-scale soft-formation bits that related the WOB, rotary speed, bit size, rock strength, and bit type to the ROP based on laboratory experiments. His model was developed based on the premise that the effect of the mechanical conditions could be determined in the laboratory using full-scale drill bits and that the model could be coupled with other models that would be appropriate for the drilling fluid properties and hydraulic effects [16].

Equation (2-4) presents the Warren's correlation.

$$R = \left(\frac{aS^2D^3}{N^bW^2} + \frac{c}{ND}\right)^{-1} \tag{2-4}$$

Where *a*, *b*, and *c* are constants, *S* is the rock strength (kPa), *D* is the bit diameter (cm), *N* is the rotary speed (rev/s), *W* is the WOB (N), and *R* is the ROP (ft/h).

Based on the analysis of the derivative of Eqn. (2-4), the drilling performance curve generated by Warren's correlation does not have a maximum local point that limited this correlation to the region of the curve before the founder point.

In 1987, Bourdon *et al.* described the progress of the development and implementation of a system for the acquisition of rig-site DOT data as well as the laboratory simulation of DOTs. In their work, more than 50 DOTs performed in onshore vertical wells and deviated wells (up to 40º) and different lithology types were analyzed. Roller-cone bits of 215.9 mm and 152.4 mm diameter were applied in these DOTs. In the laboratory DOTs, roller-cone bits of 215.9 mm were used in several rock types, including Carrara marble, Bolton Wood sandstone, Portland limestone, and a limestone aggregate concrete. They highlighted the importance of good sensors and data logging in collecting valuable information for the evaluation of drilling performance. They did not observe significant transient effects in the ROP response during either field or laboratory DOTs [17].

Bourdon *et al.* considered the ROP directly proportional to the WOB introducing the correlation shown in Equation (2-4).

$$R = KWf(v) \tag{2-5}$$

Where K is the drilling-model coefficient, W is the WOB (N), f is the function of rotary speed, and v is the rotary speed (rpm).

The linear relation between the ROP and WOB presented by Eqn. (2-5) makes evident the inexistence of a local maximum point on the drilling performance curve. This observation introduces a significant limitation to this correlation to represent the whole drilling performance curve.

In 1991, Wijk showed that drilling rates for percussion drilling and roller-cone drill bit operations can be predicted through the use of stamp test data. The use of stamp test data to predict the drilling performance for roller-cone drill bit operation is based on the author's affirmation that its rock fragmentation process is very similar to the percussive drilling. Additionally, Wijk presented a power consumption prediction for rotary drilling and discussed its economics [14].

Equation (2-6) shows the correlation proposed by Wijk to predict the drilling performance for rotary drilling.

$$B = \bar{B} n S_c^{1/4} \left[\frac{F}{D\sigma_{RD}}\right]^{3/2} \tag{2-6}$$

Where B is the ROP, n is the rotary speed, $\bar{B}$ is a non-dimensional constant, S_c is the button density (see Eqn. (2-7)), F is the WOB, D is the hole diameter, and σ_{RD} is the stamp test strength index.

$$S_c = \frac{4N_c}{3\pi D^2 \sin\theta} \tag{2-7}$$

Where N_c is the number of buttons on the cone mantle surface in roller-cone drill bit, and θ is the half of the cone top angle.

Analyzing the derivate (derivative?) of Eqn. (2-7) in relation to F, the inexistence of a local maximum point on the curve generated by this equation is observed. Then, Wijk's correlation is restricted to predict the drilling performance curve before the founder point.

In 1996, Autio and Kirkkomäki presented a novel full-face boring technique based on rotary drilling and vacuum flushing to remove the rock cuttings. In this work, a model to predict the ROP was established for application to boring machines. Their work covered the evaluation of the excavation disturbance, hole quality, particle size distribution and shape of the crushed rock, energy consumption, greenhouse emissions, and occupational conditions [18].

According to Autio and Kirkkomäki, the advance rate or ROP is a relation to cutters, WOB, rotary speed and the rock properties being affecting by the vacuum flushing efficiency. They highlighted that the advance per rotation was used as a test parameter because it is more accurate than the net advance rate and because of the difficult to keep the rotation spend stable during the tests.

Based on the field tests results, Autio and Kirkkomäki applied the method of least squares to define a linear, logarithmic, and exponential curves that best fit to the measured data, using the regression coefficient as a parameter of quality control to the fit curves. They concluded that the differences between these fit curves are very small in low range of WOB but become expressive in large range of WOB, being the exponential regression (Eqn. (2-8)) for most of the tests.

$$R = AW^B \tag{2-8}$$

Where R is the rate of penetration (net advance rate) (m/h), W is the WOB, and A and B adjustment coefficients.

Based on Eqn. (2-8), the limitation of the Autio and Kirkkomäki's approach to predict the whole drilling performance curve is evident because the inexistence of a local maximum point (positive value) in this curve restricting its application to point before the founder point.

In 2008, Detournay *et al.* presented a model to predict the drilling performance of a drag bit (i.e. showed a relationship between the WOB, torque on bit (TOB), ROP, and angular velocity). One of the outcomes highlighted in their work was the possibility of obtaining the rock's or the bit's properties from the knowledge of the existence of different phases in the response of the bit to a drilling operation [19].

Detournay *et al.*'s model assumes the presence of three different operational drilling regimes which are associated with the relation between the contact forces and the depth of cut per revolution. In the first regime, it is assumed that the relationship between the increase of the contact forces and the increase of the depth of cut per revolution is mainly a consequence of a geometrical effect. In the second regime, after a critical value of depth of cut per revolution, that is a relation to the bit bluntness, the contact force is totally applied. In this regime, any increase of the WOB will result in an increase of the depth of cut per revolution. In the last drilling regime, the sharing of material between the rock face and the drill bit is started (consequence of poor cleaning), increasing the contact area. The threshold for this regime is a relation to the bit geometry, mud properties, flow rate, and rock properties.

Detournay *et. al.* presented a mathematical model for the first and second drilling regimes. Eqns. (2-9) (2-10) and shows the relation between the scaled weight and the depth of cut per revolution for first and second drilling regimes, respectively.

$$w = (\zeta\varepsilon + k\sigma)d \tag{2-9}$$

$$w = \zeta\varepsilon(d - d_*) + w_* \tag{2-10}$$

Where w is the scaled weight (N/mm) (Eqn. (2-11)), d is the cut per revolution (mm) (Eqn. (2-12)), d_* is the depth of cut per revolution at the transition between the first and second drilling regimes (mm), w_* is the scaled weight at the transition between the first and second drilling regimes (N/mm), σ is the internal friction angle of the rock, ζ is a constant that varies between 0.5 and 0.8, and ε is the energy required to remove a unit volume of rock under ideal conditions (MPa).

$$w = \frac{W}{a(1-\rho)} \tag{2-11}$$

$$d = \frac{2\pi V}{\Omega} \tag{2-12}$$

Where a is the bit radius, ρ is the ratio between the inner and outer bit radius (for full face bit $\rho = 0$), and Ω is the angular velocity (rad/s).

Based on the previous discussion and the linearity relationship between the scaled weight and the cut per revolution, the model presented by Detournay *et al.* is limited to the regions of the drilling performance curve before the founder point.

In 2009, Shirkavand *et al.* presented a theoretical correlation between the rock strength applied to both the overbalanced and underbalanced drilling conditions and predictions of the bottom hole pressure in underbalanced drilling operations with aerated or foam drilling fluid [20]. They used the Eqn. (2-13) to derivate the rock strength as a relation to the drilling depth. This

equation is applied for PDC bits, which was based on the conservation of mass considering the ROP equivalent to the rate of rock removal during the drilling process.

$$R = W_f \frac{14.14W.N^b.\cos\alpha}{S.D_B.\tan\theta} \tag{2-13}$$

Where R is the ROP, W is the WOB, N is the rotary speed, α and θ are the cutter rake angles, S is the confined compressive strength, D_B is the bit diameter, and W_f is the wear constant that varies between 1 (new drill bit) and 0 (cutters totally worn).

Equation (2-13) shows a linear relationship between the ROP and the WOB. This relationship limits its application to a restricted region of the drilling performance curve excluding the region of this curve after the founder point.

In 2012, Kowakwi et *al.* developed a ROP prediction model that is a normalized hydraulic model with a two-term roller-cone bit that considers the available hydraulic level at a drill bit, chip hold down and bit wear effects (Eqn. (2-14)). This model is based on Warren's two-term model (Eqn. (2-4)) [12]. Their model was compared with a field dataset which showed good accuracy to predict the drilling rate. They also presented a model to predict the unconfined compressive strength (UCS) of a formation based on the drilling parameter [21].

$$R = \left(\frac{0.082\sigma^2 D^3}{N^{0.6}W^2} + \frac{5.034}{ND}\right)^{-1}.f(x).f_c(P_e).W_f \tag{2-14}$$

$$f(x) = -0.8736\,\frac{R}{HSI} + 0.9982 \tag{2-15}$$

$$f(x) = -0.736\,\frac{R}{HSI} + 0.9501 \tag{2-16}$$

$$f_c(P_e) = c_c + a_c(P_e - 120)^{b_c} \quad (2\text{-}17)$$

$$W_f = 1 - \frac{\Delta BG}{8} \quad (2\text{-}18)$$

Where σ is the rock strength (kPa), *D* is the bit diameter (cm), *N* is the rotary speed (rev/s), *W* is the WOB (N), *R* is the ROP (ft/h), $f(x)$ is the hydraulic energy function, $f_c(P_e)$ is the chip hold down effect, W_f is the bit wear effect, *HSI* is the bit hydraulic horsepower per area of drill bit, (a_c, b_c, and c_c) are chip hold down constants, P_e is the confinement pressure (psi), and ΔBG is the tooth dull grad (IADC).

As Eqn. (2-14) is an extension of Warren's model that does not change the relationship between the WOB and the ROP, the model proposed by Kowakwi et *al.* carries the same limitation of Warren's model with respect to the limitation to predict the behaviour the drilling performance curve after the founder point.

In 2012, Yagiz *et al.* presented an approach for predicting TBM performance, the CSM model. The CSM model is an evolution that started with a semi-theoretical model based on the cutting forces of individual cutters in 1977 [22], incorporated estimated cutting forces as a function of intact rock properties such as UCS and tensile strength in 1993 [23], and, finally, added the intact rock brittleness (BI) and fracture properties of rock masses in 2002 and 2006 [24] [25]. In general terms, the cutterhead requirements (thrust, torque and power) related to the maximum ROP are determined based on the individual cutter forces performing on the rock mass. In this study, the CSM model is discussed based on its application in massive and fractured hard rock conditions. The authors mentioned the difficulty of a simple formula to model the TBM performance due to the complexity of mechanical tunneling processes and the distinct rock properties and features and

affirmed that the CSM model has low accuracy to predict faulted fractured rock mass conditions where the ROP is affected by the fractures and plane of weakness. In the CSM model, the relation between the normal force per cutter and the ROP is a potential function [26].

Eqns. (5-1), (5-2), and (5-3) represent the CSM model.

$$\phi = cos^{-1}\left(\frac{R-P}{R}\right) \tag{2-19}$$

$$P' = c\sqrt[3]{\frac{\sigma_u^2.\sigma_t.s}{\phi\sqrt{R.T}}} \tag{2-20}$$

$$F_N = \frac{T.R.\phi.P'.\cos(\phi/2)}{1000} \tag{2-21}$$

Where ϕ is the angle of the arc of contact, R is the cutter radius, P is the penetration rate, P' is the pressure of contact area, c is the cutting constant, σ_u is the uniaxial compressive strength, σ_t is the Brazilian tensile strength, s is the spacing of cutters, T is the cutter trip width, F_N is the normal force per cutter.

In 2014, Chen *et al.* used a new variation of the mechanical specific energy (MSE) developed from the evaluation of available MSE models. This new approach was used as a tool for real-time monitoring, predicting, avoiding down hole accidents, reducing costs and so on. They stated that the ROP can be predicted by the new approach of the MSE. Additionally, they introduced a rate of penetration model based on the mechanical specific Energy (Eqn. (2-22)) [27].

$$R = \frac{13.33\mu_b N}{D_B\left(\frac{CCS}{E_m W\, e^{-\mu\gamma_b}} - \frac{1}{A_B}\right)} \tag{2-22}$$

Where R is the ROP (ft/h), μ_b is the bit-specific coefficient of sliding friction, N is rotary speed (rpm), D_B is the bit diameter (inches), *CCS* is the confined compressive strength (psi), E_m is the mechanical efficiency of new bit, W is the WOB (lbf), μ is the coefficient of friction of drill string, γ_b is the inclination of the bottom hole (rad), and A_B is the bit area (in2).

Analyzing the derivative of Eqn. (2-22), the lack of a local maximum point in the drilling performance curve predicted by it is observed.

In 2015, Deng *et al.* analyzed the drilling resistance in the rock breaking process and proposed a new approach to predict the ROP (Eqn. (2-23)). In their work, the energy consumption in the drilling process and the rock fragmentation fractal characteristics were studied, which was supported by laboratory experiments with roller-cone bits [29].

$$\nu = \frac{2\pi nM}{\frac{\pi}{4}D^2 a - P} \tag{2-23}$$

Where ν is the ROP, n is the rotary speed, M is the torque, D is the bit diameter, a is the specific energy, and P is the WOB.

The behaviour of the Eqn. (2-23) is very similar to Eqn. (2-22) including the inexistence of a local maximum point in the curved generated by this equation.

In 2015, Ataei *et al.* studied 11 different zones of an open-pit iron mine to classify them with respect to rock drillability. Laboratory tests and geological mapping of the rock faces were carried out, and rock-mass structural parameters were recorded to develop a model for ROP

prediction that could also predict the UCS in terms of Schmidt hammer rebound values (Eqn. (2-24)). This model was compared with previous models from literature based on analyzed scenarios in their paper. The authors affirmed that their model for ROP prediction is limited to the geological and drilling conditions that were studied in their paper [30].

$$R = 2.31 \frac{W^{0.094} N^{0.95} RDi^{0.099}}{P^{0.075} D^{3.04}} \quad (2\text{-}24)$$

Where *R* is the ROP (m/min), *W* is the WOB (kg), *N* is the rotary speed (rpm), *RDi* is the rock mass drillability index, *P* is the air pressure for flushing the blast hole (psi), and *D* is the bit diameter (mm).

Analyzing graphically Eqn. (2-24), the lack of a local maximum to this curve is easily observed. Based on this observation, Eqn. (2-24) is limited to represent the drilling performance curve before the founder point.

In 2015, Mamaghani *et al.* presented experimental studies focused on the determination of a penetration index related to RBMs applications. Their study is based on indentation test laboratory experiments using hydraulic press in rock samples obtained from Eti Copper Kure Asikoy underground mine located in Turkey. Their study results were validated by a comparative analysis between the ROP prediction (Eqn. (2-25)) and field results [31].

$$T_{max} = 0.005 N' \frac{F}{d} p \quad (2\text{-}25)$$

Where T_{max} is the maximum thrust or reaming thrust of the raise borer (kN), *N'* is the number of carbide inserts in the reamer head times the number of roller cutters, *F/d* is the

penetration index value (which is obtained from an indentation test) and p is the penetration per revolution of the cutterhead (mm/rev).

Eqn. (2-25) shows a linear relationship between the maximum thrust or reaming thrust of the raise borer and the penetration per revolution of the cutterhead, which limited the correlation to predict the region of the drilling performance curve before the founder point.

In 2016, He *et al.* investigated the relationship between five brittleness indices and the various petrophysical and geomechanical properties of rocks. In addition, they developed a correlation that relates the brittleness indices to Young's modulus, P-wave velocity, and porosity. A ROP prediction approach for PDC bits was established based on gamma ray, neutron, density, and sonic log data derived from correlations in the literature. Their approach is based on Eqn. (2-26) [32].

$$R = W_f G \frac{W^a N^b}{S D_b} \tag{2-26}$$

Where R is the ROP, W is the WOB, W_f is the bit wear function, N is the rotary speed, S is the confined rock compressive strength, D_b is the drill bit diameter, and a, b and G are constants.

The exponential relationship between the ROP and the WOB, presented in Eqn. (2-26), limited its application to the whole drilling performance curve because of the inexistence of a local maximum point for the curve generated by this equation.

In 2016, Deng *et al.* presented a ROP prediction model for roller-cone bits (Eqn. (2-27)) that considered the combined effect of the main drilling parameters and the rock dynamic compressive strength. Their model is based on the rock fragmentation mechanism of a single indenter. They applied the rock's dynamic compressive strength to reflect the real process of rock dynamic crushing by a roller-cone bit during the drilling process. They conducted a laboratory drilling experiment on sandstone and limestone rock samples with a full-scale bit to validate their ROP prediction model as well as compare their model with the other available models based on rock static compressive strength. They affirmed that the ROP prediction models based on rock static compressive strength presented an error between 45% and 50% and their model presented an average error of about 15% during their drilling laboratory experiments [33].

$$v = An_b \left(\frac{W}{\sigma_d}\right)^{3/2} \tag{2-27}$$

$$A = \frac{0.126K}{(k_1 + k_2 + k_3)^{3/2}\pi R_0^2 \sin\varphi_0} \tag{2-28}$$

$$K = \sum_{i=1}^{3}\sum_{j=1}^{m_i}(k_i)_j \tag{2-29}$$

Where v is the ROP, n_b is the bit rotary speed, W is the WOB, σ_d is the rock ultimate dynamic compressive strength, k_i $(i = 1, 2, and\ 3)$ is the number of teeth embedded in each cone in contact with rock at the same time, and m_i is the number of generatrixes on the each cone.

Equation (2-27) shows an exponential relationship between the ROP and the WOB what results in the inexistence of a local maximum point in the drilling performance curve generated by this equation. Therefore, this equation is restricted to predict the drilling performance before the founder point.

In 2016, Rostami reviewed existing models and ongoing research to predict the TBM performance. According to Rostami, ROP, utilization rate, advance rate, and cutter life are some parameters that, in general, are estimated in the TBM performance analysis. He affirmed that the force balance or theoretical approach, and the empirical models are two camps that, normally, are used to predict the TBM performance in hard rock formations. According to the author, the theoretical approach is based on estimation of cutting forces and the empirical models are based on the analysis and observations of the past projects. Additionally, he concluded that the accuracy of a TBM performance prediction is very low due to the high variability of the application scenarios [34].

In 2018, Shaterpour-Mamaghani *et al.* presented a new empirical model to predict the RBM performance using simple and multiple regression methods. Their study was based on statistical analysis of field results and laboratory studies. They used the UCS to estimate the rotational speed and consumed reamerhead torque, and Brazilian tensile strength (BTS) associated with elasticity modulus to estimate the field specific energy [35]. As the contribution of the thrust force on the cutterhead for the rate of penetration is not explicit in the empirical model proposed by Shaterpour-Mamaghani *et al.*, these methods do not represent the drilling performance curve based on the relation between the ROP and WOB.

In 2018, Armetti *et al.* proposed a new model to predict the TBM performance which correlates the ROP and FPI with the singular rock-mass parameters such as UCS, quartz content, and spacing between fractures. Their study was based on the field data continuously recorded during the construction of the “La Maddalena” exploratory tunnel, situated in northern Italy. The rock-mass quality indices: rock mass rating (RMR) and geological strength index (GSI) were used

to estimate the excavatability of a given material showing the importance of an accurate geological-geotechnical characterization to TBM prediction performance. The authors listed eight known empirical predictive methods for TBM performances. In all methods adding the method develop by the authors , the rate of penetration is not a function of the thrust force on the cutterhead (WOB) [36]. Then, for obvious reasons, these methods do not represent the drilling performance curve based on the relation between the ROP and WOB.

In 2020, Arbabsiar *et al.* presented a new model to improve the accuracy of ROP prediction for a TBM in distinct geotechnical conditions. This model is based on TBM operational parameters and media characteristics (geotechnical risk levels in the modelling). The authors presented five known TBM performance prediction empirical models that does not present an explicit relationship between the rate of penetration and the cutter normal force. Additionally, the authors presented two models (Graham's (Eqn. (2-30)) and Farmer and Glossop's (Eqn. (2-31)) models) that stablish a relationship between the rate of penetration and the cutter normal force [37].

$$PR_{ev} = 3940\frac{F_n}{TS} \tag{2-30}$$

$$RPR_{ev} = 624\frac{F_n}{TS} \tag{2-31}$$

Where PR_{ev} is the penetration per revolution, F_n is the cutter normal force, and the TS is the tensile strength.

Equations (2-30) and (2-31) present a linear relationship between the penetration per revolution (equivalent to the ROP) and the cutter normal force (equivalent to the WOB). Due to

this relationship, these equations are limited to predict the region of the drilling performance curve before the founder point.

The scarce of the models to predict the whole drilling performance curve including the founder point location is evidenced in this section.

2.2.2 Data-driven Models

In 2010, Bataee *et al.* investigated the accuracy and the validity of various ROP predictions and applied computer optimization to yield drilling parameter recommendations for PDC and roller-cone bits application in the Shadegan Oil Field. Furthermore, they observed that different models showed more accuracy in different moments of the drilling operation (depth, bit diameter, bit type, and type of formation) [38].

In 2010, Hedayatzadeh *et al.* developed a model to predict the TBM performance using an artificial multi-layer neural network with a back propagation (BP) learning algorithm. The authors affirmed that a ROP prediction for a TBM is influenced by a large number of parameters that can be divided into four main categories: Intact-rock characteristics; rock-mass properties; rock-mass conditions; and machine characteristics. They highlighted the complexity in developing a model that covers all four categories and that there is not a single universal model to predict the TBM performance [39].

In 2011, Hassampour *et al.* developed a new ROP prediction model for TBMs based on the analysis and compilation of a database from different hard rock tunneling projects. Their model used statistical methods and the relationship between geological and operational parameters.

Additionally, an approach for estimation of rock-mass boreability and TBM performances was introduced [40].

In 2012, AlArfaj *et al.* compared the traditional multiple regression method with Extreme Learning Machines (ELM) and Radial Basis Function Network (RBF) to predict the ROP [41].

In 2013, Ge *et al.* proposed a ROP prediction model to TBM based on the least-square support vector machine. This model correlated the ROP and rock properties such as UCS, BTS, peak slope index, DPW and the alpha angle [42].

In 2014, Bataee *et al.* applied the Artificial Neural Network (ANN) model for prediction of ROP and optimization of the drilling parameters through choosing a proper model of ROP prediction among the Bourgoyne and Young model, Bingham model, and the modified Warren model [43].

In 2014, Ghasemi *et al.* developed a fuzzy logic model to predict the ROP of a TBM application in hard rock. They used a data-set from the Queens Water Tunnel 3, Stage 2 that was drilled in New York City. Their model used intact-rock and mass-rock properties such as UCS, rock brittleness, distance between planes of weakness (DPW), and the discontinuities orientation in the rock-mass to predict the drilling performance of a TBM. They affirmed that the major advantage of the use of a fuzzy model for ROP prediction is that human judgment and intuition can be used. Additionally, they concluded that additional improvement is necessary to their fuzzy model to extend to other tunnel drilling operations [28].

In 2015, Duan *et al.* proposed a model to predict the ROP based on BP neural network technologies. The prediction model is built based on the known of the wells drilling logs to predict the ROP to the new well [44].

In 2016, Moraveji, and Naderi investigated the simultaneous effect of the well depth, WOB, rotary speed, bit jet impact force, yield point to plastic viscosity ratio, and the 10 min to 10 s gel strength ratio on the ROP using drilling field data. They used Response Surface Methodology (RSM) to determine the relationship between these six drilling parameters and the ROP. Additionally, they used the Bat Algorithm (BA) to maximize the ROP through the identification of the respective optimal range for the six drilling parameters [45].

In 2017, Eskandarian *et al.* presented a procedure for predicting the ROP using a ranking technique and applying data mining algorithms to build predictive models [46].

In 2017, Hegde *et al.* studied the drilling performance to predict the ROP through two different approaches: physics-based and data-driven. Their approach (data-based) used the machine learning algorithms and surface measured input (WOB, rpm, and flow rate) to predict the ROP in PDC bit application [10].

In 2017, Diaz *et al.* analyzed the drilling parameters to improve the ROP prediction in the context of geothermal systems. A fast Fourier transform filter was used to smooth the fluctuation of the ROP values and two optimization methods, multiple regression and ANN, were used to evaluate the data smoothing effects. They observed that the drilling parameter's trends were

influenced by many factors such as stratigraphy, formation strength, change of drilling operator, mud properties, and change of drill bit [47].

In 2017, Adoko *et al.* presented a study about ROP prediction for TBM applications based on the rock-mass parameters including the UCS, BI, angle between the plane of weakness, TBM driven direction, and DPW. A tunneling project in New York City was used as the base to establish the proposed models in their paper. This work used the Bayesian inference approach to identify the most appropriate models to predict the ROP among the eight models that were selected. They used the Markov chain Monte Carlo (MCMC) technique, by WinBUGS software, to obtain the mean values of the model parameters that were considered in the model prediction performance evaluation. Deviance information criterion (DIC) was used as a model accuracy indicator and to rank the models conforming to their fit and complexity [48].

In 2018, Salimi *et al.* analyzed the performance of a hard rock TBM in a 12.24 km tunnel to assess the relationship between the TBM operation and different lithology. Non-linear Regression Analysis, Classification and Regression Tree, and Genetic Programming were used to analyse the TBM performance with respect to the ground conditions. In their work, they affirmed that all existing rock-mass classification systems have limited accuracy in TBM performance prediction. They proposed new models to predict the TBM performance based on the principle components analysis approach [49].

In 2018, Elkatatny applied the self-adaptive differential evolution technique to optimize the ANN variable parameters that were used to predict the ROP as a function of the WOB, TOB, stand pipe pressure, flow rate, UCS, drilling fluid density, plastic viscosity, and rotary speed. He

concluded that the ROP is a strong function of the WOB, rotary speed, TOB, and house power while the ROP is a moderate function of UCS [50].

In 2018, Mnati and Hadi presented a new approach to predict ROP using the ANN technique. They used the data set collected from five drilling operations in the Alhalfaya oil field to train and validate their ANN models. Additionally, they used the proposed model to optimize the drilling costs [51].

In 2018, Diaz *et al.* explored the relations between the drilling parameters to improve the ROP prediction accuracy. This study was based on a drilling data-set from a geothermal project that drilled a well with 4.2 km depth. Their approach applied traditional multiple regression and ANN [47].

In 2019, Gan *et al.* proposed a ROP prediction hybrid model considering the process characteristics. Their model was divided into three stages: Stage I – a wavelet filtering method is applied to reduce the noise presented in the drilling data; Stage II – the mutual information method is used to determine the model inputs with the purpose of decreasing model redundancy; Stage III – a hybrid BA is applied to optimize the hyper-parameters of the support vector regression model [52].

In 2019, Gan *et al*. proposed a novel two-level intelligent modelling method for the ROP prediction in complex geological drilling processes considering incomplete drilling parameters, coupling, and strong nonlinearities. A formation drillability fusion sub-model was established to categorize the influence of the drilling parameter in the ROP by using Nadaboost extreme learning

machine algorithm. The ROP prediction model was established by an ANN with radial basis function optimized by the particle swarm optimization [53].

In 2020, Samaei *et al.* proposed a new equation and introduced novel techniques for TBM performance prediction. They investigated the relationship between the ROP and rock-mass properties using regression analysis. Due to this investigation, two non-linear multi-variable equations were presented and optimized by the Imperialist Competitive Algorithm, and two other models were examined by the Classification and Regression Tree and Genetic Expression Programming techniques [54].

In a general, the data-driven models do not have focus in the prediction the whole drilling performance curve limiting to the region of this curve that present high drilling efficiency, i.e., the region before the founder point. This can be considered a limitation of this type of the prediction model because of the difficulty of comparison between different drilling scenarios and limit the optimization capability.

2.3 References

[1] R. F. Mitchell and S. Z. Miska, Eds., *Fundamentals of Drilling Engineering*, vol. 12. Richardson, UNITED STATES: Society of Petroleum Engineers, 2010.

[2] J. J. Azar and G. R. Samuel, *Drilling engineering*. Tulsa, Okla: PennWell Corp, 2007.

[3] "PDC Bit vs Tricone Bit, Which is The Best Option for You," *FIRMTECH*, Nov. 04, 2019. https://www.firmtechco.com/pdc-vs-tricone/ (accessed Dec. 06, 2020).

[4] "Kelly-Drive Rotary Drilling Operations," *Equipment Operator Advanced - Advanced construction equipment operators manual*, Kelly-Drive Rotary Drilling Operations.

http://enginemechanics.tpub.com/14080/css/Kelly-Drive-Rotary-Drilling-Operations-207.htm (accessed Dec. 06, 2020).

[5] Y. L. Zheng, Q. B. Zhang, and J. Zhao, "Challenges and opportunities of using tunnel boring machines in mining," *Tunnelling and Underground Space Technology*, vol. 57, pp. 287–299, Aug. 2016, doi: 10.1016/j.tust.2016.01.023.

[6] G. Barla and S. Pelizza, "TBM tunneling in difficult ground conditions," Melbourne, Australia, Nov. 2000, vol. 1, p. 19, Accessed: Dec. 06, 2020. [Online]. Available: https://www-onepetro-org.qe2a-proxy.mun.ca/search?q=TBM+tunneling+in+difficult+ground+conditions&peer_reviewed=&published_between=&from_year=&to_year=&rows=25.

[7] G. B. Hemphill, *Practical tunnel construction*. Hoboken, New Jersey: John Wiley & Sons, Inc, 2013.

[8] A. Shaterpour-Mamaghani, N. Bilgin, C. Balci, E. Avunduk, and C. Polat, "Predicting Performance of Raise Boring Machines Using Empirical Models," *Rock Mech Rock Eng*, vol. 49, no. 8, pp. 3377–3385, Aug. 2016, doi: 10.1007/s00603-015-0900-1.

[9] Atlas Copco Rock Drills, *Mining Methods in Underground Mining*, 2nd ed. Ulf Linder.

[10] C. Hegde, H. Daigle, H. Millwater, and K. Gray, "Analysis of rate of penetration (ROP) prediction in drilling using physics-based and data-driven models," *Journal of Petroleum Science and Engineering*, vol. 159, pp. 295–306, Nov. 2017, doi: 10.1016/j.petrol.2017.09.020.

[11] W. C. Maurer, "The 'Perfect - Cleaning' Theory of Rotary Drilling," *Journal of Petroleum Technology*, vol. 14, no. 11, pp. 1270–1274, Nov. 1962, doi: 10.2118/408-PA.

[12] A. Bauer and P. N. Calder, "Open Pit Drilling - Factors Influencing Drilling Rates," presented at the 4th Rock Mechanics Symposium, Ottawa, ON, 1967.

[13] B. V. GOKHALE, *Rotary drilling and blasting in large surface mines.*, 1st ed. Place of publication not identified: CRC Press, 2018.

[14] G. Wijk, "Rotary Drilling Prediction," *International Journal of Rock Mechanics and Mining Sciences & Geomechanics*, vol. 28, no. 1, pp. 35–42, 1991.

[15] A. Bauer, "Open pit drilling and blasting," *Journal of the South African Institute of Mining and Metallurgy*, vol. 71, no. 7, pp. 115–121, 1971.

[16] T. M. Warren, "Drilling Model for Soft-Formation Bits," *JOURNAL OF PETROLEUM TECHNOLOGY*, pp. 963–970, 1981.

[17] J.-C. Bourdon, G. A. Cooper, D. A. Curry, D. McCann, and B. Peltier, "Comparison of Field and Laboratory-Simulated Drill-Off Tests," *SPE Drilling Engineering*, p. 6, 1989.

[18] J. Autio and T. Kirkkomäki, *Boring of full scale deposition holes using a novel dry blind boring method*. Helsinki: Posiva, 1996.

[19] E. Detournay, T. Richard, and M. Shepherd, "Drilling response of drag bits: Theory and experiment," *International Journal of Rock Mechanics and Mining Sciences*, vol. 45, no. 8, pp. 1347–1360, Dec. 2008, doi: 10.1016/j.ijrmms.2008.01.010.

[20] F. Shirkavand, G. Hareland, and B. S. Aadnoy, "Rock Mechanical Modelling for a Underbalanced Drilling Rate of Penetration Prediction," in *43rd Rock Mechanics Symposium and 4th US-Canada Rock Mechanics Symposium*, Asheville, NC, Jun. 2009, p. 5.

[21] I. Kowakwi, H. Chen, G. Hareland, and B. Rashidi, "The Two-Term Rollercone Rate of Penetration (ROP) Model With Integrated Hydraulics Function," presented at the 46th U.S. Rock Mechanics/Geomechanics Symposium, Jan. 2012, Accessed: Dec. 06, 2020. [Online]. Available: https://www-onepetro-org.qe2a-proxy.mun.ca/conference-paper/ARMA-2012-246?sort=&start=0&q=The+Two-Term+Rollercone+Rate+of+Penetration+%28ROP%29+Model+with+Integrated+Hydraulic

s+Function&from_year=&peer_reviewed=&published_between=&fromSearchResults=true&to_year=&rows=25#.

[22] S. Yagiz, J. Rostami, and L. Ozdemir, "Colorado School of Mines Approaches For Predicting TBM Performance," presented at the ISRM International Symposium - EUROCK 2012, May 2012, Accessed: Dec. 06, 2020. [Online]. Available: https://www-onepetro-org.qe2a-proxy.mun.ca/conference-paper/ISRM-EUROCK-2012-047?sort=&start=0&q=Colorado+School+of+Mines+approaches+for+predicting+TBM+performance&from_year=&peer_reviewed=&published_between=&fromSearchResults=true&to_year=&rows=25#.

[23] J. Rostami and L. Ozdemir, "A new model for performance prediction of hard rock TBMs," in *11th Rapid Excavation and Tunneling Conference*, Boston, MA, 1993, p. 18.

[24] S. Yagiz, "Development of rock fracture and brittleness indices to quantify the effects of rock mass features and toughness in the CSM model basic penetration for hard rock tunneling machines," Thesis, Colorado School of Mines, 2001.

[25] S. Yagiz, "A Model for prediction of tunnel boring machine performance," presented at the 10th congress of the International Association for Engineering Geology and the Environment, London, Nottingham, Sep. 2006.

[26] I. W. Farmer and N. H. Glossop, "Mechanics of disc cutter penetration," *International Journal of Rock Mechanics and Mining Sciences & Geomechanics Abstracts*, vol. 12, no. 6, pp. A123–A124, Jul. 1980, doi: 10.1016/0148-9062(80)90769-X.

[27] X. Chen, H. Fan, B. Guo, D. Gao, H. Wei, and Z. Ye, "Real-Time Prediction and Optimization of Drilling Performance Based on a New Mechanical Specific Energy Model," *Arab J Sci Eng*, vol. 39, no. 11, pp. 8221–8231, Nov. 2014, doi: 10.1007/s13369-014-1376-0.

[28] E. Ghasemi, S. Yagiz, and M. Ataei, “Predicting penetration rate of hard rock tunnel boring machine using fuzzy logic,” *Bull Eng Geol Environ*, vol. 73, no. 1, pp. 23–35, Feb. 2014, doi: 10.1007/s10064-013-0497-0.

[29] Y. Deng *et al.*, “A New Prediction Model of Energy Consumption on Rock Fragmentation and Rate of Penetration Based on Fractal Theory,” presented at the 49th US Rock Mechanics/Geomechanics Symposium, San Francisco, CA, Jun. 2015.

[30] M. Ataei, R. KaKaie, M. Ghavidel, and O. Saeidi, “Drilling rate prediction of an open pit mine using the rock mass drillability index,” *International Journal of Rock Mechanics and Mining Sciences*, vol. 73, pp. 130–138, Jan. 2015, doi: 10.1016/j.ijrmms.2014.08.006.

[31] A. S. Mamaghani, E. Avunduk, and N. Bilgin, “Rock mechanical aspects of excavation related to raise boring machine – A typical example from Asikoy underground mine, Kastamonu, Turkey,” presented at the EUROCK 2015 & 64th Geomechanics Colloquium, Salzburg, Oct. 2015.

[32] J. He, Y. Chen, L. Zhengchun, and R. Samuel, “Global Correlation of Rock Brittleness Indices With Petrophysical and Geomechanical Properties and its Application to the Prediction of Rate of Penetration (ROP),” presented at the IADC/SPE Asia Pacific Drilling Technology Conference, Singapore, 2016, doi: 10.2118/180518-MS.

[33] Y. Deng, M. Chen, Y. Jin, Y. Zhang, D. Zou, and Y. Lu, “Theoretical and experimental study on the penetration rate for roller cone bits based on the rock dynamic strength and drilling parameters,” *Journal of Natural Gas Science and Engineering*, vol. 36, pp. 117–123, Nov. 2016, doi: 10.1016/j.jngse.2016.10.019.

[34] J. Rostami, “Performance prediction of hard rock Tunnel Boring Machines (TBMs) in difficult ground,” *Tunnelling and Underground Space Technology*, vol. 57, pp. 173–182, Aug. 2016, doi: 10.1016/j.tust.2016.01.009.

[35] A. Shaterpour-Mamaghani, H. Copur, E. Dogan, and T. Erdogan, “Development of new empirical models for performance estimation of a raise boring machine,” *Tunnelling and Underground Space Technology*, vol. 82, pp. 428–441, Dec. 2018, doi: 10.1016/j.tust.2018.08.056.

[36] G. Armetti, M. R. Migliazza, F. Ferrari, A. Berti, and P. Padovese, “Geological and mechanical rock mass conditions for TBM performance prediction. The case of ‘La Maddalena’ exploratory tunnel, Chiomonte (Italy),” *Tunnelling and Underground Space Technology*, vol. 77, pp. 115–126, Jul. 2018, doi: 10.1016/j.tust.2018.02.012.

[37] M. H. Arbabsiar, M. A. Ebrahimi Farsangi, and H. Mansouri, “A new model for predicting the advance rate of a Tunnel Boring Machine (TBM) in hard rock conditions,” *MGPB*, vol. 35, no. 2, pp. 57–74, 2020, doi: 10.17794/rgn.2020.2.6.

[38] M. Bataee and M. Kamyab, “Investigation of Various ROP Models and Optimization of Drilling Parameters for PDC and Roller-cone Bits in Shadegan Oil Field,” p. 10.

[39] M. Hedayatzadeh, K. Shahriar, and J. K. Hamidi, “An Artificial Neural Network model to predict the performance of hard rock TBM,” in *ISRM International Symposium 2010 and 6th Asian Rock Mechanics Symposium - Advances in Rock Engineering*, New Delhi, India, Oct. 2010, p. 7.

[40] J. Hassanpour, J. Rostami, and J. Zhao, “A new hard rock TBM performance prediction model for project planning,” *Tunnelling and Underground Space Technology*, vol. 26, no. 5, pp. 595–603, Sep. 2011, doi: 10.1016/j.tust.2011.04.004.

[41] I. AlArfaj, A. Khoukhi, and T. Eren, “Application of Advanced Computational Intelligence to Rate of Penetration Prediction,” in *2012 Sixth UKSim/AMSS European Symposium on Computer Modeling and Simulation*, Malta, Malta, Nov. 2012, pp. 33–38, doi: 10.1109/EMS.2012.79.

[42] Y. Ge, J. Wang, and K. Li, “Prediction of hard rock TBM penetration rate using least square support vector machine,” *IFAC Proceedings Volumes*, vol. 46, no. 13, pp. 347–352, 2013, doi: 10.3182/20130708-3-CN-2036.00105.

[43] M. Bataee, S. Irawan, and M. Kamyab, “Artificial Neural Network Model for Prediction of Drilling Rate of Penetration and Optimization of Parameters,” *J. Jpn. Petrol. Inst.*, vol. 57, no. 2, pp. 65–70, 2014, doi: 10.1627/jpi.57.65.

[44] Jinan Duan, Jinhai Zhao, Li Xiao, Chuanshu Yang, and Huinian Chen, “A ROP prediction approach based on improved BP neural network,” in *2014 IEEE 3rd International Conference on Cloud Computing and Intelligence Systems*, Shenzhen, China, Nov. 2014, pp. 668–671, doi: 10.1109/CCIS.2014.7175818.

[45] M. Keshavarz Moraveji and M. Naderi, “Drilling rate of penetration prediction and optimization using response surface methodology and bat algorithm,” *Journal of Natural Gas Science and Engineering*, vol. 31, pp. 829–841, Apr. 2016, doi: 10.1016/j.jngse.2016.03.057.

[46] S. Eskandarian, P. Bahrami, and P. Kazemi, “A comprehensive data mining approach to estimate the rate of penetration: Application of neural network, rule based models and feature ranking,” *Journal of Petroleum Science and Engineering*, vol. 156, pp. 605–615, Jul. 2017, doi: 10.1016/j.petrol.2017.06.039.

[47] M. B. Diaz, K. Y. Kim, T.-H. Kang, and H.-S. Shin, “Drilling data from an enhanced geothermal project and its pre-processing for ROP forecasting improvement,” *Geothermics*, vol. 72, pp. 348–357, Mar. 2018, doi: 10.1016/j.geothermics.2017.12.007.

[48] A. C. Adoko, C. Gokceoglu, and S. Yagiz, “Bayesian prediction of TBM penetration rate in rock mass,” *Engineering Geology*, vol. 226, pp. 245–256, Aug. 2017, doi: 10.1016/j.enggeo.2017.06.014.

[49] A. Salimi, J. Rostami, C. Moormann, and J. Hassanpour, “Examining Feasibility of Developing a Rock Mass Classification for Hard Rock TBM Application Using Non-linear Regression, Regression Tree and Generic Programming,” *Geotech Geol Eng*, Oct. 2017, doi: 10.1007/s10706-017-0380-z.

[50] S. Elkatatny, “Rate of Penetration Prediction Using Self-Adaptive Differential Evolution-Artificial Neural Network,” presented at the SPE Kingdom of Saudi Arabia Annual Technical Symposium and Exhibition, Dammam, Saudi Arabia, 2018, doi: 10.2118/192186-MS.

[51] K. Hmood Mnati and H. Abdul Hadi, “Prediction of penetration Rate and cost with Artificial Neural Network for Alhafaya Oil Field,” *IJCPE*, vol. 19, no. 4, pp. 21–27, Dec. 2018, doi: 10.31699/IJCPE.2018.4.3.

[52] C. Gan *et al.*, “Prediction of drilling rate of penetration (ROP) using hybrid support vector regression: A case study on the Shennongjia area, Central China,” *Journal of Petroleum Science and Engineering*, vol. 181, p. 106200, Oct. 2019, doi: 10.1016/j.petrol.2019.106200.

[53] C. Gan *et al.*, “Two-level intelligent modeling method for the rate of penetration in complex geological drilling process,” *Applied Soft Computing*, vol. 80, pp. 592–602, Jul. 2019, doi: 10.1016/j.asoc.2019.04.020.

[54] M. Samaei, M. Ranjbarnia, V. Nourani, and M. Zare Naghadehi, “Performance prediction of tunnel boring machine through developing high accuracy equations: A case study in adverse geological condition,” *Measurement*, vol. 152, p. 107244, Feb. 2020, doi: 10.1016/j.measurement.2019.107244.

Chapter 3 Physics-Based Rate of Penetration Prediction Model for Fixed Cutter Drill Bits

This Chapter is based on section 1.3.1 and was approved for publication in the Journal of Energy Resources Technology – American Society of Mechanical Engineers (ASME) in December 2020 and will be entered into production soon. This chapter is an improvement of the paper "Widening Drilling Operation: Performance Analysis on the Application of Fixed Cutter Drill Bits in Hard Rock Formation" that was presented in ASME 39th International Conference on Ocean, Offshore and Arctic Engineering in August 2020 [1] . This improvement and consecutive submission to a journal was a recommendation of the conference paper reviewers.

Authors: Jeronimo de Moura, Jianming Yang, and Stephen D. Butt.

3.1 Co-authorship Statement

The authors' contributions in this work are described below:

- **Jeronimo de Moura**: Identification of research topic, literature review, experiments design and performance, post processing and data analysis, and manuscript preparation.
- **Jianming Yang**: Technical support, and manuscript review.
- **Stephen D**. **Butt**: Experiment supervision, technical support, and manuscript review.

3.2 Abstract

The drilling process is one of the most important and expensive aspects of the oil and gas industry. Its economic feasibility is a directly related to a good planning that has high dependence on an accurate prediction of the rate of penetration (ROP). Knowledge of drilling performance through ROP prediction models is a vital tool in the development of a consistent drilling plan and allows industry players to anticipate issues that may occur during a drilling operation. Additionally, as some drilling parameters (such rotary speed, weight on bit (WOB), and drilling fluid flow rate), an accurate prediction of the ROP is crucial to the optimization of drilling performance and contributes to reducing drilling costs. Several approaches to predict the drilling performance have been tried with varying degrees of success, complexity and accuracy. In this paper, a review of the history of drilling performance prediction is conducted with emphasis on rotary drilling with fixed cutter drill bits. The approaches are grouped into two categories: physics-based and data-driven models. The paper's main objective is to present an accurate model to predict the drilling performance of fixed cutter drill bits including the founder point location. This model was based on a physics-based approach due to its low complexity and good accuracy. This development is based on a quantitative analysis of drilling performance data produced by laboratory experiments. Additionally, the validation and applicability tests for the proposed model are discussed based on Drill-off tests (DOTs) and field trials in several different drilling scenarios. The proposed model presented high accuracy to predict the fixed cutter drill bit drilling performance in the twenty-seven different drilling scenarios which were analyzed in this paper.

3.3 Introduction

Recent ROP prediction studies have focused on the bit-rock interaction and experiments subject to high confining pressure. Normally, these studies use the finite element to model the drilling scenario [2].

ROP prediction models can be divided into two major approaches: physics-based and data-driven. Physics-based prediction models, or traditional models, are empirical models designed for specific types of drilling parameters and are based on laboratory experiments. Data-driven models are based purely on data, and either incorporate machine learning, implementation of Artificial Neural Networks to the ROP prediction, or both [3].

Except in a few rare cases, both major approaches need calibration when faced with real drilling data-sets. Normally, the prediction models that do not need calibration present low accuracy in an embracing drilling scenario. Additionally, research on the prediction of drilling performance including the founder point location are scarce. The founder point represents the point of a drilling performance curve at which an increase in WOB no longer corresponds to an increase in ROP [4]. The founder point is not the point of maximum drilling efficiency but shows the maximum ROP possible in a specific drilling scenario.

During the research activities presented in this paper, it was identified that the proportionality constant of Maurer's correlation Eqn. (3-1), called “drillability constant” (k), presents a linear relationship with the WOB. This linear relationship was observed for different

types of drill bits, such as the coring bit, drag bit, polycrystalline diamond compact (PDC) bit, and natural diamond bit in laboratory experiments, field trials and in different rock formations.

Considering the linear relationship of the drillability constant with the WOB, an extension of Maurer's model to predict the drilling performance, including the localization of the founder point for different drilling scenarios, was proposed. A new correlation was developed that not only presents two constants that need to be calibrated but also covers the drilling performance completely including the founder point location.

3.3.1 Physics-Based Prediction Models

Maurer (1962) presented a model to predict the drilling performance for roller-cone bits. This model is detailed in Subsection 3.4.1 [5].

Bauer and Calder (1967) used previously published field data to develop an empirical equation to predict the rotary drilling performance, which relates the ROP to the rock strength, WOB, rotary speed and hole diameter. To validate the developed model by using field data, they conducted laboratory indenter tests to study rock failure in hard rock. Their results provide a method to describe and predict the ROP through indenter penetration and sub-surface fracturing [6].

In 1971, Bauer presented methodologies to both estimate drill requirements and optimize the drilling process and blasting costs in a given context. He discussed the rotary drill performance based on Bauer and Calder equation [7] that included recommended pull-down weight, ROP versus confined compressive strength (CCS), bit life versus rock strengths, and drilling costs [8].

Warren (1979) presented a drilling prediction model for full-scale soft-formation bits that related the WOB, rotary speed, bit size, rock strength, and bit type to the ROP based on laboratory experiments. His model was developed based on the premise that the effect of the mechanical conditions could be determined in the laboratory using full-scale drill bits and that the model could be coupled with other models that would be appropriate for the drilling fluid properties and hydraulic effects [9].

In 1991, Wijk showed that drilling rates for percussion and rotary drilling can be predicted through the use of stamp test data. Additionally, Wijk presented a power consumption prediction for rotary drilling and discussed its economics [7].

Detournay, Richard, and Shepherd (2008) presented a model to predict the drilling performance of a drag bit (i.e. showed a relationship between the WOB, torque on bit (TOB), ROP, and angular velocity). One of the outcomes highlighted in their work was the possibility of obtaining the rock's or the bit's properties from the knowledge of the existence of different phases in response to the bit of a drilling operation [10].

Shirkavand, Hareland and Aadnoy (2009), presented a theoretical correlation between the rock strength applied to both the overbalanced and underbalanced drilling conditions and predictions of the bottom hole pressure in underbalanced drilling operations with aerated or foam drilling fluid [11].

In 2014, Chen *et al.* used a new variation of the mechanical specific energy (MSE) developed from the evaluation of available MSE models. This new approach was used as a tool for

real-time monitoring, predicting, avoiding down hole accidents, reducing costs and so on. They stated that the ROP can be predicted by the new approach of the MSE [12].

In 2015, Deng *et al.* analyzed the drilling resistance in the rock breaking process and proposed a new approach to predict the ROP. In their work the energy consumption in the drilling process and the rock fragmentation fractal characteristics were studied, which was supported by laboratory experiments with roller-cone bits [13].

He, Chen, Zhengchun and Samuel (2016) investigated the relationship between five brittleness indices and the various petrophysical and geomechanical properties of rocks. In addition, they developed a correlation that relates the brittleness indices to Young modulus, P-wave velocity, and porosity. A ROP prediction approach for PDC bits was established based on gamma ray, neutron, density, and sonic log data derived from correlations in the literature [14].

3.3.2 Data-Driven Prediction Models

Bataee, Kamyab, and Ashena (2010) investigated the accuracy and the validity of various ROP predictions and applied computer optimization to yield drilling parameter recommendations for PDC and Roller-cone bits application in the Shadegan Oil Field. Furthermore, they observed that different models showed more accuracy in different moments of the drilling operation (depth, bit diameter, bit type, and type of formation) [15].

In 2012, AlArfaj, Khoukhi, and Eren compared the traditional multiple regression method with Extreme Learning Machines (ELM) and Radial Basis Function Network (RBF) to predict the ROP [16].

Bataee, Irawan, and Kamyab (2014) applied the Artificial Neural Network (ANN) model for prediction of ROP and optimization of the drilling parameters through choosing a proper model of ROP prediction among the Bourgoyne and Young model, Bingham model, and the modified Warren model [17].

In 2015, Duan, Zhao, Xiao, and Chen proposed a model to predict the ROP based on Back Propagation (BP) neural network technologies. The prediction model is built based on the known wells drilling logs to predict the ROP for the new well [18].

In 2016, Moraveji, and Naderi investigated the simultaneous effect of the well depth, WOB, rotary speed, bit jet impact force, yield point to plastic viscosity ratio, and the 10 min to 10 s gel strength ratio on the ROP using drilling field data. They used Response Surface Methodology (RSM) to determine the relationship between these six drilling parameters and the ROP. Additionally, they used the Bat Algorithm (BA) to maximize the ROP through the identification of the respective optimal range for the six drilling parameters [19].

Eskandarian, Bahrami, and Kazemi (2017) presented a procedure for predicting the ROP using a ranking technique and applying data mining algorithms to build predictive models [20].

In 2017, Hegde, Daigle, Millwater, and Gray studied the drilling performance to predict the ROP through two different approaches: physics-based and data-driven. Their approach (data-based) used the machine learning algorithms and surface measured input (WOB, revolutions per minute (rpm), and flow rate) to predict the ROP in PDC bit application [3].

In 2018, Diaz, Kim, Kang, and Shin analyzed the drilling parameters to improve the ROP prediction in the context of geothermal systems. A fast Fourier transform filter was used to smooth the fluctuation of the ROP values and two optimization methods, multiple regression and ANN, were used to evaluate the data smoothing effects. They observed that the drilling parameters' trends were influenced by many factors such as stratigraphy, formation strength, change of drilling operator, mud properties, and change of drill bit [21].

Elkatatny (2018) applied the self-adaptive differential evolution technique to optimize the ANN variable parameters that were used to predict the ROP as a relation to the WOB, TOB, stand pipe pressure, flow rate, unconfined compressive strength (UCS), drilling fluid density, plastic viscosity, and rotary speed. He concluded that the ROP is a strong relation to the WOB, rotary speed, TOB, and house power while the ROP is a moderate relation to the UCS [22].

In 2018, Mnati and Hadi presented a new approach to predict ROP using the ANN technique. They used the data set collected from five drilling operations in the Alhalfaya oil field to train and validate their artificial neural network models. Additionally, they used the proposed model to optimize the drilling costs [23].

Gan *et al.* (2019) proposed a ROP prediction hybrid model considering the process characteristics. Their model was divided into three stages: Stage I -- a wavelet filtering method is applied to reduce the noise presented in the drilling data; Stage II -- the mutual information method is used to determine the model inputs with the purpose of decreasing model redundancy; Stage III -- a hybrid bat algorithm is applied to optimize the hyper-parameters of the support vector regression model [24].

In 2019, Gan *et al.* proposed a novel two-level intelligent modelling method for the ROP prediction in complex geological drilling processes considering incomplete drilling parameters, coupling, and strong nonlinearities. A formation drillability fusion sub-model was established to categorize the influence of the drilling parameter in the ROP by using Nadaboost extreme learning machine algorithm. The ROP prediction model was established by an ANN with radial basis function optimized by the particle swarm optimization [25].

3.4 Background

In normal drilling conditions, the ROP and the WOB can usually be plotted on a characteristic curve (see Figure 3-1). From the graph, three different regions can be identified: Region A -- inadequate depth of cut is presented in the drilling operation; Region B -- the region of higher drilling efficiency where there is an approximately linear relationship between ROP and the WOB; Region C -- the region where the drilling problems such as bit balling and vibrations appear resulting in low drilling efficiency and no-linearity of the relationship between the ROP and the WOB [26]. One of the most important aspects of this graphic is the local maximum point, called the “founder point”. The founder point represents the point at which an increase in WOB no longer corresponds to an increase in ROP [4]. The founder point is not the point of maximum drilling efficiency but shows the maximum ROP possible in a specific drilling scenario. However, it is fundamental to know the complete drilling performance and subsequently to identify the maximum drilling efficiency.

Many studies focused on the ROP prediction have been published in recent years. Some of the identified prediction techniques are very consistent and robust and are currently being applied

worldwide. Among these, we can highlight a physics-based ROP prediction correlation that was developed by Maurer (1962).

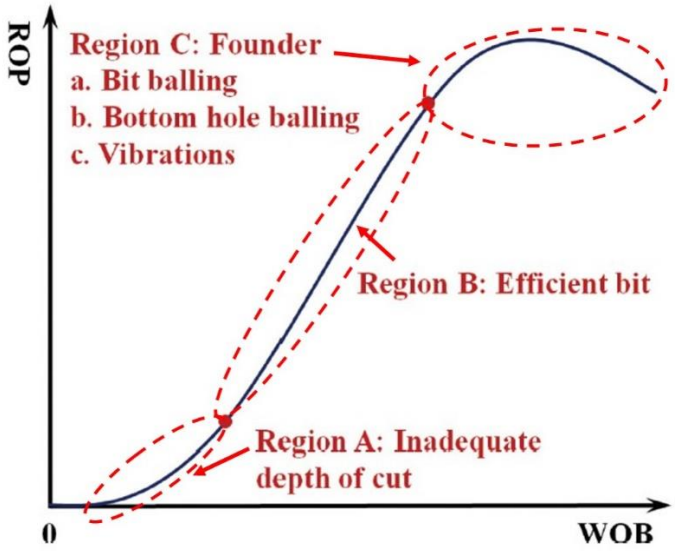

Figure 3-1 Relationship between the ROP versus WOB plot *[26]*.

3.4.1 Maurer's Correlation

Maurer (1962) presented a model to predict the drilling performance for roller-cone bits, which is derived from rock cratering mechanisms. This model is called "perfect cleaning" because it assumes that all of the rock debris is removed during the drilling operation. His work was compared with experimental data where full-scale W7R bits were applied to drill in impermeable Beekmantown dolomite rocks using water as the drilling fluid under near "perfect cleaning" conditions [5].

Equation (3-1) presents the Maurer's correlation [5].

$$R = k\left(\frac{N(W - W_0)^2}{60D^2S^2}\right) \; for \; W > W_0 \tag{3-1}$$

Where *k* is called "drillability constant", *N* is the rotary speed (rpm), *W* is the WOB (kN), W_0 is the threshold WOB before cratering is initiated (kN), *D* is the bit diameter (mm), *S* is the rock strength (MPa), and *R* is the ROP (m/h).

Due to high WOB involved in the drilling operations, normally it is assumed that $W \gg W_0$, which reduces Eqn. (3-1) to Eqn. (3-2).

$$R = k\left(\frac{NW^2}{60D^2S^2}\right) \tag{3-2}$$

3.5 Development of a New Physics-based ROP Prediction Model

The physics-based ROP prediction model presented in this paper was developed by using the results of the DOTs performed in the Drilling Technology Laboratory (DTL) localized at Memorial University of Newfoundland (MUN). These DOTs are derived from experiments which analyzed drilling performance using a coring drill bit in natural granite. This bit type was chosen due to the ease of determining the founder point location (low WOB) during the drilling experiments. Complete details about the development of this model, as well as presentation of the related DOTs, are discussed in the next sections.

3.5.1 Coring Bit – Drill-off Tests

Figure 3-1 shows a schematic diagram of a drilling simulator that was designed and manufactured by researchers at MUN. This drilling simulator, called Small Drilling Simulator (SDS), was designed to perform DOTs involving drilling operations with small diameter drill bits that required low loads and low torques.

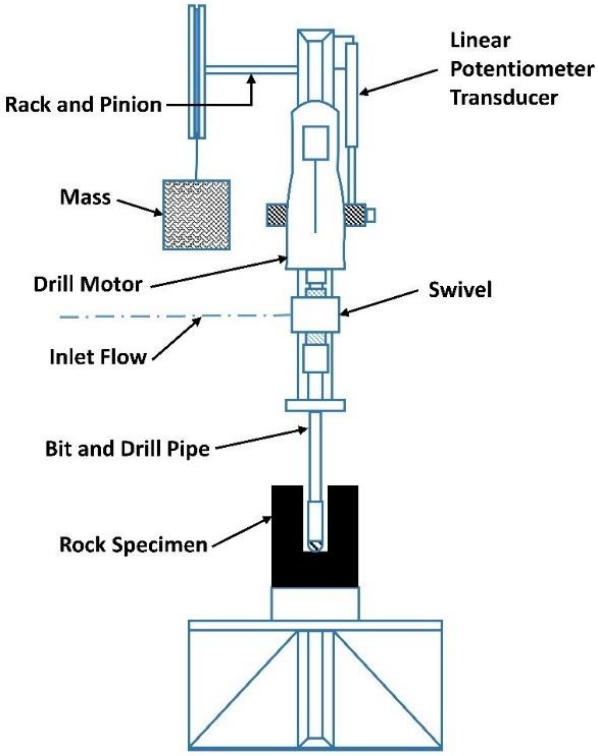

Figure 3-2 Schematic of Small Drilling Simulator (SDS) used to conduct of DOTs. Adapted from [27].

The DOTs were performed under atmospheric pressure and water as the drilling fluid. The water flows from a reservoir to the coring drill bit, passing through a hose, swivel and the drill pipe. After the drilling process has stabilized, water is collected in the cut collection system drain where the water flow is measured. The water flow rate was measured using both a graduated glass beaker of 3000 ml capacity (graduation range 250-2500 ml, graduation interval 250 ml, and accuracy ±5%) and a digital high precision stopwatch. In all phases of these experiments, the flow rate was about 35 L/m.

The power to rotate the drill string is provided by an electrical motor. A suspended mass and a rack and pinion mechanism provide the weight on the bit necessary for the drilling operation. A correlation between the suspended mass and the static WOB was established. This correlation

considers all mechanical losses of the rack and pinion mechanism. Therefore, an increase in suspended mass produces an increase in the WOB and vice versa.

SDS has a linear potentiometer transducer that is used to monitor the drilling depth. This sensor is accurate up to 1.376 mm (0.18% of the full scale). A data acquisition system records the drilling parameters necessary to analyse drilling performance.

During the DOTs, a coring drill bit with a 26.4 mm outer diameter (OD) and a 19.6 mm inner diameter (ID) was tested on natural granite rock. The natural granite rock had an average UCS of 145 MPa. The drill bit rotary speed was 300 rpm.

The penetration process of a coring bit is detailed by Xiao, Hurich, and Butt (2018). In this process, the main drilling parameters are the WOB and rotary speed [1].

Figure 3-3 shows the drilling performance curve of the DOTs. For assumption, Maurer's correlation (Eqn. (3-2)) was applied to a coring bit outer diameter ($ROP\text{-}Maurer_{OD}$), as shown in the graph. The drillability constant (k) of Maurer's correlation was calibrated in order to obtain the best fit between the real and predicted drilling performance curves.

From the graph, the founder point location can be estimated in a WOB of about 1.4 kN and a ROP of about 5.6 m/h.

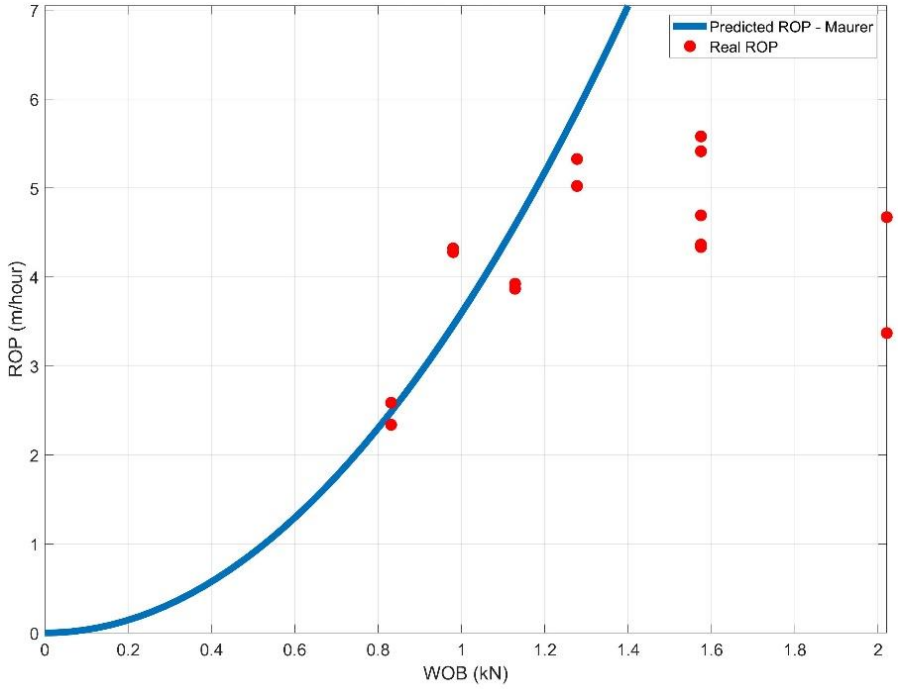

Figure 3-3 Comparison between Core drilling operation (DOT) and Maurer's correlation applied to drill bit outer (26.4mm) and inner diameter (19.6mm).

3.5.2 The New Physics-based ROP Prediction Model

To study the drilling performance, a parametric analysis of the drillability constant (k) (Maurer's correlation) was realized. Initially, by an algebraic manipulation, Eqn. (3-1) was rewritten to calculate the k at each point of the graph of Figure 3-3. Equation (3-3) shows k as a relation to the drilling parameters.

$$k = \frac{60RS^2}{N}\left(\frac{D}{W - W_0}\right)^2 \tag{3-3}$$

Figure 3-4 shows a curve that correlates the drillability constant (k) to WOB, considering DOT mentioned in the previous section. From the graph, it is possible to identify the linear dependence of k in relation to WOB. Because of its dependence on WOB, the drillability constant will henceforth be referred to as the drillability linear equation and will be indicated by the capital

letter *K* (see Eqn. (3-4)). Similarly, *a* will be called the "drillability coefficient" and *b* will be called the "drillability constant term".

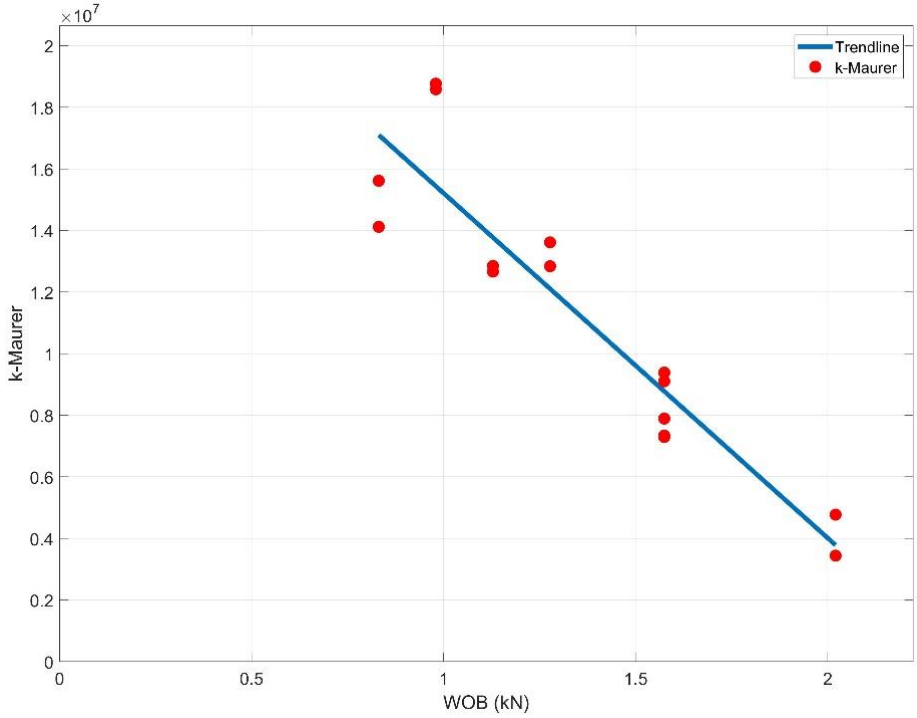

Figure 3-4 Drillability constant *k* (Eqn. (3-3)) as a relation to the WOB to core drilling operation (DOT) considering the drill bit outer diameter.

$$K = aW + b \tag{3-4}$$

From Figure 3-4, drillability coefficient (*a*) and drillability constant term (*b*) (Eqn. (3-4)) can be determined (*a = -11,197,629* and *b = 26,411,624*).

Replacing the drillability linear equation *K*, Eqn. (3-4), into Eqn. (3-1), a new ROP prediction correlation can be determined establishing a cubic dependence of the ROP in relation to the WOB. Equation (3-5) represents this new physics-based ROP prediction correlation.

$$R = (aW + b)\left[\frac{N(W - W_0)^2}{60D^2S^2}\right] \; for \; W > \; W_0 \tag{3-5}$$

Due to the high WOB involved in the drilling operations, normally it is assumed that $W \gg W_0$, which reduces the Eqn. (3-5) to Eqn. (3-6).

$$R = (aW^3 + bW^2)\left[\frac{N}{60D^2S^2}\right] \tag{3-6}$$

Figure 3-5 shows a comparison between the DOT and a curve generated by Eqn. (3-5) (ROP-JdM). From the graph, it can be seen that Eqn. (3-5) generated a highly accurate representation of the DOT, which includes the founder point location.

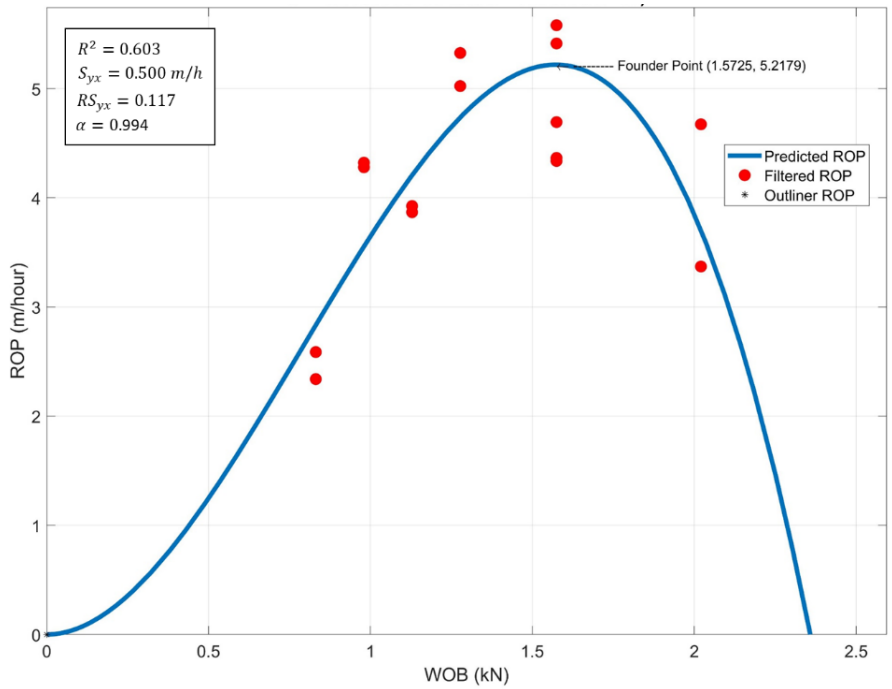

Figure 3-5 Comparison between the core drilling operation (DOT) and the curve derived of the Eqn. (3-5).

According to previous discussions, Eqn. (3-5) presents promising results to predict the drilling performance and locate the founder point. The ability of Eqn. (3-5) to locate the founder point is possible because of the cubic relation between ROP and WOB, that is a local maximum

point in this relation. The derivative of Eqn. (3-5) shows the existence of this local maximum point (Eqn. (3-7)) that is the founder point.

$$\frac{dR}{dW} = AW^2 + BW \tag{3-7}$$

Where:

$$A = \left[\frac{3aN}{60D^2S^2}\right] \tag{3-8}$$

$$B = \left[\frac{2bN}{60D^2S^2}\right] \tag{3-9}$$

The inability of the physics-based prediction models presented by Maurer (1962) [5], Bauer and Calder (1967) [6], Warren (1979) [9], Wijk (1991) [7], Shirkavand (2009) [11] and Chen *et al.* (2014) [12] to locate the point of foundation is proven through the analysis of the derivative of their respective equations, considering a parametric analysis where all drilling parameters are constant, with the exception of WOB.

3.6 Applicability and Accuracy Tests of the New Model

As a way to test the applicability and accuracy of the new physics-base ROP prediction correlation, in this section, some drilling laboratory experiments and field trial results will be compared. This data was presented by different authors in different research programs, with respective curves generated by Eqn. (3-5).

3.6.1 PDC Drill Bit Field Trial (Rana, Abugharara, Molgaard and Butt (2015) [28])

Rana, Abugharara, Molgaard and Butt (2015) presented a field trial where a PDC-bit of 152.4 mm diameter was used in a red-shale formation (UCS = 56 MPa) [28].

Similarly to the previous section, the drillability constant was plotted as a relation to the WOB by Eqn. (3-3) and verified its linear relationship with the WOB (Figure 3-6).

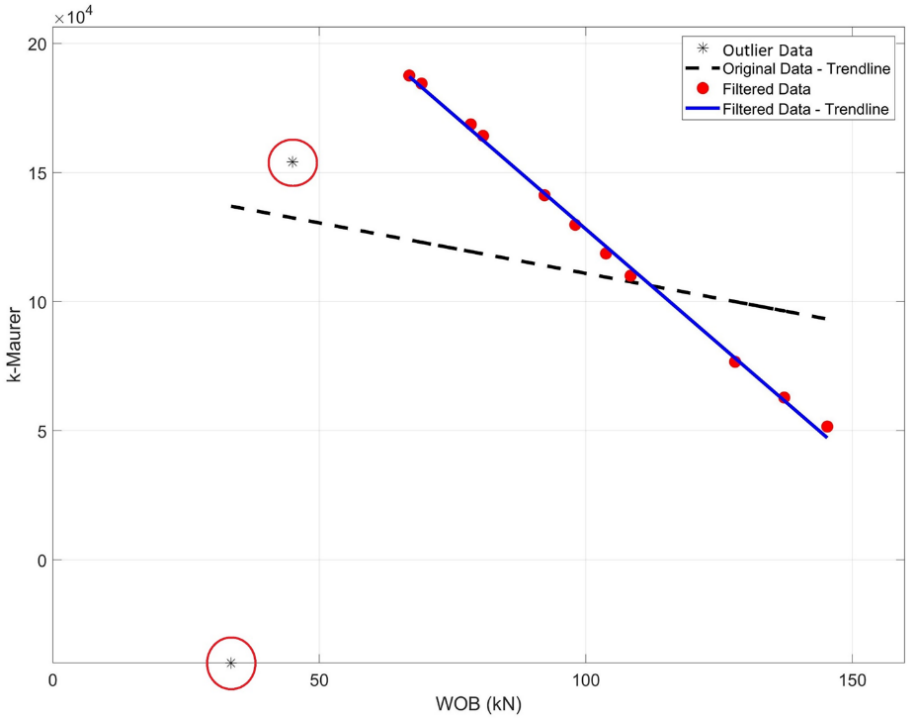

Figure 3-6 Drillability constant k as a relation to the WOB for a drilling operation with PDC-bit of 152.7 mm diameter in a red-shale formation.

The drillability coefficient *a* and drillability constant term *b* were calibrated in order to determine the drillability linear equation (Eqn. (3-4)) that best fit the graph, Figure 3-6. Specific to this data-set, the two initial data points were considered outliers and were disregarded in this analysis.

Finally, the values of *a* and *b* were inserted in Eqn. (3-5) to calculate the predicted ROP for this data-set. Figure 3-7 shows a comparison between the field trial data and the predicted drilling performance curve by Eqn. (3-5).

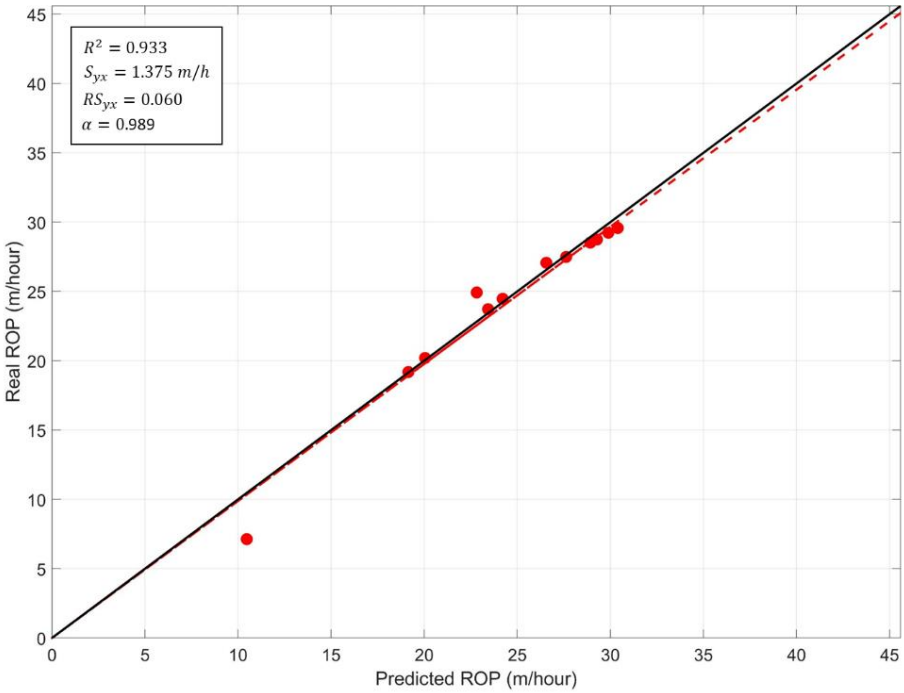

Figure 3-7 Comparison between the ROP of the drilling operation with PDC-bit of 152.7 mm diameter in a red-shale formation and the ROP predicted by Eqn. (3-5).

From the graph, we can see the high accuracy of Eqn. (3-5) in predicting the drilling performance of this field trial. In this graph, real ROP was plotted in relation to the predicted ROP. Due to the fact that the closer the dashed line to the solid line, the values predicted by Eqn. (3-5) are considered a good representation of the drilling performance curve.

To measure the accuracy of Eqn. (3-5) using Figure 3-7, four parameters were used.

The first parameter is the coefficient of determination, denoted by R^2, which is given by Eqn. (3-10). The coefficient of determination is a statistical measure that indicates how close the

data (real ROP) is to a simple linear regression model (predicted ROP), which is indicated by a solid line with slope equal to 1 (see Figure 3-7). A perfect fit is when $R^2 = 1$ [29], [30].

$$R^2 = 1 - \frac{\sum(\gamma x_i + \beta - y_i)^2}{\sum(y_i - average(y))^2} \tag{3-10}$$

The second parameter is the slope of least-squares linear fit curve with the origin fixed at (0,0), denoted by α, related to real ROP, which is indicated by a dotted line (see Figure 3-7) and is given by Eqn. (3-11) [2]. Due to that, if $\alpha > 1$ then Eqn. (3-5) underestimated the ROP values and if $\alpha < 1$ then Eqn. (3-5) overestimated the ROP values.

$$\alpha = \frac{\sum(x_i \,.\, y_i)}{\sum(x_i^2)} \tag{3-11}$$

Two alternative ways to measure of how well Eqn. (3-5) represents the drilling performance are the standard error of estimate, given by Eqn. (3-12), and the relative standard error of estimate, given by Eqn. (3-13) [30].

$$S_{y,x} = \sqrt{\frac{\sum(y_i^2) - \beta\sum(y_i) - \gamma\sum(x_i \,.\, y_i)}{n-2}} \tag{3-12}$$

$$SR_{y,x} = \frac{S_{y,x}}{\sum(x_i)} \tag{3-13}$$

In Eqn. (3-10), Eqn. (3-11), Eqn. (3-12) and Eqn. (3-13), the predicted ROP is denoted by *x*, the real ROP is denoted by *y*, and *n* is the amount of drilling data. If we consider that the perfect fit linear curve contains all points $(x_i\,, x_i)$ then $\gamma = 1$ and $\beta = 0$.

Conceptually, R^2, $S_{y,x}$, and $SR_{y,x}$ represent the dispersion of the drilling data and α shows if Eqn. (3-5) underestimates or overestimates the ROP values in a drilling performance.

For this analysis, $R^2 = 0.933$, $\alpha = 0.989$, $S_{y,x} = 1.37\ m/h$, and $RS_{y,x} = 6.05\%$ based on Figure 3-7 and Eqn. (3-10), Eqn. (3-11), Eqn. (3-12), and Eqn. (3-13).

3.6.2 Natural Diamond Bits Laboratory DOT (Winters and Warren (1983) [31])

Winters and Warren (1983) provide a detailed explanation of how the pump-off test works in the field applications and present two methods related to a drill-off test and a slack-off test, which presented accurate measurement of the resultant hydraulic lift and a diamond bit's pressure drop. Basically, they used two different bit designs, which differ only by flow geometries. Natural diamond bits of 215.9 mm diameters with radial flow, standard cross-flow, and modified cross-flow were used. Carthage Limestone rock samples (*UCS = 76 MPa*) were drilled [32].

For this analysis, the DOT that compared a modified and standard cross-flow bits were used. In this DOT, drilling fluid of 1,558 kg/m^3 with a flow rate of 68 m^3/h was used. The rotary speeds were 75 and 100 rpm being that the ROP of 75 rpm was normalized to 100 rpm.

Similar to subsection 3.6.1, the drillability constant (*k*) was calculated for each point of the DOT performed by Winters and Warren (1983).

Figure 3-8 shows a graph that relates the calculated drillability constants and their respective WOB.

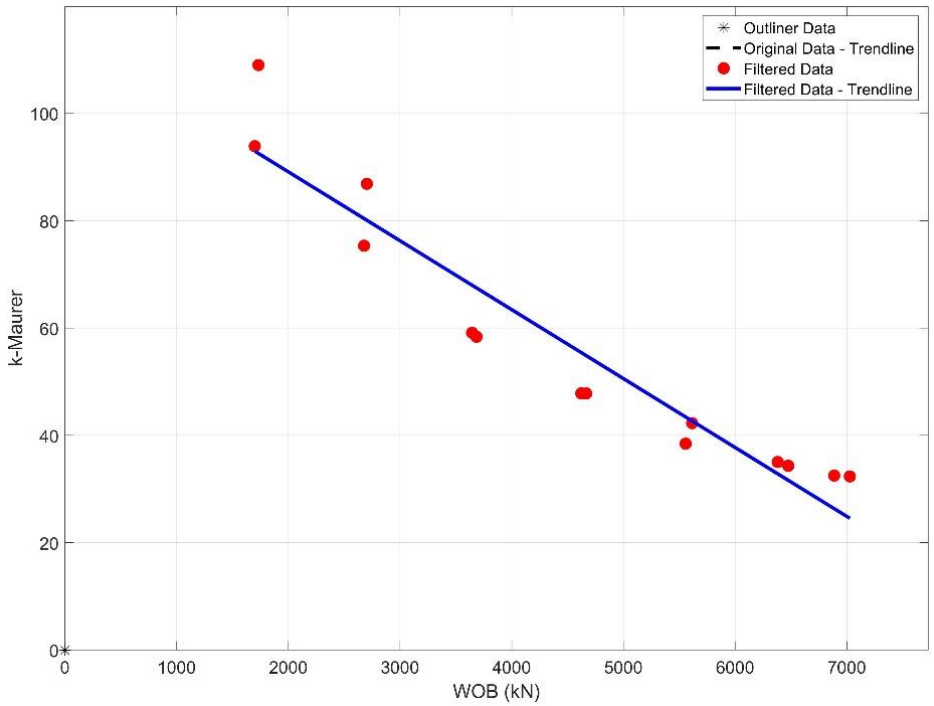

Figure 3-8 Drillability constant *k* as a relation of the WOB for a drilling operation with natural diamond bit of 215.9 mm diameter in a carthage limestone formation.

From the graph, drillability coefficient (*a*) and drillability constant term (*b*) are calibrated.

The values of *a* and *b* are inserted in Eqn. (3-5) to calculate the predicted ROP for this data-set. Figure 3-9 shows a comparison between the field trial data and the predicted drilling performance curve by Eqn. (3-5).

In Figure 3-9, we can see the high accuracy of Eqn. (3-5) for predicting the drilling performance to this laboratory DOT based on Figure 3-9 and Eqn. (3-10), Eqn. (3-11), Eqn. (3-12), and Eqn. (3-13), $R^2 = 0.8595$, $\alpha = 1.020$, $S_{y,x} = 1.47\ m/h$, and $RS_{y,x} = 23.74\%$.

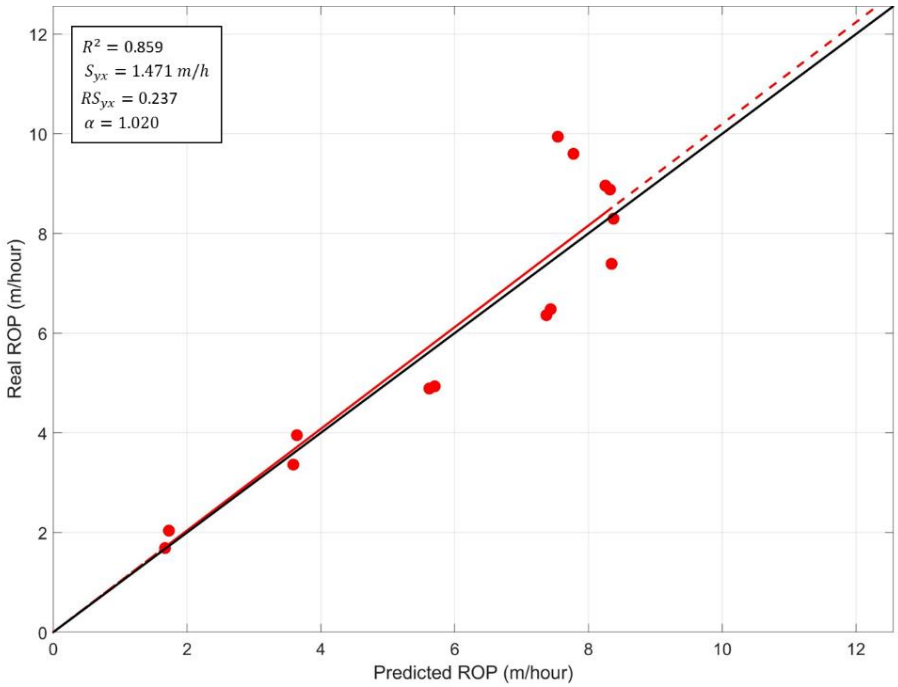

Figure 3-9 Comparison between the ROP of the drilling operation with natural diamond bit of 215.9 mm diameter in a carthage limestone formation and the ROP predicted by Eqn. (3-5).

3.6.3 Other DOTs and Field Trials

Table 3-1 summarizes 27 distinct evaluations of applicability and accuracy of Eqn. (3-5) to predict the drilling performance to fixed cutter drill bits. As previously mentioned, the accuracy of Eqn. (3-5) was measured by Eqn. (3-11) and the data dispersion by Eqns. (3-10), (3-12) and (3-13) following the same procedure mentioned in the previous subsections.

Lines 1 and 2 of Table 3-1 refer to the study presented by Winters and Warren (1983) where they provide a detailed explanation of how the pump-off test works in the field applications and present two methods related to a DOT and a slack-off test, which presented accurate measurement of the resultant hydraulic lift and a diamond bit's pressure drop. Basically, they used two different bit designs, which differ only by flow geometries. Natural diamond bits of 215.9 mm diameter with radial flow, standard cross-flow, and modified cross-flow were used. Carthage Limestone rock

samples (*UCS = 76MPa*) were drilled [32]. For this analysis, the DOT that compared a modified and standard cross-flow bits were used. In this DOT, drilling fluid of 1,558 kg/m^3 with a flow rate of 68 m^3/h was used. The rotary speeds were 75 and 100 rpm being that the ROP of 75 rpm was normalized to 100 rpm.

Table 3-1 Applicability and Accuracy Evaluation for Fixed Cutter Drill Bits

	Bit OD mm	**UCS MPa**	R^2	α	$S_{y,x}$ **m/h**	$RS_{y,x}$ **%**	**Samples**	**Ref.**
1	215.9	76	0.971	0.997	0.20	4.68	13	[31]
2	215.9	76	0.859	1.020	1.47	23.74	14	[31]
3	152.4	56	0.933	0.989	1.37	6.05	12	[28]
4	35.0	51	0.898	1.005	1.67	18.59	5	[28]
5	35.0	51	0.909	1.013	2.25	19.70	5	[28]
6	35.0	51	0.962	1.008	1.55	16.25	5	[28]
7	35.0	51	0.139	0.997	4.12	34.31	5	[28]
8	35.0	51	0.847	0.973	2.00	13.60	5	[28]
9	35.0	51	0.942	1.006	2.26	17.24	5	[28]
10	35.0	51	0.893	0.994	1.98	16.36	5	[28]
11	35.0	51	0.833	0.967	1.54	13.64	5	[28]
12	35.0	51	0.891	0.996	1.88	14.68	5	[28]
13	35.0	51	0.761	1.000	2.09	18.32	5	[28]
14	35.0	51	0.960	0.993	0.85	5.92	5	[28]
15	35.0	51	0.875	0.986	0.83	6.73	5	[28]
16	35.0	51	0.990	1.003	1.13	8.01	5	[28]
17	35.0	51	0.758	0.977	1.30	11.41	5	[28]
18	35.0	51	0.803	1.017	3.39	25.44	5	[28]
19	35.0	51	0.854	0.985	0.57	5.43	5	[28]
20	311.2	186	0.720	1.095	0.52	41.48	13	[32]
21	215.9	207	0.905	1.027	0.88	32.48	5	[33]
22	215.9	207	0.989	0.995	0.77	11.40	3	[33]
23	215.9	62	0.964	1.007	0.60	18.62	17	[34]
24	215.9	62	0.946	0.978	0.27	9.39	12	[34]
25	311.2	276	0.827	1.007	1.06	22.25	9	[35]
26	26.8	46	0.900	1.000	0.34	5.27	5	[36]
27	26.8	46	0.912	1.001	0.56	6.42	5	[36]

Lines 3 to 19 refer to DOTs and field trials conducted by Rana, Abugharara, Molgaard and Butt (2015). Their work presented a series of DOTs and a field trial in which the performance of a passive vibration assisted rotational drilling (pVARD) tool, a drilling tool that was developed to

enhance the ROP with 3 different configurations, denoted by pVARD 1, pVARD 2, and pVARD 3, in comparison with a conventional drilling operation. The conventional drilling operation did not use a pVARD tool during the drilling operation. In the field trial, a PDC-bit of 152.4 mm in diameter was used in a red-shale formation (*UCS = 56 MPa*) and in the series of DOTs, a drag bit of 35 mm was used in concrete samples (*UCS = 51 MPa*) [28].

Line 20 refers to a paper written by Brooks, Dean and Wilton (1962). In that paper, they indicated the conclusion of four years of research related to electronic drilling recording system. The bit type and flow rate are not presented in their paper [32].

Lines 21 and 22 refer to the study presented by Langeveld (1992). In that paper, he studied the PDC bit dynamics based on numerical modelling of PDC bit/drill string and torsional vibration control systems. A 50-tonne drilling machine was used to measure the reduction in ROP due to backward whirl in hard limestone rock specimens (*UCS = 207MPa*). The drilling fluid flow rate was not mentioned. The penetration per revolution was converted to ROP and normalized to 100 rpm [33].

Lines 23 and 24 refer to DOTs, which measured simulated down-hole conditions and the performance of a PDC bit over application of a PDM and turbine drilling. Black, Walker, Tibbitts, and Sandstorm (1984) performed these DOTs at a constant pressure using a standard water-based drilling fluid. A high speed hydraulic drive system, connected to the rotary table with rotary speeds, with a range of 450 to 900 rpm, was used during these DOTS. A new PDC bit of 215.9 mm diameter was used to drill four samples of Mancos shale, which present UCS of about 62 MPa. The tests

used in the applicability and accuracy of Eqn. (3-5) are referred as Test 2 and Test 3 in their paper [34].

Line 25 refers to the Roehrlich and Belohlavek (2006) research, which analyzed historical drilling data and the development of bottom hole assembly (BHA) components to ROP enhancement in an ultra-hard rock application. The tests used in this applicability and accuracy of Eqn. (3-5) refer to results from a down-hole motor runs with impregnated bits of 311.2 mm diameter. Bunter rock samples, which are a hard (UCS of about 276 MPa), and very abrasive formation, consisting of layers of quartzitic sandstone and silificated claystone, were drilled during these DOTs. The rotary speed varied between 750 and 975 rpm and the flow rate was about 3180 L/m. ROPs were normalized to 1000 rpm in this analysis [35].

Finally, Lines 26 and 27 refer to the Abtahi, Butt, Molgaard, and Arvani study, which investigated the optimization of bit wear using the vibration assisted rotary drilling (VARD) tool. The tests used in this applicability and accuracy of Eqn. (3-5) refer to results from coring bit applications with 26.8 mm OD and 19 mm ID. The rotary speed was 600 rpm and water flow rate was about 0.2 L/m in two different drilling scenarios: with drilling vibration of 48 mm and without vibration. A concrete block specimen, with a UCS of about 46 MPa, was drilled [36].

Line 1 of Table 3-1 presented the lowest standard error of estimate (between all drilling data ($S_{y,x} = 0.20$ m/h, and $RS_{y,x} = 4.68$ %)) and Eqn. (3-5) presented high accuracy to predict the drilling performance ($\alpha = 0.971$).

Considering Table 3-1, Lines 7 and 11 present the highest data dispersion and the lowest accuracy of the Eqn. (3-5) respectively.

To a specific drilling scenario, line 7 of Table 3-1, despite high dispersion of the drilling data ($R^2 = 0.139$, $S_{y,x} = 4.12$ m/h, and $RS_{y,x} = 34.31\%$), Eqn. (3-5) presented high capability to represent the drilling performance curve in this scenario ($\alpha = 0.997$). Specifically, in this experiment, Rana, Abugharara, Molgaard, and Butt (2015) performed a DOT considering a conventional drilling operation with flow rate of 100 L/m and 5 distinct WOBs (1.03, 1.36, 1.69, 2.03, and 2.35 kN) (see [28] for more details).

Figure 3-10 and Figure 3-11 show a comparison between the real ROP and the predicted ROP related to Lines 7 and 11 respectively in Table 3-1.

Eqn. (3-5) presented the lowest accuracy to predict the drilling performance ($\alpha = 0.967$) in the drilling data related to line 11 of Table 3-1. In this case, Eqn. (3-5) overestimates the ROP values but, even in this scenario, Eqn. (3-5) presents good accuracy to predict the drilling performance.

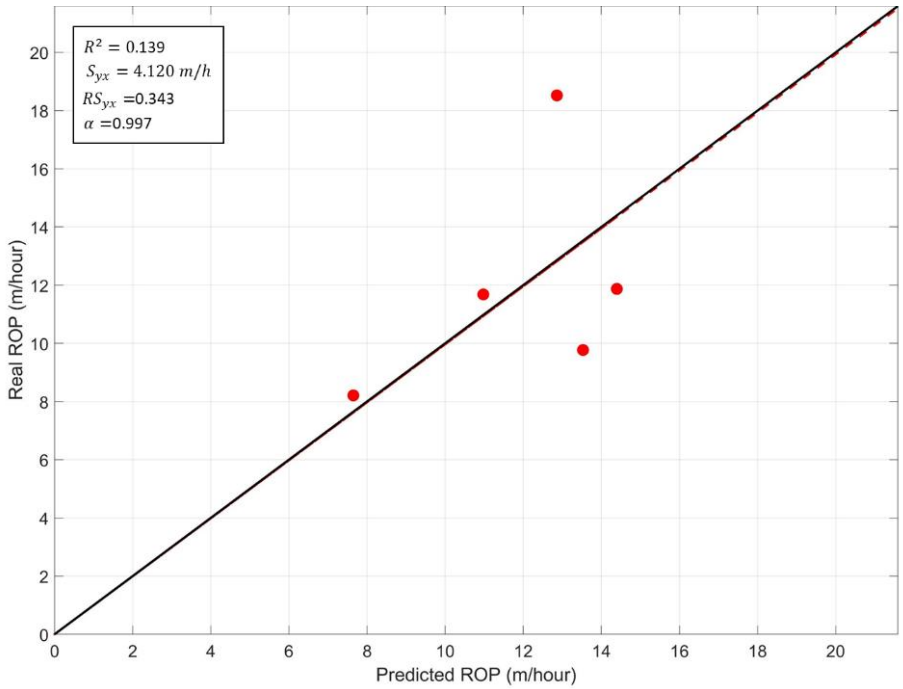

Figure 3-10 Comparison between the ROP of the drilling operation with drag bit of 35.0 mm with a concrete specimen and flow rate equal 100 L/m and with conventional configuration and the ROP predicted by Eqn. (3-5).

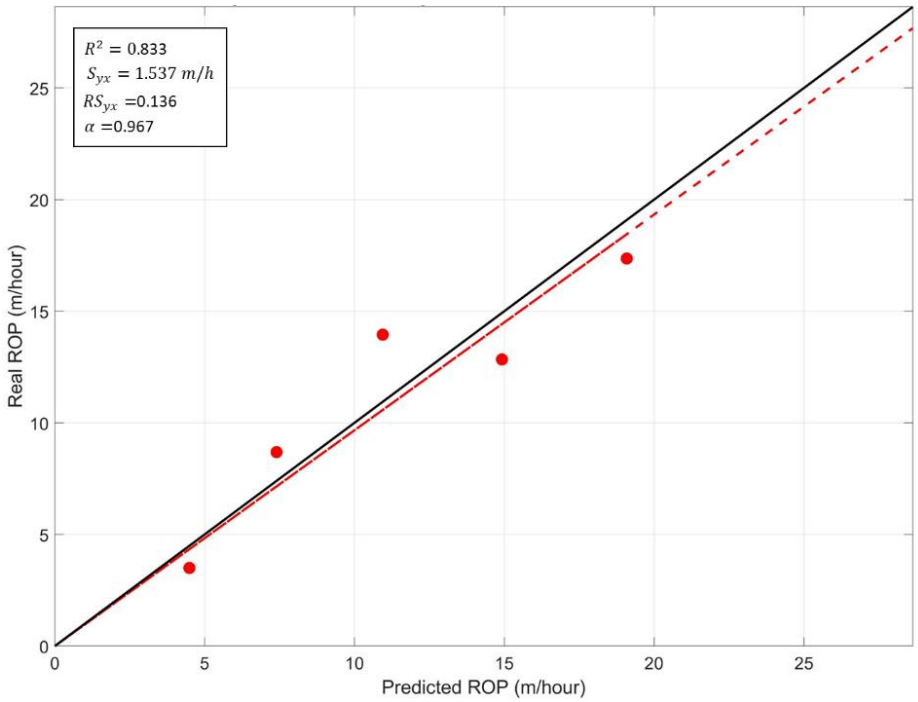

Figure 3-11 Comparison between the ROP of the drilling operation with drag bit of 35.0 mm with a concrete specimen and flow rate equal 100 L/m and with pVARD configuration 1 and the ROP predicted by Eqn. (3-5).

3.7 Conclusion

The new correlation presented in this paper is based on the linearity of the relationship between the drillabiliy constant *k* (Eqn. (3-1)) and WOB. This relationship produces a cubic dependence between the ROP and WOB.

A coring bit DOT performance in DTL and 27 other different fixed cutter drilling scenarios were analyzed as a way to test the applicability and accuracy of Eqn. (3-5) to predict the drilling performance including the founder point location. In all drilling scenarios, *k* presented an approximately linear dependence of the WOB. Due to this dependence, *k* was designated by a capital letter *K* and called the drillability linear equation, which presents two constants: *a*, called the drillability coefficient; and *b*, called the drillability constant term.

In general terms, the new correlation (Eqn. (3-5)) presented high accuracy in predicting the drilling performance of the drilling scenarios analyzed in this paper (R^2 of 0.8967, α of 1.0012, $S_{y,x}$ of 1.39 L/m, and $SR_{y,x}$ of 15.83 %). These drilling scenarios covered PDC bits, natural diamond bits, drag bits, coring bits, and impregnated bit applications in several rock types with UCS ranging from 51 to 276 MPa and bit OD diameter ranging from 26.4 to 311.2 mm. In addition to being included in these scenarios, drilling vibration conditions, modified cross-flow bits, and three different configurations of a pVARD tool.

An extension of the applicability and accuracy analysis of the new correlation, presented in this paper, is ongoing. In this extension, the new correlation will be applied to predict the drilling performance to roller-cone drilling and large diameter drilling operations such as raise-boring and

TBM operations. Additionally, it will analyze the relationship between the constants that are present in the new correlation and the drilling and rock parameters such as flow rate, bit diameter, rock strength, rock mass index, etc. Lastly, the possibility of prediction of the drillability coefficient and the drillability constant term will be analyzed based on the drilling and rock parameters, allowing the application of the new correlation without the need calibration of constant terms of Eqn. (3-5).

3.8 Acknowledgments

The authors acknowledge the technical contributions of Novamera Inc. and Memorial University of Newfoundland, developers of Sustainable Mining by Drilling (SMD) project. Without their support and funding, this paper could not have reached its goal.

3.9 References

[1] J. de Moura, Y. Xiao, D. Ahmed, J. Yang and S. D. Butt, "Widening Drilling Operation: Performance Analysis on the Application of Fixed Cutter Drill Bits in Hard Rock Formation," in *ASME 39th International Conference on Ocean, Offshore and Arctic Engineering*, Virtual Conference-online, Aug. 2020, p. 10.

[2] G. Pettit, "Case Study: Reactive Torque Failure Prevention," presented at the IADC/SPE Drilling Conference and Exhibition, Fort Worth, Texas, USA, 2018, doi: 10.2118/189660-MS.

[3] C. Hegde, H. Daigle, H. Millwater, and K. Gray, "Analysis of rate of penetration (ROP) prediction in drilling using physics-based and data-driven models," *Journal of Petroleum Science and Engineering*, vol. 159, pp. 295–306, Nov. 2017, doi: 10.1016/j.petrol.2017.09.020.

[4] H. Khorshidian, S. D. Butt, and F. Arvani, “Influence of high velocity jet on drilling performance of PDC bit under pressurized condition,” presented at the 48th US Rock Mechanics/Geomechanics Symposium, Minneapolis, MN, Jun. 2014.

[5] W. C. Maurer, “The ‘Perfect - Cleaning’ Theory of Rotary Drilling,” *Journal of Petroleum Technology*, vol. 14, no. 11, pp. 1270–1274, Nov. 1962, doi: 10.2118/408-PA.

[6] A. Bauer and P. N. Calder, “Open Pit Drilling - Factors Influencing Drilling Rates,” presented at the 4th Rock Mechanics Symposium, Ottawa, ON, 1967.

[7] G. Wijk, “Rotary Drilling Prediction,” *International Journal of Rock Mechanics and Mining Sciences & Geomechanics*, vol. 28, no. 1, pp. 35–42, 1991.

[8] A. Bauer, “Open pit drilling and blasting,” *Journal of the South African Institute of Mining and Metallurgy*, vol. 71, no. 7, pp. 115–121, 1971.

[9] T. M. Warren, “Drilling Model for Soft-Formation Bits,” *JOURNAL OF PETROLEUM TECHNOLOGY*, pp. 963–970, 1981.

[10] E. Detournay, T. Richard, and M. Shepherd, “Drilling response of drag bits: Theory and experiment,” *International Journal of Rock Mechanics and Mining Sciences*, vol. 45, no. 8, pp. 1347–1360, Dec. 2008, doi: 10.1016/j.ijrmms.2008.01.010.

[11] F. Shirkavand, G. Hareland, and B. S. Aadnoy, “Rock Mechanical Modelling for a Underbalanced Drilling Rate of Penetration Prediction,” in *43rd Rock Mechanics Symposium and 4th US-Canada Rock Mechanics Symposium*, Asheville, NC, Jun. 2009, p. 5.

[12] X. Chen, H. Fan, B. Guo, D. Gao, H. Wei, and Z. Ye, “Real-Time Prediction and Optimization of Drilling Performance Based on a New Mechanical Specific Energy Model,” *Arab J Sci Eng*, vol. 39, no. 11, pp. 8221–8231, Nov. 2014, doi: 10.1007/s13369-014-1376-0.

[13] Y. Deng *et al.*, "A New Prediction Model of Energy Consumption on Rock Fragmentation and Rate of Penetration Based on Fractal Theory," presented at the 49th US Rock Mechanics/Geomechanics Symposium, San Francisco, CA, Jun. 2015.

[14] J. He, Y. Chen, L. Zhengchun, and R. Samuel, "Global Correlation of Rock Brittleness Indices With Petrophysical and Geomechanical Properties and its Application to the Prediction of Rate of Penetration (ROP)," presented at the IADC/SPE Asia Pacific Drilling Technology Conference, Singapore, 2016, doi: 10.2118/180518-MS.

[15] M. Bataee and M. Kamyab, "Investigation of Various ROP Models and Optimization of Drilling Parameters for PDC and Roller-cone Bits in Shadegan Oil Field," p. 10.

[16] I. AlArfaj, A. Khoukhi, and T. Eren, "Application of Advanced Computational Intelligence to Rate of Penetration Prediction," in *2012 Sixth UKSim/AMSS European Symposium on Computer Modeling and Simulation*, Malta, Nov. 2012, pp. 33–38, doi: 10.1109/EMS.2012.79.

[17] M. Bataee, S. Irawan, and M. Kamyab, "Artificial Neural Network Model for Prediction of Drilling Rate of Penetration and Optimization of Parameters," *J. Jpn. Petrol. Inst.*, vol. 57, no. 2, pp. 65–70, 2014, doi: 10.1627/jpi.57.65.

[18] Jinan Duan, Jinhai Zhao, Li Xiao, Chuanshu Yang, and Huinian Chen, "A ROP prediction approach based on improved BP neural network," in *2014 IEEE 3rd International Conference on Cloud Computing and Intelligence Systems*, Shenzhen, China, Nov. 2014, pp. 668–671, doi: 10.1109/CCIS.2014.7175818.

[19] M. Keshavarz Moraveji and M. Naderi, "Drilling rate of penetration prediction and optimization using response surface methodology and bat algorithm," *Journal of Natural Gas Science and Engineering*, vol. 31, pp. 829–841, Apr. 2016, doi: 10.1016/j.jngse.2016.03.057.

[20] S. Eskandarian, P. Bahrami, and P. Kazemi, “A comprehensive data mining approach to estimate the rate of penetration: Application of neural network, rule based models and feature ranking,” *Journal of Petroleum Science and Engineering*, vol. 156, pp. 605–615, Jul. 2017, doi: 10.1016/j.petrol.2017.06.039.

[21] M. B. Diaz, K. Y. Kim, T.-H. Kang, and H.-S. Shin, “Drilling data from an enhanced geothermal project and its pre-processing for ROP forecasting improvement,” *Geothermics*, vol. 72, pp. 348–357, Mar. 2018, doi: 10.1016/j.geothermics.2017.12.007.

[22] S. Elkatatny, “Rate of Penetration Prediction Using Self-Adaptive Differential Evolution-Artificial Neural Network,” presented at the SPE Kingdom of Saudi Arabia Annual Technical Symposium and Exhibition, Dammam, Saudi Arabia, 2018, doi: 10.2118/192186-MS.

[23] K. Hmood Mnati and H. Abdul Hadi, “Prediction of penetration Rate and cost with Artificial Neural Network for Alhafaya Oil Field,” *IJCPE*, vol. 19, no. 4, pp. 21–27, Dec. 2018, doi: 10.31699/IJCPE.2018.4.3.

[24] C. Gan *et al.*, “Prediction of drilling rate of penetration (ROP) using hybrid support vector regression: A case study on the Shennongjia area, Central China,” *Journal of Petroleum Science and Engineering*, vol. 181, p. 106200, Oct. 2019, doi: 10.1016/j.petrol.2019.106200.

[25] C. Gan *et al.*, “Two-level intelligent modeling method for the rate of penetration in complex geological drilling process,” *Applied Soft Computing*, vol. 80, pp. 592–602, Jul. 2019, doi: 10.1016/j.asoc.2019.04.020.

[26] X. Chen, J. Yang, and D. Gao, “Drilling Performance Optimization Based on Mechanical Specific Energy Technologies,” in *Drilling*, A. Samsuri, Ed. InTech, 2018, pp. 133–162.

[27] Y. Xiao, C. Hurich, J. Molgaard, and S. D. Butt, “Investigation of active vibration drilling using acoustic emission and cutting size analysis,” *Journal of Rock Mechanics and*

Geotechnical Engineering, vol. 10, no. 2, pp. 390–401, Apr. 2018, doi: 10.1016/j.jrmge.2017.10.002.

[28] P. S. Rana, A. N. Abugharara, J. Molgaard, and S. D. Butt, "Experimental evaluation of passive-vibration assisted rotary drilling (p-VARD) tool to enhance drilling performance," presented at the 49th US Rock Mechanics/Geomechanics Symposium, San Francisco, CA, Jun. 2015.

[29] A. J. Wheeler and A. R. Ganji, "Correlation of Experimental Data," in *Introduction to engineering experimentation*, 2nd ed., Upper Saddle River, NJ: Prentice Hall, 2003, pp. 151–168.

[30] J. L. Devore, "Estimating Model Parameters," in *Probability and statistics for engineering and the sciences*, 6th ed., Belmont, CA: Thomson-Brooks/Cole, 2004, pp. 505–516.

[31] W. J. Winters and T. M. Warren, "Determining the True Weight-on-Bit for Diamond Bits," presented at the 58th Annual Technical Conference and Exhibition, San Francisco, California, Oct. 1983, doi: 10.2118/11950-MS.

[32] W. B. Brooks, J. T. Dean, and W. Gravley, "Mobile Electronic Recording System and Drill-off Data Illustrating Its Use," *Journal of Petroleum Technology*, vol. 15, no. 01, pp. 11–16, 1963.

[33] C. J. Langeveld, "PDC bit dynamics," presented at the SPE/IADC drilling conference, New Orleans, LO, 1992.

[34] A. D. Black, B. H. Walker, G. A. Tibbitts, and J. L. Sandstrom, "PDC Bit Performance for Rotary, Mud Motor, and Turbine Drilling Applications," *SPE Drilling Engineering*, vol. 1, no. 06, pp. 409–416, Dec. 1986, doi: 10.2118/13258-PA.

[35] M. Roehrlich and K.-U. Belohlavek, "ROP Enhancement in Ultrahard Rock," in *IADC/SPE Drilling Conference and Exhibition*, Miami, FL, Feb. 2006, p. 6.

[36] A. Abtahi, S. Butt, J. Molgaard, and F. Arvani, “Wear analysis and optimization on impregnated diamond bits in vibration assisted rotary drilling (VARD),” presented at the 45th US Rock Mechanics/Geomechanics Symposium, San Francisco, CA, Jun. 2011.

Chapter 4 An Empirical Model for the Drilling Performance Prediction for Roller-Cone Drill Bits

This Chapter is based on section 1.3.2 and was submitted to the Journal of Petroleum Science & Engineering on November 2020 and is currently under review.

Authors: Jeronimo de Moura, Yingjian Xiao, Jianming Yang, and Stephen D. Butt

4.1 Co-authorship Statement

The authors' contributions in this work are described below:

- **Jeronimo de Moura**: Identification of research topic, literature review, experiments design and performance, post processing and data analysis, and manuscript preparation.
- **Yingjian Xiao**: Technical support, rock specimen preparation, and manuscript review.
- **Jianming Yang**: Technical support and manuscript review.
- **Stephen D**. **Butt**: Experiment supervision, technical support, and manuscript review.

4.2 Abstract

The drilling process is a challenge in the oil and gas industry. These challenges are usually associated with the high costs involved in this process. Technological advances in the past few years, specifically in the drilling process, have allowed the exploitation of oil and gas fields that were uneconomical before. The economic feasibility of drilling a well is directly associated with the accuracy of the plan before the drilling starts, called “well planning”. Therefore, an accurate drilling performance prediction is crucial. Usually, the approaches to drilling performance prediction are divided into two categories: physics-based and data-driven models. Physics-based prediction models, or traditional models, are based on laboratory experiments, being empirical models designed for specific types of drilling parameters. Data-driven models are based purely on data, incorporating either machine learning or the implementation of neural networks to predict the rate of penetration. de Moura *et al.* [1] developed a new drilling performance prediction model that includes the founder point location for fixed cutter drill bit operations. This model was based on the physics-based prediction approach because it usually presents low complexities and good accuracy. Based on several drilling datasets, the applicability and accuracy of the new model for roller-cone bit operations is discussed. Based on an analysis of the drilling data-sets from drill-off tests and field operations, the linear relationship between the “drillability constant” of the Maurer model and the weight on bit (WOB) was confirmed. The results of this study show that the new model presented high accuracy to predict the drilling performance in 25 distinct scenarios that included roller-cone bits with diameters that varied between 63.50 and 444.50 mm and in different rock specimens with rock strength varying between 30 and 317.16 MPa.

4.3 Introduction

Drilling performance prediction models are divided usually into two categories: physics-based and data-driven prediction models. The physics-based models, or traditional models, use empirical correlations to model drilling performance. These models normally present constants in their equations that need to be calibrated by drill-off tests (DOTs). On the other hand, the data-driven prediction models need historical drilling data-sets to train their algorithms to predict drilling performance by either machine learning, neural networks, or both [2].

In 1962, Maurer developed one of the most famous models used globally for drilling performance prediction. He introduced an empirical correlation to predict the rate of penetration (ROP) for roller-cone bits. His work, called “perfect cleaning”, was based on rock cratering mechanisms and assumed that cuttings are totally removed during the drilling process. Drilling experiments with full-scale W7R bits in impermeable Beekmantown dolomite rocks using water as a drilling fluid, were used to analyse the accuracy of the Maurer’s correlation [3].

The new empirical drilling performance prediction model, which is presented in this paper, explores a linear relationship that was identified during the DOTs with tricone bits in hard rock, between the drillability constant (Maurer model) and WOB. The reach of the new correlation covers the drilling performance modelling and the location of the founder point. The applicability and accuracy of this correlation is tested through a comparative analysis between prediction curves and real drilling data-sets.

For decades, many researchers studied drilling performance and developed drilling performance prediction models.

In 1987, Bourdon *et al.* described the progress of the development and implementation of a system for the acquisition of rig-site DOT data as well as the laboratory simulation of DOTs. In their work, more than 50 DOTs performed in onshore vertical wells and deviated wells (up to 40º) and different lithology types were analyzed. Roller-cone bits of 215.9 mm and 152.4 mm diameter were applied in these DOTs. In the laboratory DOTs, roller-cone bits of 215.9 mm were used in several rock types, including Carrara marble, Bolton Wood sandstone, Portland limestone, and a limestone aggregate concrete. They highlighted the importance of good sensors and data logging in collecting valuable information for the evaluation of drilling performance. They did not observe significant transient effects in the ROP response during either field or laboratory DOTs [4].

In 2001, Robinson and Ramsey described a rig-site procedure, with little or no wasted rig time that determined the founder point of roller-cone drill bits. A new equation to calculate the founder point was introduced. Their studies' outcomes were compared with field examples [5].

In 2010, Bataee *et al.* studied the validity of some ROP prediction models for the roller-cone and PDC bits such as the Bourgoyne and Young model, Bingham model and modified Warren model. This study covers a comparative analysis between these ROP prediction models and field data. Based on computer optimization, this study proposes to predict the ROP, optimizing the drilling parameters and, consequently, decreasing the drilling cost for future drilling operations [6].

In 2012, Kowakwi *et al.* developed a ROP prediction model that is a normalized hydraulic model with a two-term roller-cone bit that considers the available hydraulic level at a drill bit. This model is based on Warren two-term model. Their model was compared with a field dataset which showed good accuracy to predict the drilling rate. They also presented a model to predict the unconfined compressive strength (UCS) of a formation based on the drilling parameter [7].

In 2012, AlArfaj *et al.* performed a comparison analysis between the traditional multiple regression method with Extreme Learning Machines (ELM) and Radial Basis Function Network (RBF) when applied to ROP prediction. This study is a complement of previous works that added one new drilling data set to the analysis, a comparative analysis with three prediction methods and an evaluation of the difference between the real and predicted ROP [8].

In 2015, Deng *et al.* analyzed the drilling resistance in the rock breaking process and proposed a new approach to predict the ROP. In their work the energy consumption in the drilling process and the rock fragmentation fractal characteristic were studied and supported by laboratory experiments with roller-cone bits. They used rock cutting distribution size, energy dissipation analysis, and fractal dimensions to propose a new prediction model for the energy consumption on the rock fragmentation process. One of the results of their study was a prediction equation of the ROP based on the principle of energy conservation and the fractal energy consumption model. Based on the analysis of the field data, an average error below 15% on the ROP prediction was estimated [9].

In 2016, Deng *et al.* presented a ROP prediction model for roller-cone bits that considered the combined effect of the main drilling parameters and the rock dynamic compressive strength.

Their model is based on the rock fragmentation mechanism of a single indenter. They applied the rock dynamic compressive strength to reflect the real process of rock dynamic crushing by a roller-cone bit during the drilling process. They conducted a laboratory drilling experiment on sandstone and limestone rock samples with a full-scale bit to validate their ROP prediction model as well as compare their model with the other available models based on rock static compressive strength. They affirmed that the ROP prediction models based on rock static compressive strength presented an error between 45 % and 50 % and their model presented an average error of about 15 % during their drilling laboratory experiments [10].

In 2018, Diaz *et al.* explored the relations between the drilling parameters to improve the ROP prediction accuracy. This study was based on a drilling data-set from a geothermal project that drilled a well with a 4.2 km depth. Their approach applied traditional multiple regression and Artificial Neural Network [11].

In 2019, Gan *et al.* presented a two-level intelligent model to predict the ROP. This model is based on the drilling characteristics of data incompleteness, couplings and strong nonlinearities. The drilling data set is completed by applying a piecewise cubic hermit interpolation method. The two-level ROP model is composed of a formation drillability fusion sub-model and a ROP sub-model based on Nadaboost ELM algorithm and a neural network with radial basis function, respectively. This model was developed to control and optimize complex geological drilling processes [12].

In 2020, de Moura *et al.* developed a new drilling performance prediction model that includes the founder point location for fixed cutter drill bit operations. This new model is based on

the Maurer model exploring the linear relationship between the "drillability constant" of the Maurer model and the WOB. Due to this, the new model shows the existence of a cubic dependence between the ROP and WOB and introduces two constants called the "drillability coefficient" and "drillability constant term". This study showed the high accuracy of this new model to predict the drilling performance for fixed cutter drill bit and its capability to determine the founder point location [1].

Normally, all models are developed based on a specific drilling scenario. Their accuracy is affected when they are applied in a different drilling scenario than the one they were developed on. For instance, a prediction model developed to fixed cutter drill bits, will not accurately predict the drilling performance in a scenario with roller-cone bits and vice versa, because the rock fragmentation mechanism is different for these two type of drill bits (see Figure 4-1).

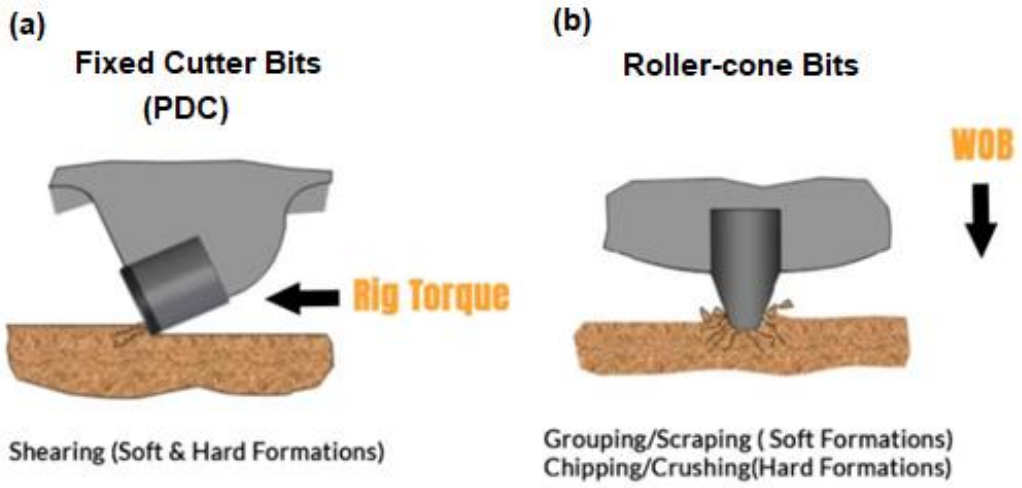

Figure 4-1 Rock fragmentation mechanism: (a) Fixed Cutter Bits Polycrystalline Diamond Compact (PDC); (b) Roller-cone Bits. Adapted from [13].

The drilling action of roller-cone bits on a soft formation requires a gouging-scraping process, while on a hard formation requires a chipping-crushing process. In both cases, the

processes depend on rolling and sliding movements of the cones. A considerable amount of sliding is required to maximize the gouging-scraping process and the chipping-crushing process requires the cones to roll with a very low slip. In fixed cutter drill bits, the fail of the rock is through a grinding process where the dragging and scraping action is present [14].

According to mentioned above, an evaluation of the applicability and accuracy of the new drilling performance model proposed by de Moura *et al.* [1] for roller-cone bit is extremely relevant due to the clear difference between the rock fragmentation mechanisms for fixed cutter drill bits and roller-cone bits. This evaluation will be detailed in the following sections.

4.4 Methodology

This study proposes to evaluate the applicability and accuracy of the new drilling performance model proposed by de Moura *et al.* [1] for roller-cone bits including the founder point location. This development is based on a quantitative analysis of drilling performance data produced by laboratory experiments and available in literature. Laboratory experiments were performed in the Drilling Technology Laboratory (DTL) located at Memorial University of Newfoundland, St. John's, Newfoundland and Labrador, Canada. A large-scale laboratory drilling rig, called Large Drilling Simulator (LDS), is the main equipment used in these experiments. In relation to the data available in the literature, this study identified research that makes available data-sets that will permit a critical analysis of the drilling performance, contemplating data such as WOB, ROP, bit type, bit diameter, rock strength, and rotary speed.

The proposed drilling performance prediction model is based on Maurer's correlation. The decision to use such an approach is in line with the low complexity and good accuracy normally

presented by Maurer's correlation in several drilling scenarios and, mainly, in the supposed linear relationship between the "drillability constant" and WOB [1].

4.4.1 Experimental Methods

Figure 4-2 (a) shows a 3D presentation of the LDS and Figure 4-2 (b) shows its simplified schematics (depicted in mid-stroke). The LDS requirements were based on the real drilling operating conditions. The systems were designed to operate with several types of drill bits being composed of three main units and subsystems able to simulate different drilling scenarios. The three main units are: the rotary system composed of a high torque motor; the WOB system composed of two pneumatic cylinders, a hydraulic servo-actuator, a load cell, accelerometers, and magnetostrictive displacement transducers; and the drill cell and mud circulation system composed of a high pressure drill cell and a high pressure positive displacement pump [15]. The LDS is used to perform DOTs, where are drilled specimens under atmospheric pressure or high pressure. In the experiments with specimens under high pressure, a drill cell is used. The drilling fluid flows to the LDS under hydraulic pressure or pumped by a positive displacement pump. The LDS is totally automatized and has sensors that monitor the WOB, torque on bit (TOB), rotary speed, drilling depth, and flow rate.

Figure 4-3 shows the tricone roller insert bit used during the DOTs that were the basis of this study. Table 4-1 shows the technical specification of this drill bit.

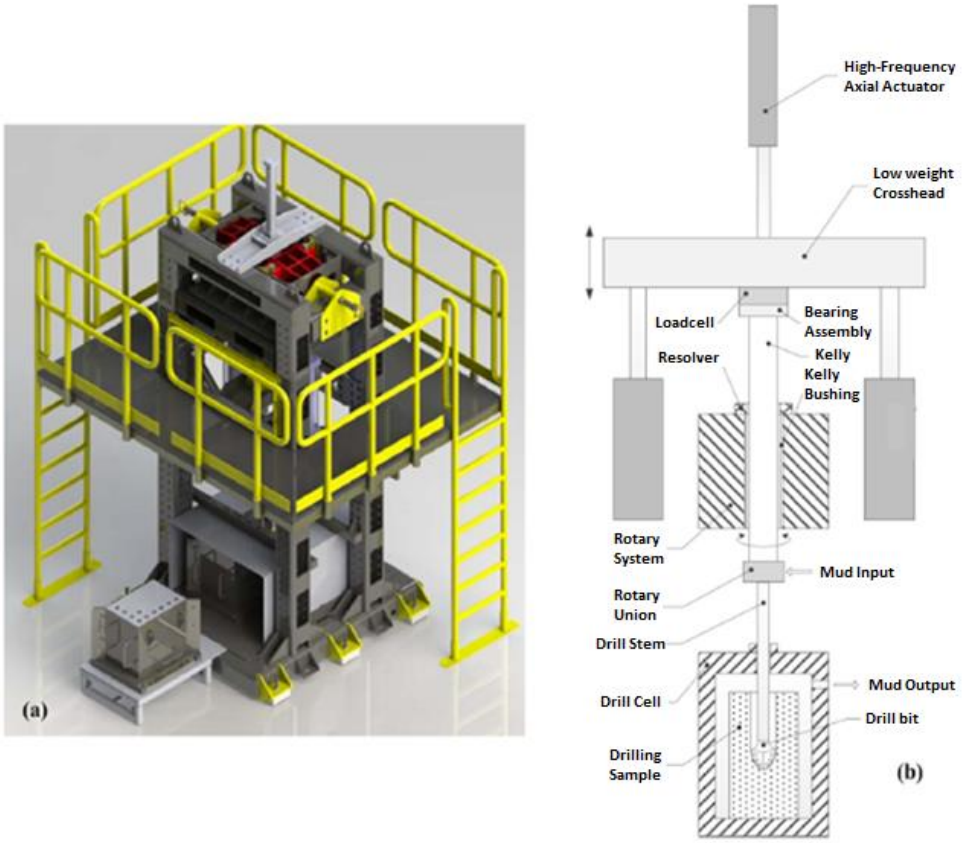

Figure 4-2 Laboratory Drill Simulator: (a) 3D Presentation; (b) Simplified Schematics (depicted in mid-stroke) [15].

Figure 4-3 Tricone roller insert bit designed to drill into very hard formations.

Table 4-1 Tricone roller insert bit technical specification.

Bit diameter	63.5 mm
Bit Type	Tricone
Cutter	Tungsten Carbide Insert (TCI)
Cone retention	Ball Bearing
Bearing	Open
Circulation	Regular-Fluid
Connection	N-4 Rod Pin
IADC code	631

Considering the International Association of Drilling Contractors (IADC) code, this tricone bit is classified as an insert-type bit applied to hard rock formations such as limestone, hard sandstone, dolomite, and anhydrite that have high compressive strength and contain abrasive materials. Additionally, considering its bearing design, this drill bit has non-sealed roller bearings (open-bearing) [14].

During the DOTs, the WOB varied between 3 and 18 kN which were performed with tap water as the drilling fluid in atmospheric pressure. The water flow rate was approximately 35 L/m and the rotary speed was approximately 35 rpm. Natural granite rock specimens were used during these DOTs.

Table 4-2 shows the natural granite rock properties that was used during the DOTs.

Table 4-2 UCS and Young Modulus of the Granite Specimen.

Sample #	UCS MPa	Young Modulus GPa
1	161.0	15.6
2	175.0	11.5
3	173.3	12.0
5	176.7	11.2
8	171.6	17.4
9	157.6	12.8
10	163.6	12.7
Average	168.4	13.3
Standard Deviation	7.0	2.1
Repeatability Limit	19.8	5.9

The repeatability limit can be determined by Eqn. (4-1) [16]. Table 4-2 shows that all values, comparing two-by-two, does not differ more than the repeatability (r). In this case, the values presented in Table 4-2 are good representations of the tested specimen properties, because the difference between the maximum and the minimum values of UCS (176.7 MPa – 157.6 MPa = 19.1 MPa) is less than the repeatability limit (19.8 MPa) [16].

$$r = 2(\sqrt{2})s_r \quad (4\text{-}1)$$

Where: r is the repeatability limit, and s_r is the repeatability standard deviation.

Figure 4-4 shows an example of specimen of natural granite rock that is quite homogeneous and isotropic, used during the DOTs.

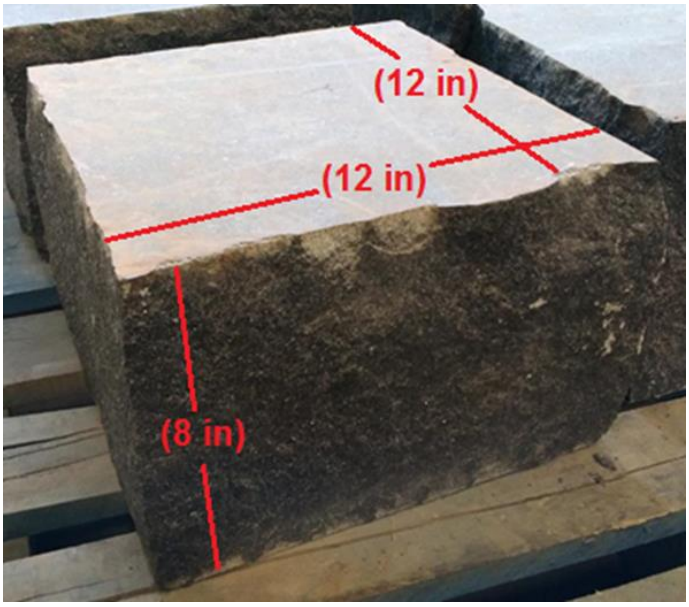

Figure 4-4 Natural granite block specimen.

4.5 Drill-Off Test Results and Discussions

Figure 4-5 shows the drilling performance curve obtained during a DOT with a tricone bit of 63.5 mm diameter in a natural granite block specimen. The DOT was detailed in the previous section. The graph shows three distinct regions: Region A – inadequate depth of cut; Region B – higher drilling efficiency where an increase in WOB results in an increase in ROP (the relation is approximately linear); Region C – drilling problems such as vibrations and bit balling start to happen during the DOT [17]. The local maximum point of a representative curve in Figure 4-5 is called the founder point. Its location can be estimated in a WOB of 14 kN and a ROP of 0.6 m/h.

Next, the methodology used by de Moura *et al.* (2020) for the development of their model will be presented, applying to roller-cone drill bits.

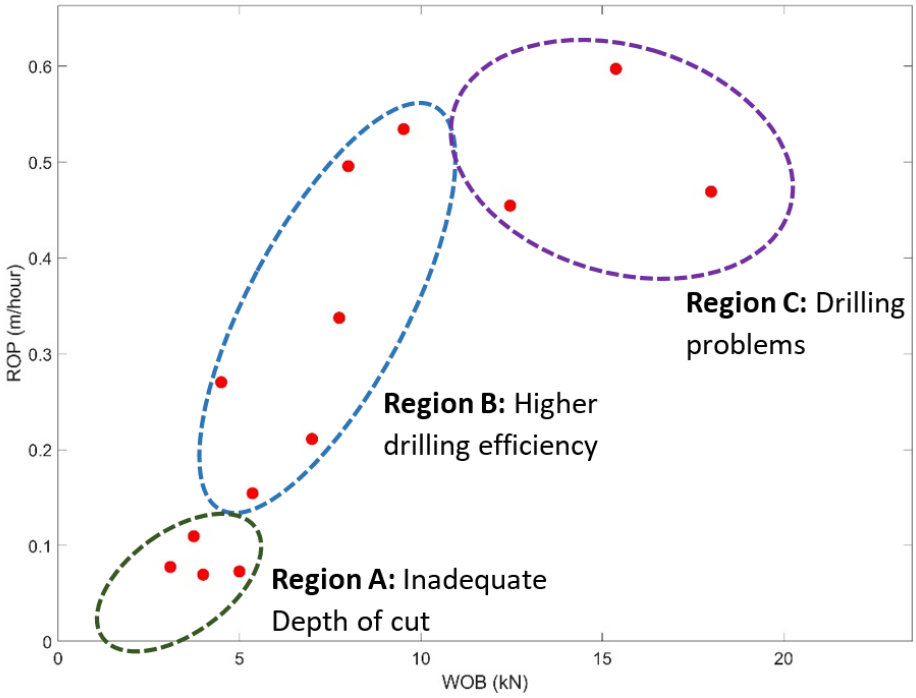

Figure 4-5 DOT for a drilling operation with a tricone bit of 2 ½ inches diameter in a granite rock specimen.

Maurer affirmed that the ROP is directly proportional to the ratio between rotary speed times the square of the difference between the WOB and threshold WOB before cratering is initiated, and the square of the drill bit diameter times the square of the rock strength (Eqn. (4-2)) [3]. The proportionality constant of this rate is called the drillability constant (k), which is shown in Eqn. (4-3). In real drilling operations normally $W \gg W_0$ resulting in Eqn. (4-4).

$$R \propto \frac{N(W - W_0)^2}{60D^2S^2} \; for \; W > W_0 \tag{4-2}$$

$$R = k\left(\frac{N(W - W_0)^2}{60D^2S^2}\right) for \; W > W_0 \tag{4-3}$$

$$R = k\left(\frac{NW^2}{60D^2S^2}\right) \tag{4-4}$$

Figure 4-6 shows a comparison between the DOT, mentioned before, and Maurer model (Eqn. (4-4)) considering a drillability constant value of 1,000,0000. The drillability constant value was estimated in order to obtain a better fit between the DOT and the Maurer model.

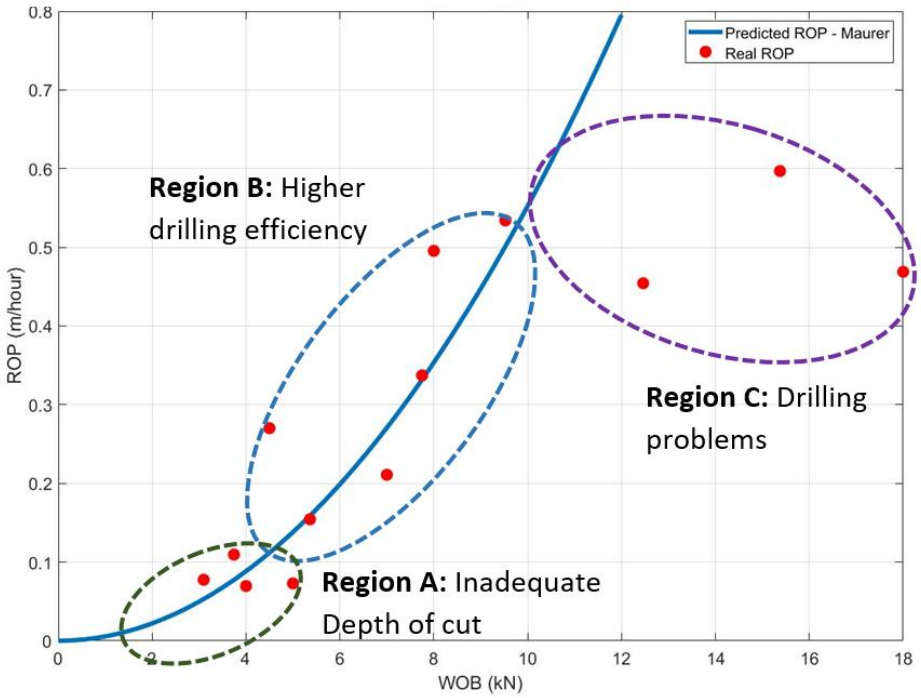

Figure 4-6 Comparison between the DOT, for a drilling operation with a tricone bit of 2 ½ inches diameter in a granite rock specimen, and Maurer model.

The limitation in Eqn. (4-4) to model the whole drilling performance is clearly shown in Figure 4-6, where just regions A and B of the graph are covered by Maurer model. This behavior of Eqn. (4-4) is due to the quadratic relation between the WOB and ROP. As the founder point was defined as the local maximum of a curve that represents the drilling performance, the derivative of Eqn. (4-4) will prove the inability of Maurer model to predict its location.

Equation (4-5) shows the derivative of Eqn. (4-4). The founder point location will be determined when Eqn. (4-5) is zero, but that is impossible because the drillability constant and the rotary speed have values bigger than zero. In other words, the founder point is not a point of the

Maurer model. This behavior is present in the vast majority of physics-based drilling performance prediction models.

$$\frac{dR}{dW} = \left(\frac{kN}{30D^2S^2}\right)W \;\; with \;\; \left(\frac{kN}{30D^2S^2}\right) > 0 \qquad (4\text{-}5)$$

For the purpose of understanding the Maurer's correlation's limitation to predict the whole drilling performance including the founder point location, the drillability constant was analyzed based on its dependency to the drilling parameters. Based on Eqn. (4-3), Eqn. (4-6) describes this dependency [1].

$$k = \frac{60RS^2}{N}\left(\frac{D}{W - W_0}\right)^2 \qquad (4\text{-}6)$$

Figure 4-7 shows the drillability constant value (Eqn. (4-6)) calculated for each data-set point of the DOT. The graph describes a relation approximately linear between the drillability constants and WOB. Thus, Eqn. (4-7) shows the linear relation between the "drillability constant", henceforth called the drillability linear equation and indicated by the capital letter *K*, and the WOB. Eqn. (4-7) presents two constants, *a* and *b*, called the drillability coefficient and the drillability constant term, respectively [1].

Specifically for Figure 4-7, the drillability coefficient and the drillability constant term presented values of approximately –75,051 and 1,606,451, respectively.

The de Moura *et al.*'s new drilling performance prediction model is presented by Eqns (4-8) and (4-9) based on Eqns (4-3), (4-4), and (4-7).

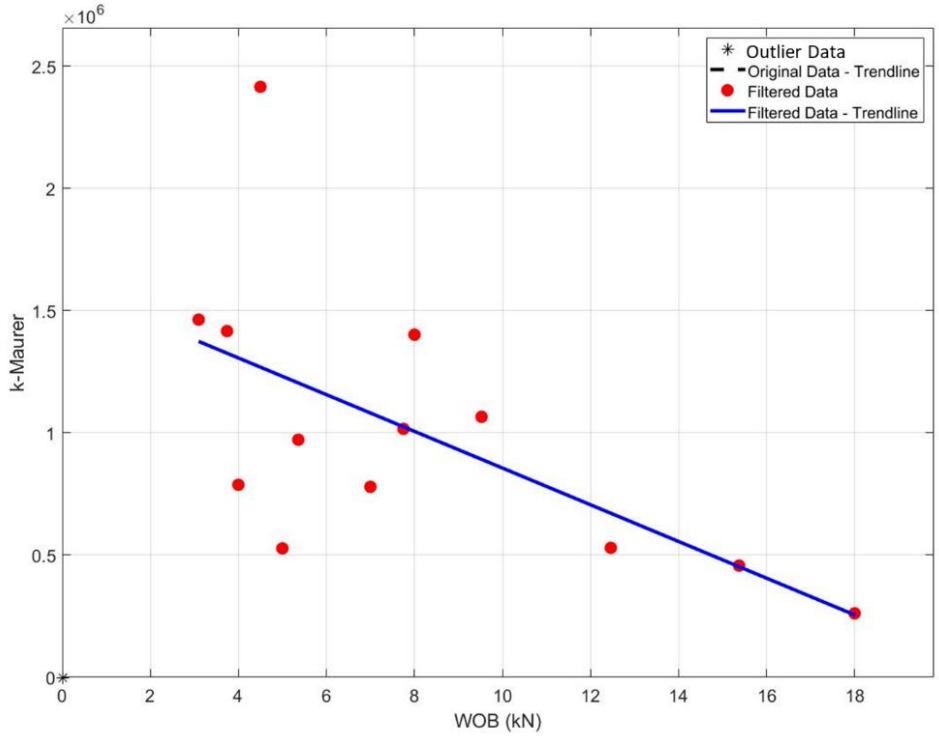

Figure 4-7 Drillability constant (Eqn. (4-6)) as a relation to the WOB for a drilling operation (DOT) with a tricone bit of 2 ½ inches diameter in a granite rock specimen.

$$K = aW + b \tag{4-7}$$

$$R = (aW + b)\left(\frac{N(W - W_0)^2}{60D^2S^2}\right) for\ W > W_0 \tag{4-8}$$

$$R = \left(\frac{N}{60D^2S^2}\right)(aW^3 + bW^2) \tag{4-9}$$

The WOB correspondent to the founder point in the new model can be determined doing the derivative of Eqn. (4-9) equal to zero. Eqn. (4-10) shows the derivative of Eqn. (4-9) and Eqns. (4-11) and (4-12) show the WOB's and the ROP's correspondence to the founder point location.

$$\frac{dR}{dW} = \left(\frac{N}{60D^2S^2}\right)(3aW^2 + 2bW) \tag{4-10}$$

$$W_{fp} = -\frac{2b}{3a} \tag{4-11}$$

$$R_{fp} = \left(\frac{N}{60D^2S^2}\right)\left(\frac{4b^3}{27a^2}\right) \tag{4-12}$$

Figure 4-8 shows a comparison between the DOT data-set and the new model (Eqn. (4-9)) as well as the founder point location based on Eqns. (4-11) and (4-12). The graph shows that the new model has high accuracy to predict the drilling performance and locates the founder point of this DOT.

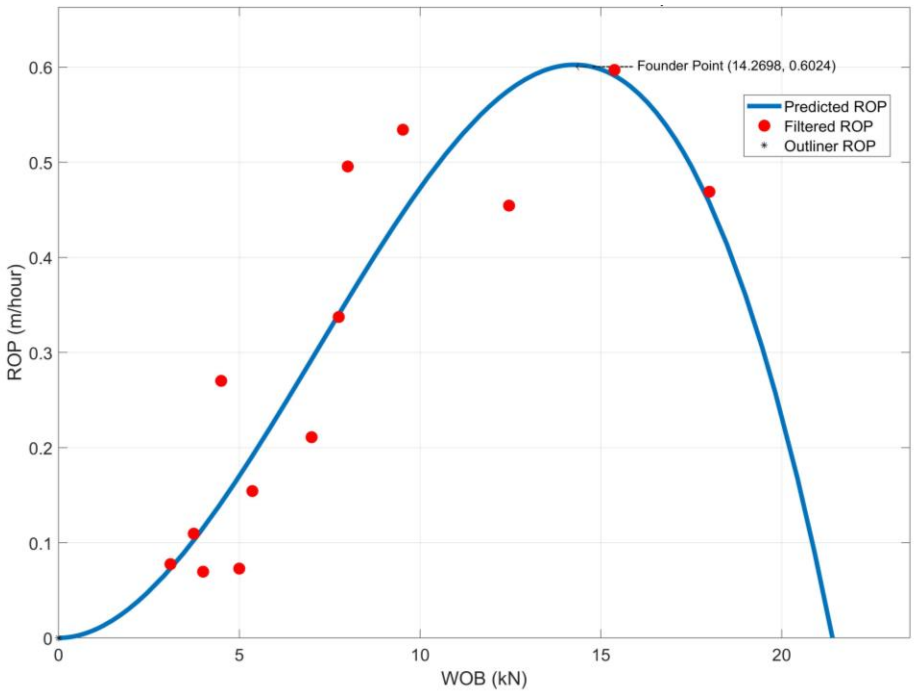

Figure 4-8 Comparison between a drilling operation (DOT) with a tricone bit of 2 ½ inches diameter in a granite rock specimen and the curve derived from Eqn. (4-9).

The coefficient of determination, denoted by R^2, the slope of least-squares linear fit curve with the origin fixed at (0,0), denoted by α, the standard error of estimate, denoted by $S_{(y,x)}$, and the relative standard error of estimate, denoted by $SR_{(y,x)}$, were used to measure the accuracy of the new model.

The coefficient of determination, Eqn. (4-13), is a way to indicate how close the real ROP data-set is to the predicted ROP, being a perfect fit is when $R^2 = 1$ [18], [19].

$$R^2 = 1 - \frac{\sum(\gamma x_i + \beta - y_i)^2}{\sum(y_i - average(y))^2} \tag{4-13}$$

Equation (4-14) shows the slope of least-squares linear fit curve with the origin fixed at (0,0) that is related to the real ROP data-set. When the Eqn. (4-9) underestimates the ROP values, $\alpha > 1$ and when the Eqn. (4-9) overestimate the ROP values, $\alpha < 1$ [19].

$$\alpha = \frac{\sum(x_i y_i)}{\sum(x_i^2)} \tag{4-14}$$

Equations (4-15) and (4-16) shows the standard error of the estimate and the relative standard error of the estimate, respectively [19].

$$S_{y,x} = \sqrt{\frac{\sum(y_i^2) - \beta\sum(y_i) - \gamma\sum(x_i y_i)}{n-2}} \tag{4-15}$$

$$SR_{y,x} = \frac{S_{y,x}}{\sum(x_i)} \tag{4-16}$$

In Eqns (4-13), (4-14), (4-15), and (4-16), the real ROP is denoted by *y*, the predicted ROP is denoted by *x*, and *n* is the amount of drilling data-set points. To Eqn. (4-15), $\gamma = 1$ and $\beta = 0$ demonstrates that the perfect fit linear curve contains all points of the drilling data-set. Eqns (4-13), (4-15), and (4-16) represent the dispersion of the drilling data-set and Eqn. (4-14) represents the accuracy of Eqn. (4-9) to predict the drilling performance.

Figure 4-9 shows a comparison between the real drilling data-set and the predicted drilling performance by Eqn. (4-9). The real drilling data-set was plotted in relation to predicted drilling performance. The closer the bubble points to the dashed line, the more accurate the predicted ROP. In Figure 4-9, $R^2 = 1$ is indicated by a solid line with a slope equal to 1.

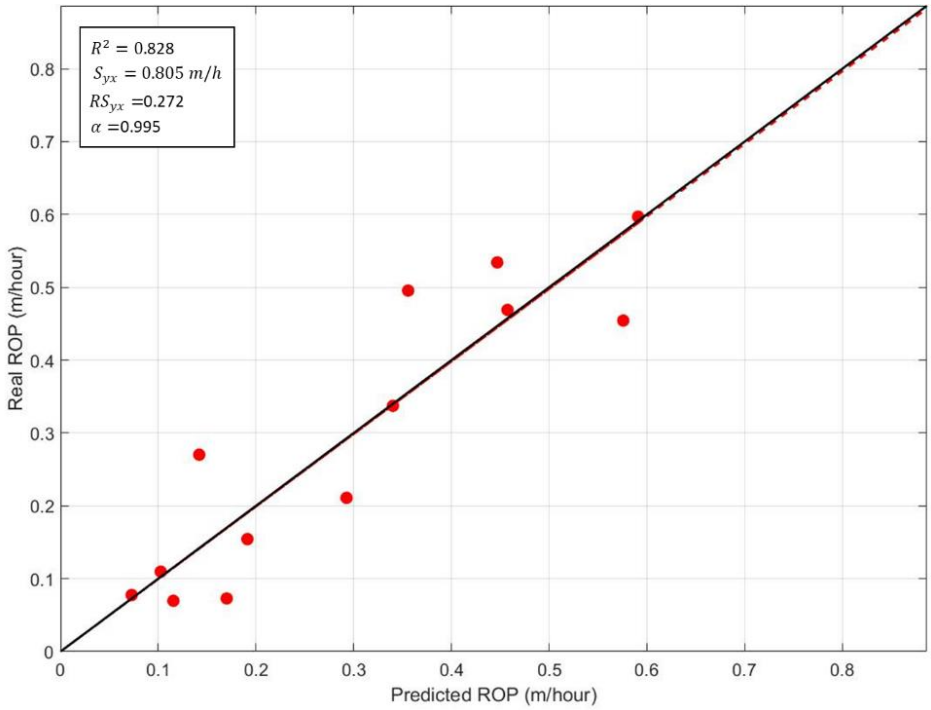

Figure 4-9 Comparison between the ROP of the DOT with a tricone bit of 2 ½ inches diameter in a granite rock specimen and the ROP predicted by Eqn. (4-9).

For this analysis, $R^2 = 0.8283$, $S_{y,x} = 0.08$ m/h, $RS_{y,x} = 27.17\ \%$, and $\alpha = 0.9955$ based on Figure 4-9 and Eqns (4-13), (4-14), (4-15), and (4-16).

4.6 Comprehensiveness Evaluation of the New Model

As a way to test the comprehensiveness of the de Moura et al.'s model for tricone drill bits, some field tests and DOT results will be analyzed in this section. These drilling data-sets come from different research available in the literature. The analysis carried out in this section will follow a process similar to that of the previous section.

4.6.1 Tricone Insert Drill Bit Field Drilling Test Performed in Compacted Shale

In 1996, Fear presented a method to identify which drilling parameters influence the ROP in a particular group of drill bits. This method is used to maximize the ROP in drilling operations. In this study, Fear analyzed, among others, the drilling performance of a 444.5 mm diameter tricone insert drill bit in compacted shale that used water based mud as drilling fluid [20].

Figure 4-10 shows a representative curve of the field drilling test mentioned above. From the graph, the drilling data point related to the highest WOB presents an anomalous behavior because in the previous data points, an increment of the WOB does not result in an increment of the ROP.

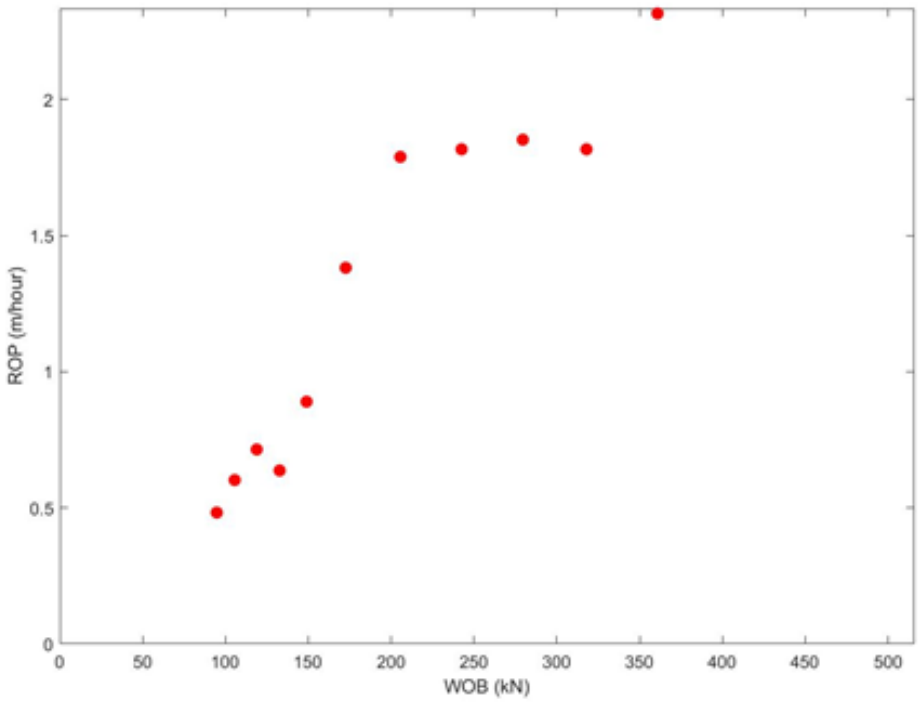

Figure 4-10 Representative curve of a field drilling test performed in compacted shale with a tricone bit of 444.5 mm diameter.

Considering all drilling data-sets including the anomalous data point, the "drillability constant", as a relation to the WOB based on Eqn. (4-6), was plotted (Figure 4-11). From the graph and Eqn. (4-7), the drillability coefficient, *a*, and the drillability constant term, *b*, were defined.

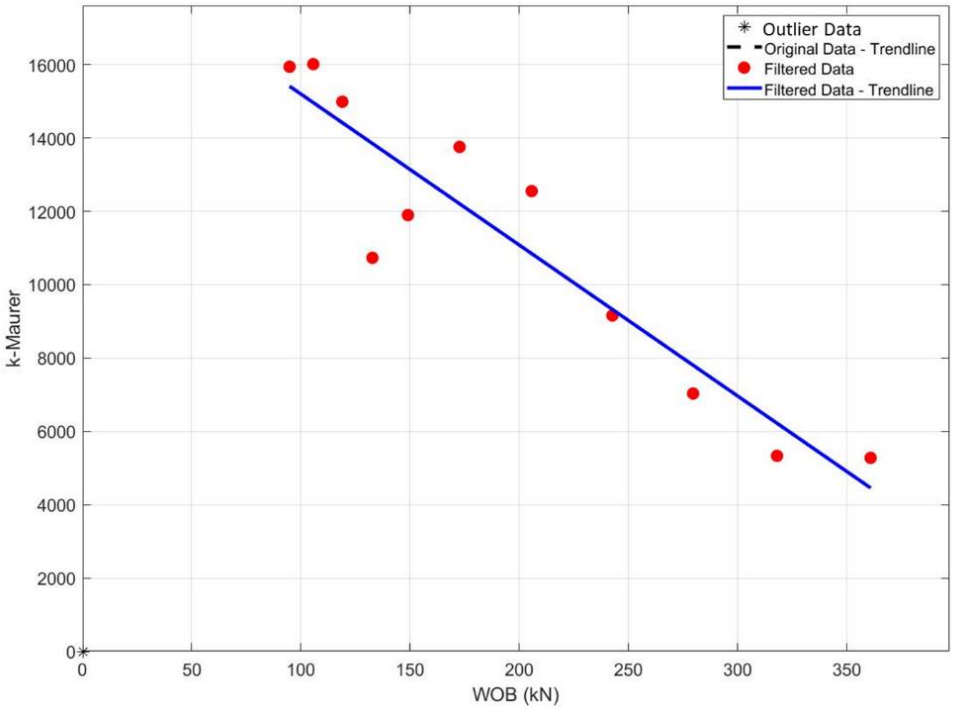

Figure 4-11 Drillability Constant as a relation to the WOB for a field drilling test performed in compacted shale with a tricone bit of 444.5 mm diameter.

Figure 4-12 shows a comparison between the real, and the predicted, ROP. The predicted ROP was calculated considering the values of the drillability coefficient and the drillability constant term that were previously determined and Eqn. (4-9).

For this analysis, $R^2 = 0.9069$, $S_{y,x} = 0.19\, m/h$, $RS_{y,x} = 15.07\%$, and $\alpha = 0.9979$ based on Figure 4-12 and Equations (4-13), (4-14), (4-15), and (4-16).

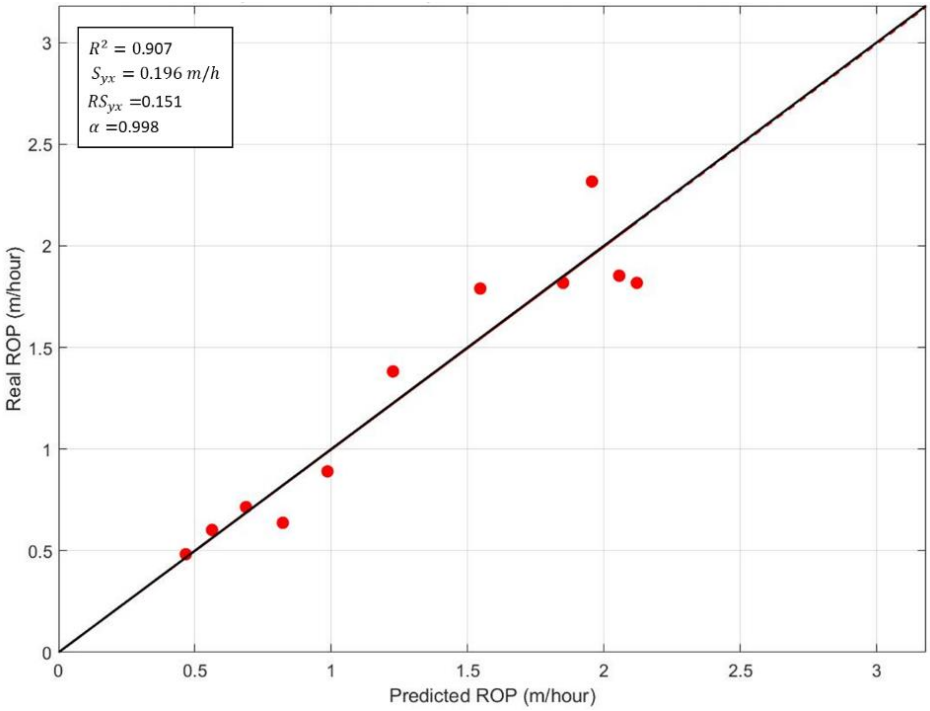

Figure 4-12 Comparison between the ROP of a field drilling test performed in compacted shale with a tricone bit of 444.5 mm diameter and the ROP predicted by Eqn. (4-9).

4.6.2 Tricone Insert Drill Bit Drilling Operation Performed in Basalt

In 2017, Vargas [21] analyzed the drilling dataset for a geothermal well drilled in Iceland in order to accomplish the following: (a) understand ways to improve drilling time; (b) identify drilling problems; (c) identify the drilling factors that influence the rate of penetration and drill bit selection. During these drilling operations, a 311.15 mm diameter TCI drill bit with 812.8/812.8 mm nozzles were used with water as the drilling fluid. The lithology was predominantly basalt with the UCS estimated at approximately 165 MPa.

Figure 4-13 shows a representative curve of the drilling operation mentioned above. The drilling data-set shows high dispersion that suggests an unstable operation but the general tendency of the ROP as a relation to the WOB presents an expected behavior. The graph suggests the existence of the founder point.

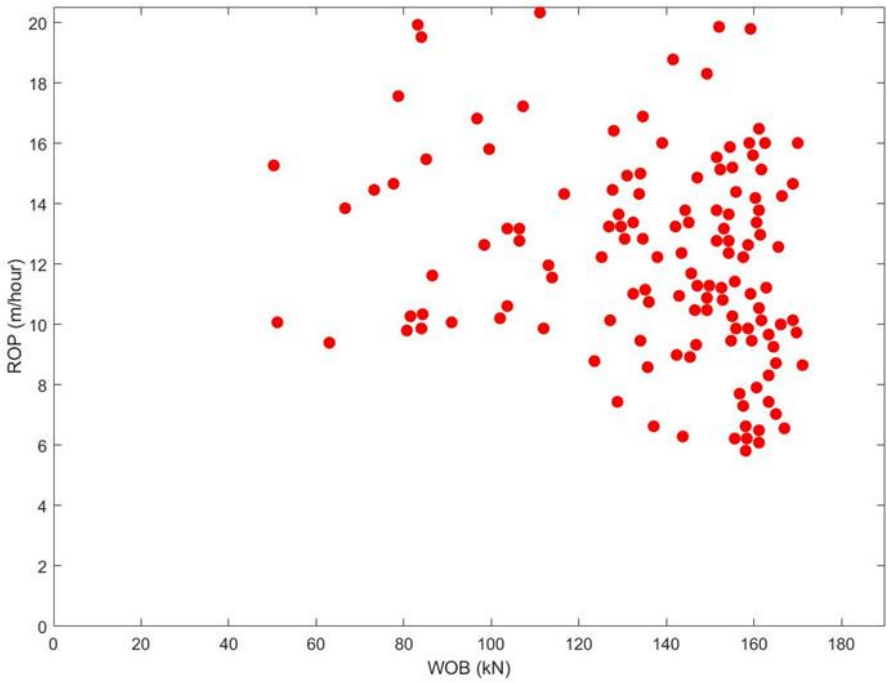

Figure 4-13 Representative curve of a drilling operation performed in basalt with a TCI drill bit of 12 ¼ inches diameter.

Figure 4-14 presents the "drillability constant" as a relation to the WOB based on Eqn. (4-6) for this drilling data-set. Despite the high dispersion and the presence of outliers, a linear relation between the "drillability constant" and WOB is observed in Figure 4-14. From the graph and Eqn. (4-7), the drillability coefficient, *a*, and the drillability constant term, *b*, were defined.

Figure 4-15 shows a comparison between the real, and the predicted, ROP. The predicted ROP was calculated considering the values of the drillability coefficient and the drillability constant term that were previously determined and Eqn. (4-9). This graph shows a high dispersion of the drilling data-set.

For this analysis, $R^2 = 0.8217$, $S_{y,x} = 3.71\ m/h$, $RS_{y,x} = 29.41\%$, and $\alpha = 0.9200$ based on Figure 4-15 and Equations (4-13), (4-14), (4-15), and (4-16).

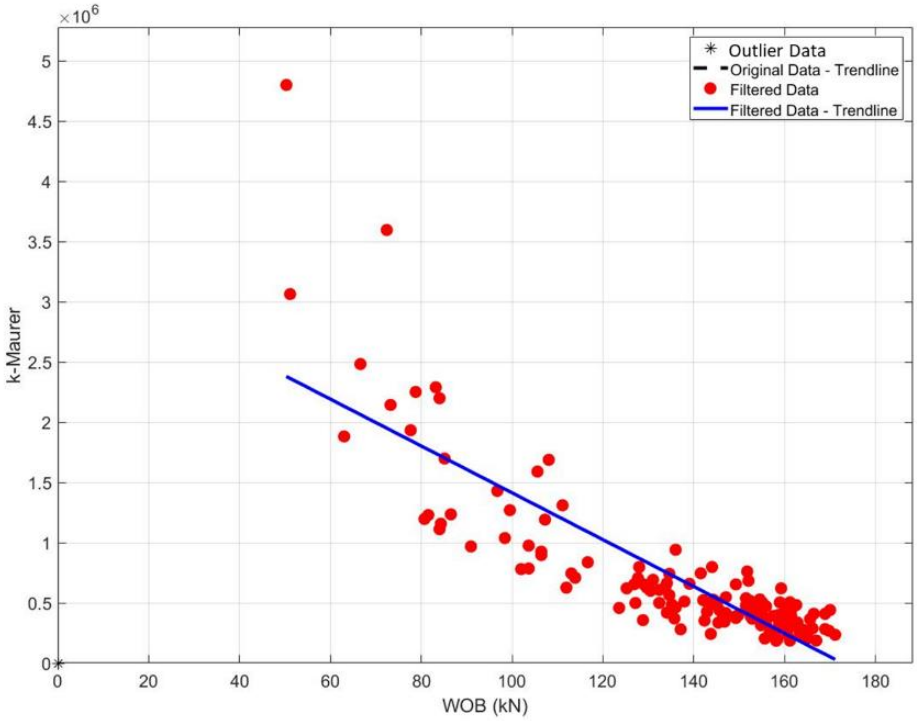

Figure 4-14 Drillability Constant as a relation to the WOB for a drilling operation performed in basalt with a TCI drill bit of 12 ¼ inches diameter.

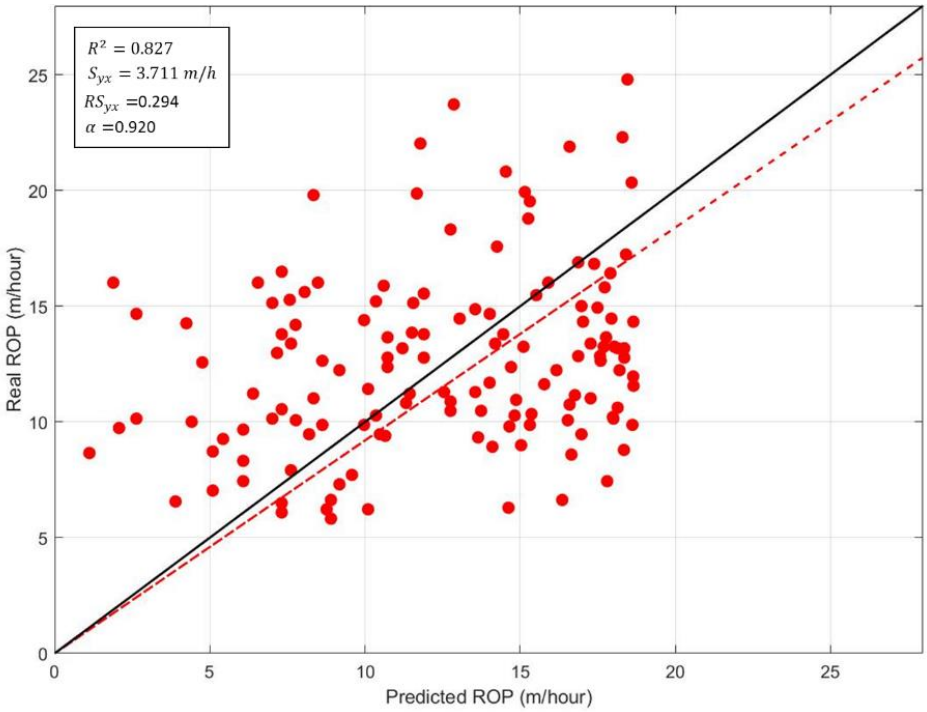

Figure 4-15 Comparison between the ROP of a drilling operation performed in basalt with a TCI drill bit of 12 ¼ inches diameter and the ROP predicted by Eqn. (4-9).

4.6.3 Roller-cone Drill Bit Drilling Operation Performed in a Rock Specimen with CCS of 113.53 MPa

In 2015, Rashidi *et al.* [22] developed a ROP prediction model for roller-cone bits that included the influence of the main drilling parameters and the cutting structure in the ROP prediction. The authors used full-scale laboratory experiments to calibrate this model. In a specific experiment, a roller-cone bit of a 216 mm diameter was used in a rock specimen with a confined compressive strength (CCS) of 113.53 MPa and rotary speed of 122 rpm.

Figure 4-16 shows a representative curve of the drilling operation mentioned above. Despite the low amount of data, there is an approximately linear relation between the ROP and WOB, which is expected in a typical drilling performance curve (Figure 4-5 - Region B).

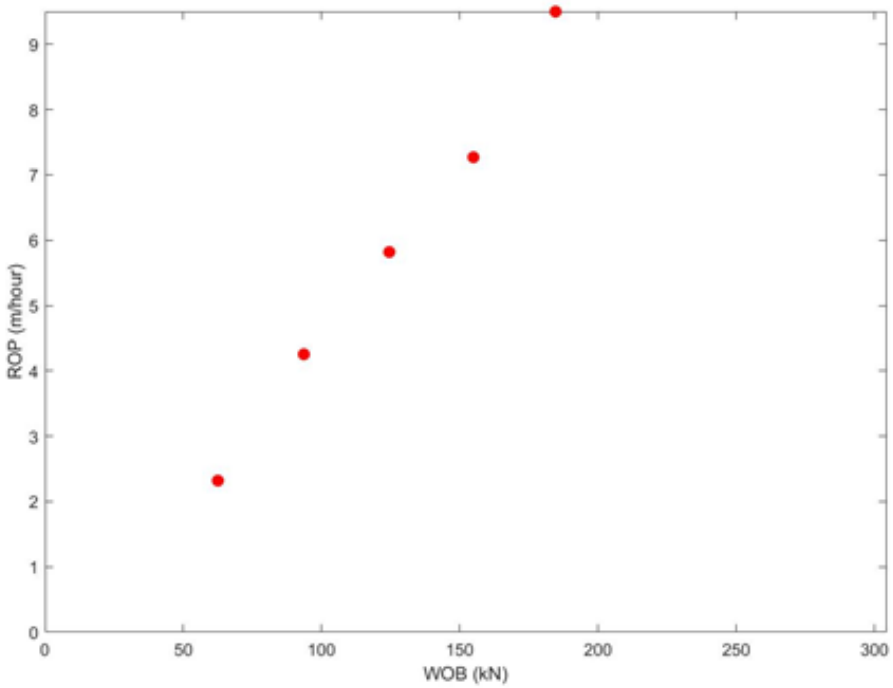

Figure 4-16 Representative curve of a laboratory experiment performed with a roller-cone drill bit of 216 mm diameter in a rock specimen with CCS of 113.53 MPa.

As seen in the previous sections, the "drillability constant" (Eqn. (4-6)) has a linear dependence with the WOB that can be seen in Figure 4-17. The drillability coefficient, *a*, and the drillability constant term, *b*, were determined through Figure 4-17 and Eqn. (4-7).

Figure 4-18 shows a comparison between the real ROP and the predicted ROP that was calculated considering the previously determined values of the drillability coefficient and the drillability constant term and Eqn. (4-9). Figure 4-18 shows that Eqn. (4-9) has high accuracy to predict the drilling performance in this specific scenario.

For this analysis, $R^2 = 0.9414$, $S_{y,x} = 1.18\, m/h$, $RS_{y,x} = 20.33\%$, and $\alpha = 1.0126$ based on Figure 4-18 and Equations (4-13), (4-14), (4-15), and (4-16).

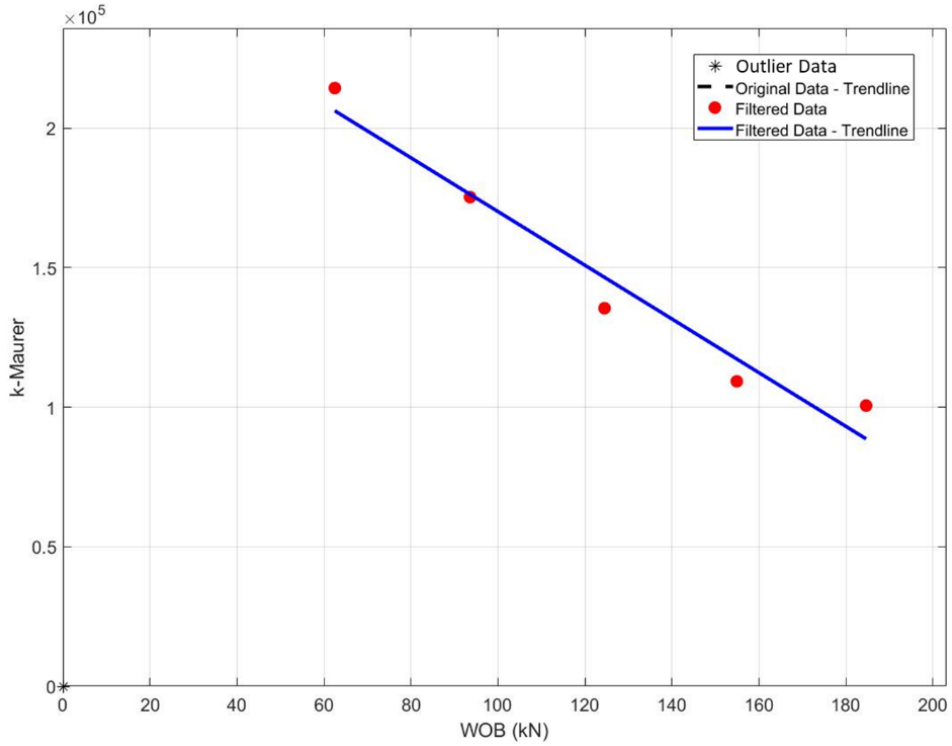

Figure 4-17 Drillability Constant as a relation to the WOB for a laboratory experiment performed with a roller-cone drill bit of 216 mm diameter in a rock specimen with CCS of 113.53 MPa.

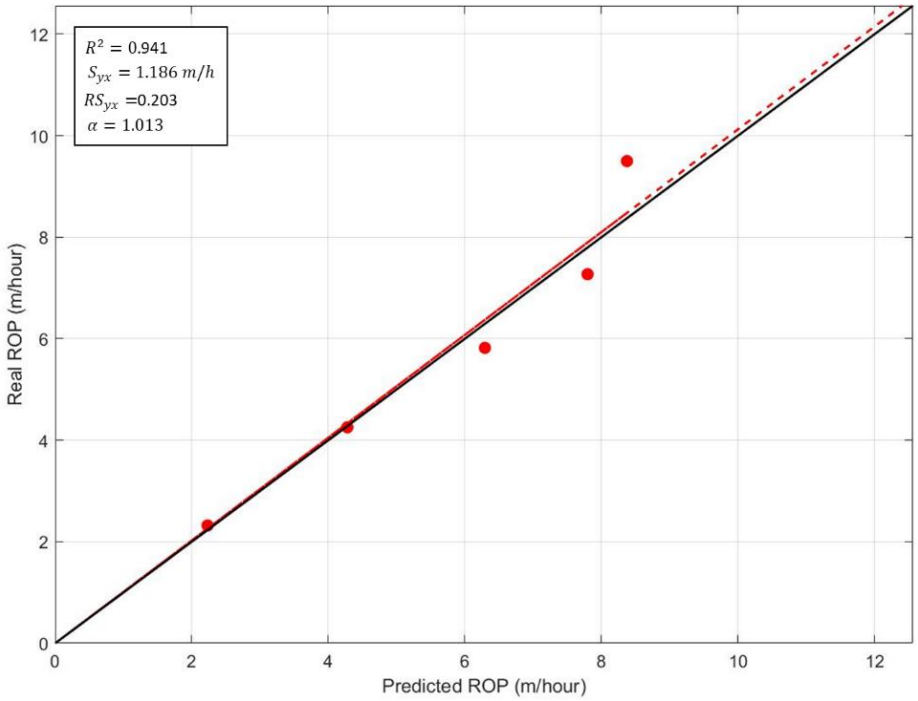

Figure 4-18 Comparison between the ROP of a laboratory experiment performed with a roller-cone drill bit of 216 mm diameter in a rock specimen with CCS of 113.53 MPa and the ROP predicted by Eqn. (4-9).

4.6.4 Other Drilling Operations

As a way to evaluate the comprehensiveness of Eqn. (4-9), 25 distinct drilling scenarios were analyzed. This analysis is similar to the analysis performed in the previous sections, where the drillability coefficient and the drillability constant term (Eqn. (4-7)) were determined, and the coefficient of determination (Eqn. (4-13)), the slope of least-squares linear fit curve with the origin fixed at (0,0) (Eqn. (4-14)), the standard error of estimate (Eqn. (4-15)), and the relative standard error of estimate (Eqn. (4-16)) were calculated.

Table 4-3 shows details of the comprehensiveness evaluation of Eqn. (4-9). In this evaluation, the drilling scenarios covered drill bit diameters varying between 63.50 mm and 444.50 mm, UCS varying between 30.0 MPa and 317.16 MPa, and different types of rock such as granite, basalt, limestone, marble, shale, dolomite, diabase, and sandstone.

Due to the complexity to measure the data-set reliability and accuracy of each drilling scenario, a global analysis of the results is necessary. In general terms, Table 3 shows that Eqn. (4-9) has high accuracy to predict the drilling performance presenting an average R^2 of 0.804 with a standard deviation of 0.204 and an average α of 1.016 with a standard deviation of 0.052.

From Table 4-3, the highest dispersion of the drilling data ($R^2 = 0.149$, $S_{y,x} = 2.23\ m/h$, and $RS_{y,x} = 54.57\%$) is presented in the scenario shown in line 17, but the Eqn. (4-9) presented high accuracy to predict its drilling performance ($\alpha = 1.017$). The scenario shown in line 2 presented the lowest accuracy of the new model ($\alpha = 0.920$), where Eqn. (4-9) overestimated the ROP values.

Figure 4-19 and Figure 4-20 shows a comparison between the predicted ROP (Eqn. (4-9)) and the real ROP related to lines 17 and 2 respectively of Table 4-3.

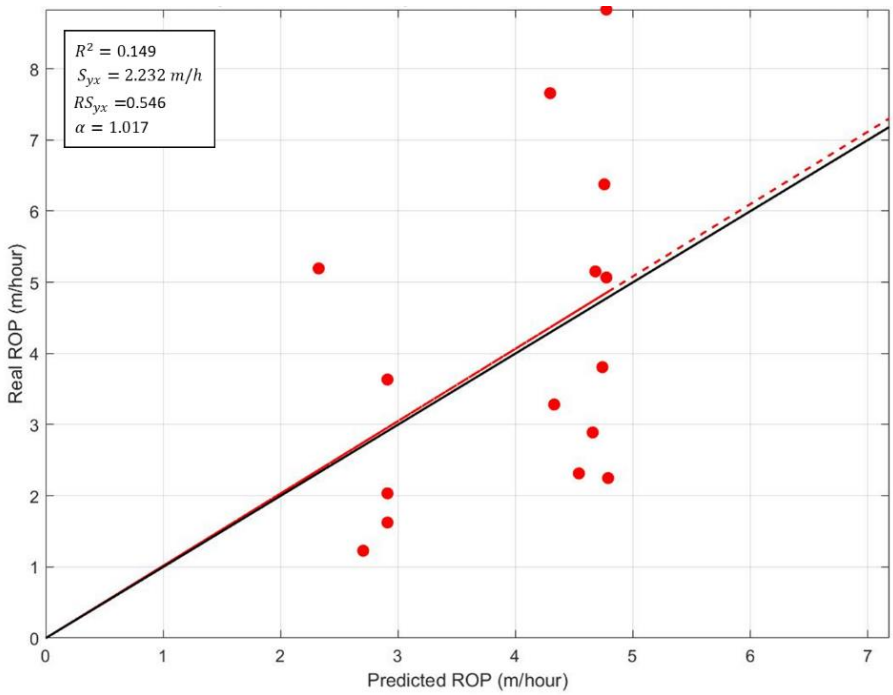

Figure 4-19 Comparison between the ROP of the drilling scenario on line 17 of Table 4-3 and the ROP predicted by Eqn. (4-9).
Table 4-3 Comprehensiveness Evaluation of Eqn. (4-9).

Bit OD [mm]	Rock Type	UCS [MPa]	Flow Rate [L/m]	R^2	α	$S_{y,x}$ [m/h]	$SR_{y,x}$ [%]	Ref.
63.50	Granite	168.40	35	0.828	0.995	0.08	27.17	-
311.15	Basalt	165.47	3300	0.827	0.920	3.71	29.41	[21]
311.15	Basalt	165.47	3300	0.681	0.995	1.89	14.91	[21]
152.40	Limestone	30.00	1250	0.949	1.005	0.38	10.51	[4]
215.90	Limestone	30.00	1250	0.792	1.070	2.99	41.39	[4]
215.90	Limestone	30.00	1250	0.575	1.030	3.74	40.89	[4]
444.50	Shale	50.00	-	0.907	0.998	0.20	15.07	[20]
120.70	Dolomite	317.16	265	0.722	0.995	6.78	68.85	[23]
120.70	Dolomite	317.16	265	0.870	1.026	6.41	71.46	[23]
120.70	Dolomite	317.16	265	0.878	1.025	3.64	73.00	[23]
216.00	-	58.34	-	0.705	1.017	3.01	29.15	[22]
216.00	-	113.49	-	0.941	1.016	1.19	20.33	[22]
310.00	Granite	215.00	-	0.598	0.994	1.38	18.79	[24]
310.00	Marble	170.00	-	0.895	0.970	1.52	13.76	[24]
200.00	Marble	170.00	-	0.572	1.007	6.89	36.94	[24]
160.00	Granite	215.00	-	0.986	0.996	0.45	6.77	[24]
160.00	Marble	170.00	-	0.149	1.017	2.23	54.57	[24]
120.00	Granite	215.00	-	0.963	1.006	0.90	17.66	[24]
120.00	Marble	170.00	-	0.775	1.035	5.95	47.35	[24]
250.00	Sandstone	50.00	-	0.523	0.996	13.36	36.47	[24]
250.00	Granite	215.00	-	0.999	1.000	0.20	2.82	[24]
250.00	Diabase	220.00	-	0.999	0.998	0.57	6.64	[24]
250.00	Diabase	220.00	-	0.997	1.000	0.46	4.19	[24]
215.90	Sandstone	60.57	-	0.988	1.000	0.62	4.41	[10]
215.90	Limestone	44.81	-	0.984	1.000	0.31	1.87	[10]
			Mean	0.804	1.016	2.75	27.77	
		Standard Deviation		0.204	0.052	3.12	21.99	

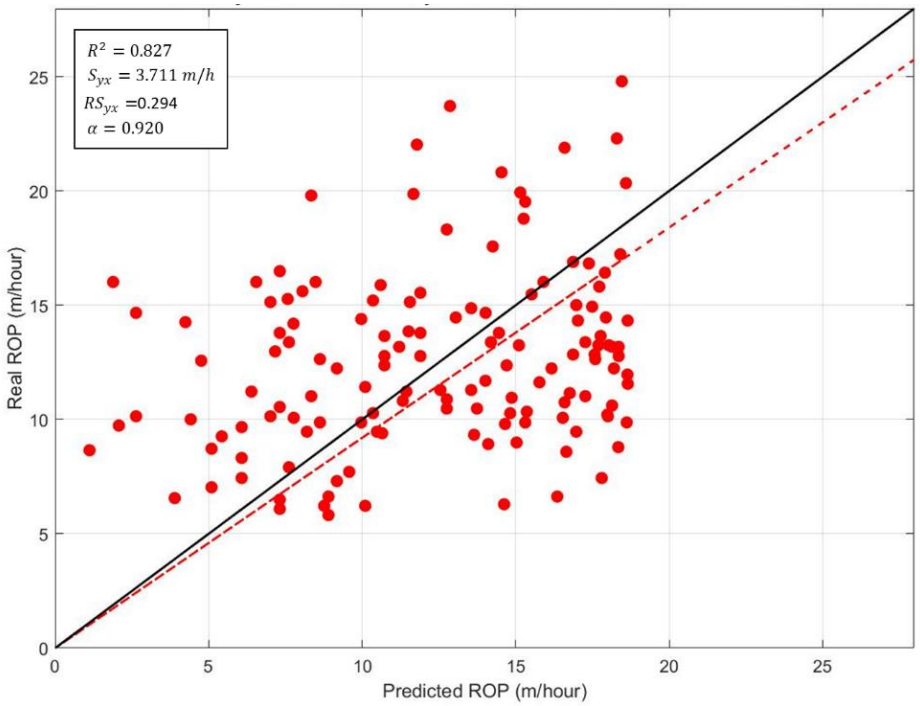

Figure 4-20 Comparison between the ROP of the drilling scenario on line 2 of Table 4-3 and the ROP predicted by Eqn. (4-9).

4.7 Conclusion

According to this research, the "drillability constant" (k) value of the Maurer ROP prediction model is relation to the WOB for roller-cone bit operations, and this dependence is approximately linear. This affirmation is based on the analysis of 25 distinct drilling scenarios that used roller-cone bits of different diameters (63.50 to 444.50 mm) and in different rock specimens (UCS varying between 30 and 317.16 MPa).

In general terms, the de Moura *et al.*'s model presented high accuracy to predict the drilling performance in the scenarios mentioned above and can be confirmed by a mean value of the slope of least-squares linear fit curve with the origin fixed at (0,0) (α) of 1.016 with standard deviation of 0.052. The α value varied between 0.920 and 1.070, being that a perfect fit ($\alpha = 1.000$) was observed in 4 drilling scenarios.

Despite the high dispersion of the drilling data-set in some analyzed scenarios, where this data dispersion was characterized by the coefficient of determination (R^2) with a minimum value of 0.149 being observed, the new model kept its high accuracy to predict the whole drilling performance. Possibly, the high data dispersion mentioned is the result of instability in the drilling process, but the classic relationship between ROP and WOB was observed in most cases.

Contrary to what is presented by most drilling prediction models, de Moura *et al.* model extrapolates its application to a specific drill bit type with high accuracy. The singularity of each drilling scenario is absorbed by the new model through the calibration of its constants (drillability coefficient and drillability constant term). This model is enhanced through its ability to determine the founder point location that is a powerful tool in the drilling optimization and in the comparative analysis between different drilling scenarios.

Research involving the extension of the new model to predict the drilling performance to large diameter drilling (RBM and TBM) is ongoing. Additionally, a parametric analysis of the impact of the drilling parameters in the constants of the new model (drillability coefficient and drillability constant term) will also be performed. This is extremely relevant due to the complexity involving the performance of DOTs during the real field drilling operations.

Research to understand the impact of the drilling parameters and rock mass characteristics in the drillability coefficient and drillability constant term of the de Moura and Butt model is ongoing. Additionally, a laboratory-scale device to simulate the large diameter drilling operation is in the final phase of development.

4.8 Acknowledgments

The authors appreciate and acknowledge the technical and financial support of Novamera Inc., Memorial University of Newfoundland, and MITACS through the Sustainable Mining by Drilling (SMD) project. Without their appreciated support, this research could not have achieved its results.

4.9 Nomenclature

a	Drillability Coefficient
b	Drillability Constant Term
CCS	Compressive Strength, MPa
D	Drill Bit Diameter, mm
DOT	Drill-Off Test
IADC	International Association of Drilling Contractors
k	Drillability Constant
K	Drillability Linear Equation
LDS	Large Drilling Simulator
N	Rotary Speed, rpm
r	Repeatability Limit, MPa
R	Rate of Penetration, m/h
ROP	Rate of Penetration, m/h
R_{fp}	ROP Correspondent to the Founder Point, kN
R^2	Coefficient of Determination
S	Rock Strength, MPa

s_r	Repeatability Standard Deviation, MPa
$S_{y,x}$	Standard Error of Estimate, m/h
$SR_{y,x}$	Relative Standard Error of Estimate
UCS	Unconfined Compressive Strength, MPa
W	Weight on Bit, kN
W_{fp}	WOB Correspondent to the Founder Point, kN
WOB	Weight on Bit, kN
W_0	Threshold WOB Before Cratering, kN
x	Predicted ROP, m/h
y	Real ROP, m/h
α	Slope of Least-Squares Linear Fit Curve with Origin Fixed at (0,0)
β	Constant Term of Least-Squares Linear Fit
γ	Constant Coefficient of Least-Squares Linear Fit

4.10 References

[1] J. de Moura, Y. Xiao, D. Ahmed, J. Yang and S. D. Butt, "Widening Drilling Operation: Performance Analysis on the Application of Fixed Cutter Drill Bits in Hard Rock Formation," in *ASME 39th International Conference on Ocean, Offshore and Arctic Engineering*, Virtual Conference-online, Aug. 2020, p. 10.

[2] C. Hegde, H. Daigle, H. Millwater, and K. Gray, "Analysis of rate of penetration (ROP) prediction in drilling using physics-based and data-driven models," *Journal of Petroleum Science and Engineering*, vol. 159, pp. 295–306, Nov. 2017, doi: 10.1016/j.petrol.2017.09.020.

[3] W. C. Maurer, “The ‘Perfect - Cleaning’ Theory of Rotary Drilling,” *Journal of Petroleum Technology*, vol. 14, no. 11, pp. 1270–1274, Nov. 1962, doi: 10.2118/408-PA.

[4] J.-C. Bourdon, G. A. Cooper, D. A. Curry, D. McCann, and B. Peltier, “Comparison of Field and Laboratory-Simulated Drill-Off Tests,” *SPE Drilling Engineering*, p. 6, 1989.

[5] L. H. Robinson and M. S. Ramsey, “Are You Drilling Optimized or Spinning Your Wheels?,” in *AADE 2001 National Drilling Conference, “Drilling Technology - The Next 100 years,”* Houston, TX, Mar. 2001, p. 11.

[6] M. Bataee and M. Kamyab, “Investigation of Various ROP Models and Optimization of Drilling Parameters for PDC and Roller-cone Bits in Shadegan Oil Field,” p. 10.

[7] I. Kowakwi, H. Chen, G. Hareland, and B. Rashidi, “The Two-Term Rollercone Rate of Penetration (ROP) Model with Integrated Hydraulics Function,” presented at the 46th U.S. Rock Mechanics/Geomechanics Symposium, Jan. 2012, Accessed: Dec. 06, 2020. [Online]. Available: https://www-onepetro-org.qe2a-proxy.mun.ca/conference-paper/ARMA-2012-246?sort=&start=0&q=The+Two-Term+Rollercone+Rate+of+Penetration+%28ROP%29+Model+with+Integrated+Hydraulics+Function&from_year=&peer_reviewed=&published_between=&fromSearchResults=true&to_year=&rows=25#.

[8] I. AlArfaj, A. Khoukhi, and T. Eren, “Application of Advanced Computational Intelligence to Rate of Penetration Prediction,” in *2012 Sixth UKSim/AMSS European Symposium on Computer Modeling and Simulation*, Malta, Malta, Nov. 2012, pp. 33–38, doi: 10.1109/EMS.2012.79.

[9] Y. Deng *et al.*, “A New Prediction Model of Energy Consumption on Rock Fragmentation and Rate of Penetration Based on Fractal Theory,” presented at the 49th US Rock Mechanics/Geomechanics Symposium, San Francisco, CA, Jun. 2015.

[10] Y. Deng, M. Chen, Y. Jin, Y. Zhang, D. Zou, and Y. Lu, “Theoretical and experimental study on the penetration rate for roller cone bits based on the rock dynamic strength and drilling parameters,” *Journal of Natural Gas Science and Engineering*, vol. 36, pp. 117–123, Nov. 2016, doi: 10.1016/j.jngse.2016.10.019.

[11] M. B. Diaz, K. Y. Kim, T.-H. Kang, and H.-S. Shin, “Drilling data from an enhanced geothermal project and its pre-processing for ROP forecasting improvement,” *Geothermics*, vol. 72, pp. 348–357, Mar. 2018, doi: 10.1016/j.geothermics.2017.12.007.

[12] C. Gan *et al.*, “Two-level intelligent modeling method for the rate of penetration in complex geological drilling process,” *Applied Soft Computing*, vol. 80, pp. 592–602, Jul. 2019, doi: 10.1016/j.asoc.2019.04.020.

[13] “PDC Bit vs Tricone Bit, Which is The Best Option for you,” *FIRMTECH*, Nov. 04, 2019. https://www.firmtechco.com/pdc-vs-tricone/ (accessed Dec. 06, 2020).

[14] R. F. Mitchell and S. Z. Miska, Eds., *Fundamentals of Drilling Engineering*, vol. 12. Richardson, UNITED STATES: Society of Petroleum Engineers, 2010.

[15] F. Arvani, M. Sarker, G. Rideout, and S. D. Butt, “Design and Development of an Engineering Drilling Simulator and Application for Offshore Drilling for MODUs and Deepwater Environments,” presented at the SPE Deepwater Drilling and Completions Conference, Galveston, Texas, USA, 2014, doi: 10.2118/170301-MS.

[16] ASTM International, “D7012-14e1 Standard Test Methods for Compressive Strength and Elastic Moduli of Intact Rock Core Specimens under Varying States of Stress and Temperatures,” ASTM International, West Conshohocken, PA, 2014. doi: 10.1520/D7012-14E01.

[17] X. Chen, J. Yang, and D. Gao, “Drilling Performance Optimization Based on Mechanical Specific Energy Technologies,” in *Drilling*, A. Samsuri, Ed. InTech, 2018, pp. 133–162.

[18] A. J. Wheeler and A. R. Ganji, “Correlation of Experimental Data,” in *Introduction to engineering experimentation*, 2nd ed., Upper Saddle River, NJ: Prentice Hall, 2003, pp. 151–168.

[19] J. L. Devore, “Estimating Model Parameters,” in *Probability and statistics for engineering and the sciences*, 6th ed., Belmont, CA: Thomson-Brooks/Cole, 2004, pp. 505–516.

[20] M. J. Fear, “How to Improve Rate of Penetration in Field Operations,” *SPE Drilling & Completion*, vol. 14, no. 01, pp. 42–49, Mar. 1999, doi: 10.2118/55050-PA.

[21] D. M. R. Vargas, “Analysis of Bit Operations: Laguna Colorada Geothermal Project, Bolivia,” Orkustofnun, Iceland, 2016.

[22] B. Rashidi, G. Hareland, and Z. Wu, “Performance, simulation and field application modeling of rollercone bits,” *Journal of Petroleum Science and Engineering*, vol. 133, pp. 507–517, Sep. 2015, doi: 10.1016/j.petrol.2015.06.003.

[23] D. S. Rowley, R. J. Howe, and F. H. Deily, “Laboratory Drilling Performance of the Full-Scale Rock Bit,” *Journal of Petroleum Technology*, vol. 13, no. 01, pp. 71–81, Jan. 1961, doi: 10.2118/1545-G-PA.

[24] G. Wijk, “Rotary Drilling Prediction,” *International Journal of Rock Mechanics and Mining Sciences & Geomechanics*, vol. 28, no. 1, pp. 35–42, 1991.

Chapter 5 A Novel Rate of Penetration Prediction Model for Large Diameter Drilling: an Approach Based on TBM and RBM Applications

This Chapter is based on section 1.3.3 and was submitted to the International Journal of Rock Mechanics and Mining Sciences in December 2020 and is currently under review.

Authors: Jeronimo de Moura, Jianming Yang, and Stephen D. Butt.

5.1 Co-authorship Statement

The authors' contributions in this work are described below:

- **Jeronimo de Moura**: Identification of research topic, literature review, experiments design and performance, post processing and data analysis, and manuscript preparation.
- **Jianming Yang**: Technical support and manuscript review.
- **Stephen D**. **Butt**: Experiment supervision, technical support, and manuscript review.

5.2 Abstract

In mining and construction as well as the oil and gas industry, the drilling process is a vital step because of its impact in the economic feasibility of many projects. An accurate rate of penetration

is an important aspect of a drilling process. Currently, a massive quantity of research is focused on the understanding of the bit-rock interaction and on the development of accuracy tools to predict the drilling performance. de Moura *et al.* [1] explored the linear relationship between the "drillability constant" of the Maurer model and the WOB to develop a high-accuracy drilling prediction model, called de Moura and Butt model, for the fixed cuter drill bits applied in oil and gas scenarios that is able to localize the local maximum point of the drilling performance curve ("founder point"). In this paper, a comprehensiveness analysis of the de Moura and Butt model is performed for the large diameter drilling. The model proved to be effective and highly accurate in predicting drilling performance in 19 distinct RBM and TBM operations, analyzed in this paper, even in the presence of data-sets with high-dispersion. A comparative analysis between the de Moura and Butt, CSM, and Gehring models were performed based on two TBM operations. This analysis indicated that the CSM and Gehring models presented low-accuracy underestimating or overestimating drilling performance while the de Moura and Butt model presented high-accuracy in predicting them. Additionally, a discussion about the existence of the founder point in large diameter drilling operations is included. The existence of this point in the drilling performance curve is strongly suggested by two RBM applications and that its location can be determined by the de Moura and Butt model.

5.3 Introduction

In mining and construction projects, the proper selection of an excavation machine and an accurate prediction of its performance are crucial to cost estimates and planning. Currently, mechanical excavation is a strong alternative to conventional drill and blasting in tunneling and mining projects. TBM and RBM are the most used excavation machines in these type of projects.

RBMs are used in mining and construction projects mainly to excavate shafts and other vertical structures. Initially, a pilot hole of 230 to 350 mm diameter is drilled down. Next, the drill bit used during the pilot hole drilling is changed to a large diameter reamer and it is pulled back up to the upper level. A RBM has the flexibility to work with different dip angles and diameters [2].

TBMs are applied in tunnel construction for traffic, hydropower, sewerage and water, underground storage, and mining. Currently, there is a wide variety of TBMs available in the marketplace including machines with different diameters and adapted to different formation conditions [3]. TBMs present considerable advantages over drill and blast in favourable ground conditions due to their normally high advance rates and lower risk levels, but in adverse ground conditions these machines present a significant increase in cost and decrease in safety [4].

In the last few decades, research related to ROP modelling has grown considerably, mainly in the determination of a relationship between the ROP and the rock-mass properties and in the application of machine learning and neural networks.

In large diameter drilling, we have highlighted the research developed by Graham in 1976 [5] and Farmer and Glossop in 1980 [6]. These were the first models used to predict the TBM performance based on the intact rock parameters such as UCS and tensile strength. The research started by Ozdemir and Johnson in 1977 [7] [8], a semi-theoretical model based on the cutting forces on individual cutter that was later called CSM model.

In general terms, drilling performance models can be divided into two categories: physics-based - these models, also called traditional models, are based on empirical equations and

laboratory experiments; data-driven - these models are based on extensive data-set that use machine learning and neural networks to predict the drilling performance [9].

This paper is one part of a research about drilling performance prediction that was initiated by de Moura et al. [1]. In that paper, the authors discuss the Maurer model and its limitation in predicting the whole drilling performance curve including the founder point location. They identified a linear relationship between the "drillability constant" of the Maurer model and the WOB, and developed a new model that establish a cubic relation between the ROP and WOB, called de Moura and Butt model. This model was applied to predict the drilling performance of small diameter fixed cutter drill bits that were normally applied in the oil and gas industry.

This paper's aim is to perform an applicability analysis of the de Moura and Butt model for large diameter drilling performance as well as to perform accuracy tests of this model to predict the TBM and RBM performance. The rationale behind this analysis is due to the different rock penetration mechanisms present in these two drilling scenarios as well as the impact of the rock-mass characteristics in large diameter drilling operations. This study is based on a quantitative analysis of TBM and RBM drilling performance data-sets available in literature.

5.3.1 Physics-Based Prediction Models

In 1996, Autio, and Kirkkomäki presented a novel full-face boring technique based on rotary drilling and vacuum flushing to remove the rock cuttings. In this work, a model to predict the ROP was established for application to boring machines. Their work covered the evaluation of the excavation disturbance, hole quality, particle size distribution and shape of the crushed rock, energy consumption, greenhouse emissions, and occupational conditions [10].

In 2012, Yagiz *et al.* presented an approach for predicting TBM performance, the CSM model. The CSM model is an evolution that started with a semi-theoretical model based on the cutting forces of individual cutters in 1977 [8], incorporated an estimative of cutting forces as a relation to intact rock properties such as UCS and tensile strength in 1993 [11], and, finally, added the intact rock brittleness and fracture properties of rock masses in 2002 and 2006 [12], [13]. In general terms, the cutterhead requirements (thrust, torque and power) related to the maximum ROP are determined based on the individual cutter forces performing on the rock mass. In this study, the CSM model is discussed based on its application in massive and fractured hard rock conditions. The authors mentioned the difficulty of a simple formula to model the TBM performance due to the complexity of mechanical tunneling processes and the distinct rock properties and features and affirmed that the CSM model has low accuracy to predict faulted fractured rock mass conditions where the ROP is affected by the fractures and plane of weakness [7].

In 2015, Ataei *et al.* studied 11 different zones of an open-pit iron mine to classify them with respect to rock drillability. Laboratory tests and geological mapping of the rock faces were carried out, and rock-mass structural parameters were recorded to develop a model for ROP prediction that could also predict the UCS in terms of Schmidt hammer rebound values. This model was compared with previous models from literature based on analyzed scenarios in their paper. The authors affirmed that their model for ROP prediction is limited to the geological and drilling conditions that were studied in their paper [14].

In 2015, Shaterpour-Mamaghani *et al.* presented experimental studies focused on the determination of a penetration index related to RBM's applications. Their study is based on indentation test laboratory experiments using hydraulic press in rock samples obtained from Eti

Copper Kure Asikoy underground mine located in Turkey. Their study results were validated by a comparative analysis between the ROP prediction and field results [15].

In 2016, Rostami reviewed existing models and ongoing research to predict the TBM performance. According to Rostami, ROP, utilization rate, advance rate, and cutter life are some parameters that, in general, are estimated in the TBM performance analysis. He affirmed that the force balance or theoretical approach, and the empirical models are two camps that, normally, are used to predict the TBM performance in hard rock formations. According to the author, the theoretical approach is based on estimation of cutting forces and the empirical models are based on the analysis and observations of the past projects. Additionally, he concluded that the accuracy of a TBM performance prediction is very low due to the high variability of the application scenarios [16].

In 2018, Shaterpour-Mamaghani *et al.* presented a new empirical model to predict the RBM performance using simple and multiple regression methods. Their study was based on statistical analysis of field results and laboratory studies. They used the UCS to estimate the rotational speed and consumed reamerhead torque, and BTS associated with elasticity modulus to estimate the field specific energy [2].

In 2018, Armetti *et al.* proposed a new model to predict the TBM performance which correlates the ROP and field penetration index (FPI) with the singular rock-mass parameters such as UCS, quartz content, and spacing between fractures. Their study was based on the field data continuously recorded during the construction of the “La Maddalena” exploratory tunnel, situated in northern Italy. The rock-mass quality indices RMR and GSI were used to estimate the

excavatability of a given material showing the importance of an accurate geological-geotechnical characterization to TBM prediction performance [17].

In 2020, Arbabsiar *et al.* presented a new model to improve the accuracy of ROP prediction for a TBM in distinct geotechnical conditions. This model is based on TBM operational parameters and media characteristics (geotechnical risk levels in the modelling) [18].

5.3.2 Data-Driven Prediction Models

In 2010, Hedayatzadeh *et al.* developed a model to predict the TBM performance using an artificial multi-layer neural network with a back propagation learning algorithm. The authors affirmed that a ROP prediction for a TBM is influenced by a large number of parameters that can be divided into four main categories: Intact-rock characteristics; rock-mass properties; rock-mass conditions; and machine characteristics. They highlighted the complexity in developing a model that covers all four categories and that there is not a single universal model to predict the TBM performance [19].

In 2011, Hassanpour *et al.* developed a new ROP prediction model for TBMs based on the analysis and compilation of a database from different hard rock tunneling projects. Their model used statistical methods and the relationship between geological and operational parameters. Additionally, an approach for estimation of rock-mass boreability and TBM performances was introduced [20].

In 2013, Ge *et al.* proposed a ROP prediction model to TBM based on the least-square support vector machine. This model correlated the ROP and rock properties such as UCS, BTS, peak slope index, distance between planes of weakness (DPW) and the alpha angle [21].

In 2017, Adoko *et al.* presented a study about ROP prediction for TBM applications based on the rock-mass parameters including the UCS, Intact Rock Brittleness (BI), angle between the plane of weakness, TBM driven direction, and DPW. A tunneling project in New York City was used as the base to establish the proposed models in their paper. This work used the Bayesian inference approach to identify the most appropriate models to predict the ROP among the eight models that were selected. They used the Markov Chain Monte Carlo (MCMC) technique, by WinBUGS software, to obtain the mean values of the model parameters that were considered in the model prediction performance evaluation. Deviance Information Criterion (DIC) was used as a model accuracy indicator and to rank the models conforming to their fit and complexity [22].

In 2017, Salimi *et al.* analyzed the performance of a hard rock TBM in a 12.24 km tunnel to assess the relationship between the TBM operation and different lithology. Non-linear Regression Analysis, Classification and Regression Tree, and Genetic Programming were used to analyse the TBM performance with respect to the ground conditions. In their work, they affirmed that all existing rock-mass classification systems have limited accuracy in TBM performance prediction. They proposed new models to predict the TBM performance based on the principle components analysis approach [23].

In 2020, Samaei *et al.* proposed a new equation and introduced novel techniques for TBM performance prediction. They investigated the relationship between the ROP and rock-mass

properties using regression analysis. Due to this investigation, two non-linear multi-variable equations were presented and optimized by the Imperialist Competitive Algorithm, and two other models were examined by the Classification and Regression Tree and Genetic Expression Programming techniques [24].

5.4 Background

Whether in construction, mining, tunneling, or oil and gas applications, the essence of the drilling process is guided by the rock fragmentation mechanisms and does not depend on its application area. The creation of a particular terminology to each application area is very normal but theoretical foundations rest on the same bases.

In oil and gas drilling, in normal drilling conditions, the relationship between the ROP and WOB is represented by a characteristic curve (see Figure 5-1). In this curve, three distinct regions can be identified: Region A, where an inadequate depth of cut takes place in the drilling process; Region B, where there is an approximate linear relationship between the ROP and WOB and a higher drilling efficiency is present; and Region C, where the approximately linear relationship between the ROP and WOB is not present and drilling problems (bit balling, bottom hole balling, and vibrations) take place impacting the drilling efficiency [25]. Figure 5-1 shows the existence of a local maximum point in the WOB-ROP curve, called the “founder point”, from which an increase in the WOB no longer results in an increase in the ROP [26].

In the TBM applications, on-site penetration tests are a way to determine TBM performance in a specific geological environment. In these tests, the TBM’s operational conditions are pre-defined to allow a comparative analysis between different machine types and projects. The start-

stop-test is an example of an on-site penetration test. This type of test consists of a TBM which starts slowly from zero to the maximum thrust and then reverses with the same conditions. A detailed geological analysis is mandatory in this test and includes an analysis of the rock discontinuity and rock strength laboratory determination [27].

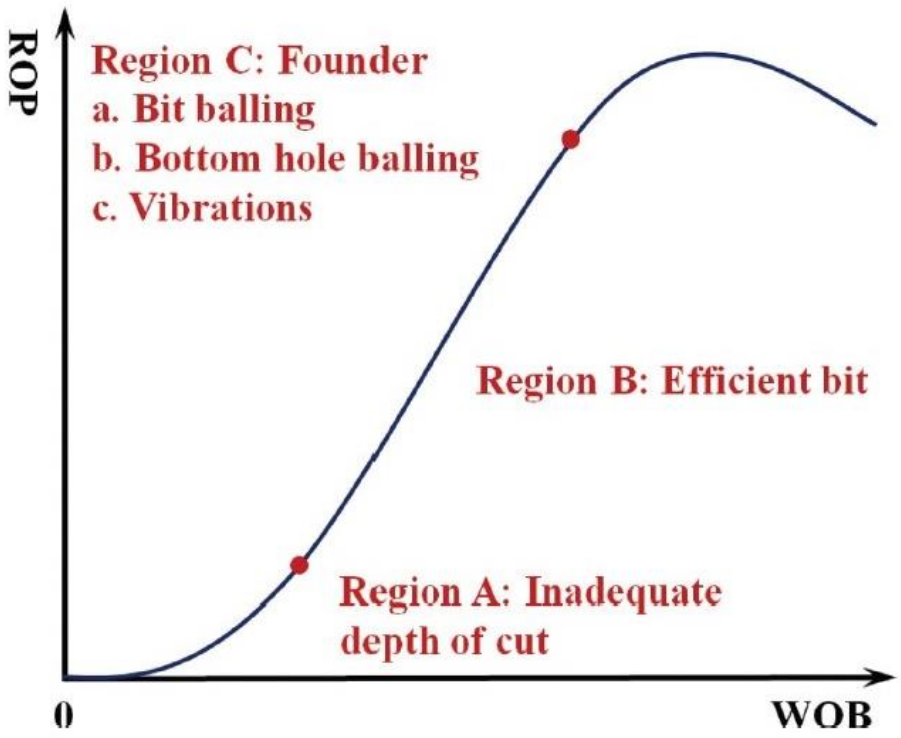

Figure 5-1 Drilling performance curve in the oil and gas drilling [25].

Figure 5-2 shows a typical TBM performance curve where a stage called the “subcritical penetration” is identified. In this stage, in low penetration rates, only the crushing process is present and a chipping process does not occur. At this stage, an increase in WOB does not result in an increase in the ROP. In the oil and gas context, this region is identified as a region where an “inadequate depth of cut” occurs and the drilling mechanism in this stage is different from the other stages of the drilling process. Another interest point of the TBM performance curve is the “friction” between the rock-mass and the TBM shield that can be determined via a friction stroke (free stroke)

before the penetration test. In the friction stroke, the friction value is determined when the cutterhead is not in contact with a rock mass but the TBM shield is. Different machine types and different tunnel routes cause different friction values [27]. Normally in the TBM performance curve, the ROP is called “penetration” and is reported in mm/rev and the WOB is equivalent to the “total thrust force” or “normal force per disc cutter” where the “normal force per disc cutter” is equal to the “total thrust force” divided by the effective number of disc cutters present on the cutterhead.

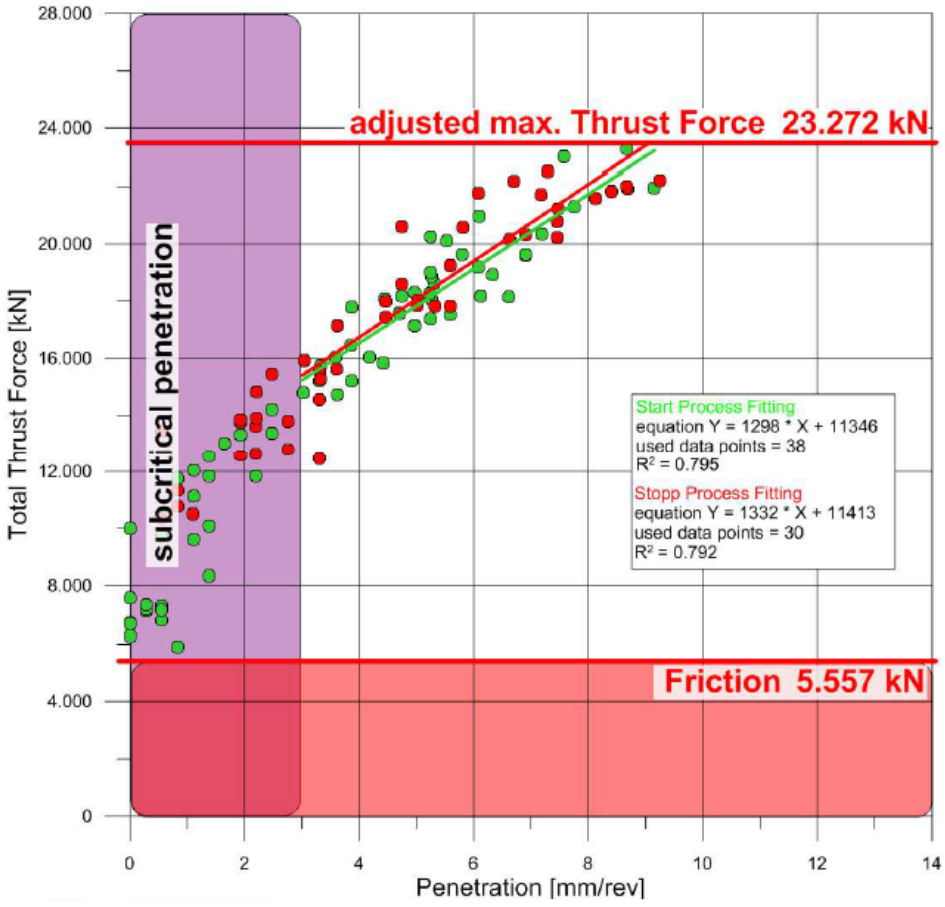

Figure 5-2 Drilling performance curve in the TBM applications [27].

The two most famous models for the TBM penetration prediction are the CSM and the Gehring model [27].

5.4.1 CSM Model

The Earth Mechanics Institute of the Colorado School of Mines has been researching on the TBM performance prediction since the early 1980's. The CSM model is based on: TBM parameters (such as thrust, torque, and power); rock properties (such as UCS, BTS and brittleness of intact rock); and orientation and frequency of discontinuities in rock mass. This model is a semi-theoretical model with an empirical database that has been updated continuously by the Earth Mechanics Institute over the last couple of decades [7]. In the CSM model, the relation between the normal force per cutter and the ROP is a potential function (see Equations (5-1), (5-2), and (5-3)) [27].

$$\phi = cos^{-1}\left(\frac{R-P}{R}\right) \tag{5-1}$$

$$P' = c\sqrt[3]{\frac{\sigma_u^2.\sigma_t.s}{\phi\sqrt{R.T}}} \tag{5-2}$$

$$F_N = \frac{T.R.\phi.P'.\cos(\phi/2)}{1000} \tag{5-3}$$

5.4.2 Gehring Model

The Gehring model is an empirical model based on different tunnel projects with a specific TBM setup (17 inches cutters - 80 mm spacing). Equation (5-4) is a linear relation between the penetration rate and the normal force per cutter that considers independent correction factors including rock mass properties, cutterhead type, and geometries. This model does not include the influence of specific failure energy and rock discontinuities [27].

$$P = \frac{F_N}{\sigma_u}.k_0.k_1.k_2.k_3.k_4.k_5 \tag{5-4}$$

5.4.3 de Moura and Butt Model

In 2020, de Moura *et al.* presented a new drilling performance prediction model based on the linear relationship between the "drillability constant" (*k*) of the Maurer model and the WOB that was identified during the DOTs performed with a coring drill bit in natural granite rock [1].

According to the procedure developed in their study, initially the "drillability constant" (*k*) is calculated to each experimental point using the Eqn. (5-5). Next, the "drillability constant" (*k*) is plotted as a relation to the WOB (as exemplified by Figure 5-3). Due to this linear relationship between the "drillability constant" (*k*) of the Maurer model and the WOB, the authors called it a "drillability linear equation" and indicated it by the capital letter *K* introducing two constants: the drillability coefficient (*a*) and the drillability constant term (*b*) (see Eqn. (5-6)). The value of these constants can be determined through the graph that related the "drillability constant" (*k*) and the WOB (exemplified by Figure 5-3).

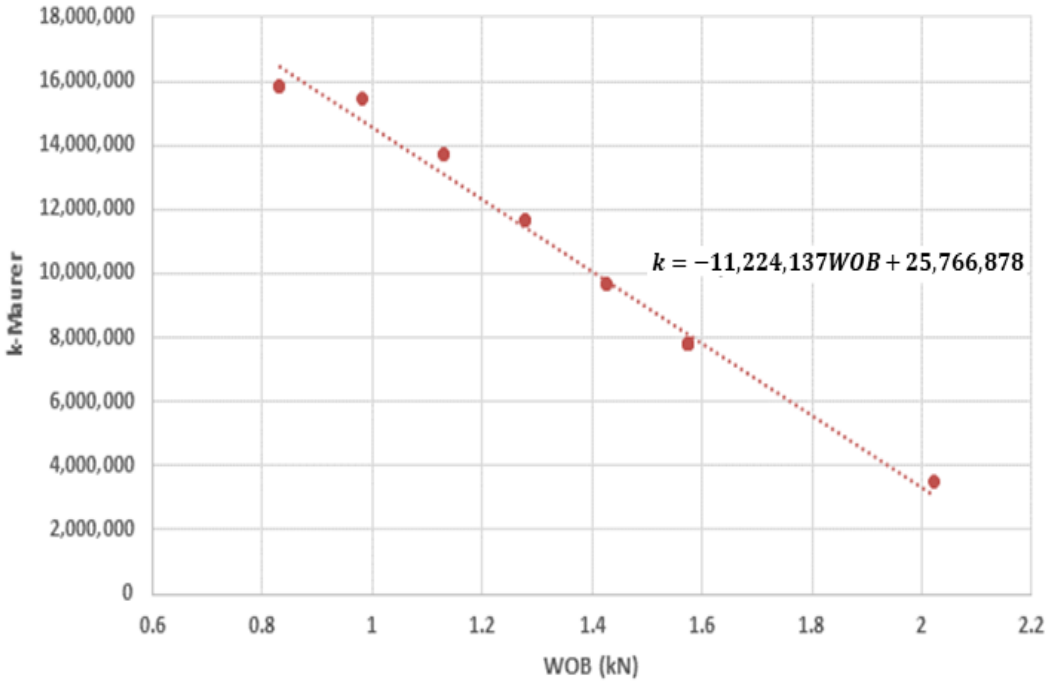

Figure 5-3 "Drillability Constant" (*k*) of the Maurer model as a relation to the WOB [1].

$$k = \frac{60RS^2}{N} \cdot \left[\frac{d_b}{W - W_0}\right]^2 \quad (5\text{-}5)$$

$$K = aW + b \quad (5\text{-}6)$$

Once the values of the drillability coefficient and the drillability constant term are identified, the ROP are determined by Eqn. (5-7) showing that the ROP has a cubic dependency on the WOB.

$$R = (aW + b)\left[\frac{N(W - W_0)^2}{60D^2S^2}\right] \; for\; W > W_0 \quad (5\text{-}7)$$

5.4.4 Data Dispersion and Model Accuracy Measurements

In this paper, four parameters are used to measure the data dispersion and the models' accuracy to predict the drilling performance.

To measure the accuracy of the predicted ROP with relation to the real ROP, the slope of the least-squares linear fit curve with origin fixed at (0,0), indicated by α, is used. Based on Eqn. (5-8), if $\alpha > 1$ then the predicted ROP value is underestimated and if $\alpha < 1$ then it is overestimated.

$$\alpha = \frac{\sum(x_i . y_i)}{\sum(x_i^2)} \quad (5\text{-}8)$$

To measure the data dispersion around the predicted values, the coefficient of determination (R^2), the standard error of estimate ($S_{y,x}$), and the relative standard error of estimate ($RS_{y,x}$) are used and are represented by Equations (5-9), (5-10), and (5-11), respectively. The coefficient of

determination indicates how close the real ROP values are to the predicted ROP values that are represented by a simple linear regression model.

$$R^2 = 1 - \frac{\sum(\gamma x_i + \beta - y_i)^2}{\sum(y_i - average(y))^2} \quad (5\text{-}9)$$

$$S_{y,x} = \sqrt{\frac{\sum(y_i^2) - \beta\sum(y_i) - \gamma\sum(x_i y_i)}{n-2}} \quad (5\text{-}10)$$

$$SR_{y,x} = \frac{S_{y,x}}{\sum(x_i)} \quad (5\text{-}11)$$

5.5 Comprehensive Analysis of de Moura and Butt Model for Large Diameter Drilling Operations

To measure the comprehensiveness of the de Moura and Butt model to predict the drilling performance of large diameter drilling operations, some TBM and RBM field tests and DOT results will be analyzed in this section. The data-sets come from distinct research available in the literature. The accuracy of the model will be measured by Eqns (5-8), (5-9), (5-10), and (5-11).

5.5.1 Tunnel Boring Machine with 80 Disc Cutters of 17 Inches in Very Hard Rock [27]

In 2015, Wilfing *et al.* performed a comparative analysis between the real ROP obtained during TBM projects and the Gehring, CSM, and Alpine prediction models [27].

The authors reduced the number of cutters from 80 to 78 cutters for the particular TBM setup analyzed in their paper because during a normal TBM operation the loading is not distributed equally by all disc cutters (the contact between the rock mass and the disc cutters is different

depending on the location of the cutterhead). The TBM projects analyzed by Wilfing et al. involved very hard rock formations with UCS of 122, 125, and 144 MPa.

To apply the de Moura and Butt model in the TBM performances reported by Wilfing *et al.*, some consideration will be necessary. Firstly, the WOB is calculated multiplying the "Normal Force per Disc Cutter" by the number of disc cutters (78 units). Next, the ROP is calculated based on the penetration and assuming a rotary speed of 3 rpm. Finally, it is assumed that the cutterhead diameter is 10 meters. These assumptions and considerations do not affect the analysis because they are constant values in Eqn. (5-7).

Figure 5-4 shows a representative curve of a TBM performance reported by Wilfing *et al.* [27] contemplating the considerations and assumptions mentioned above in order to apply the de Moura and Butt model. From the graph, the "subcritical penetration" or "inadequate depth of cut" region is present between 5,000 and 8,000 kN. As in the "subcritical penetration" region the drilling mechanism is different compared to the other stages of the drilling process, so it will be excluded in the next step of this analysis. The friction is translated to Eqn. (5-7) through the W_0.

Figure 5-5 shows that the "drillability constant" of the Maurer model has an approximately linear dependence with WOB according to de Moura *et al.* [1]. Based on this relationship, the drillability coefficient and the drillability constant term can be defined by Eqn. (5-6).

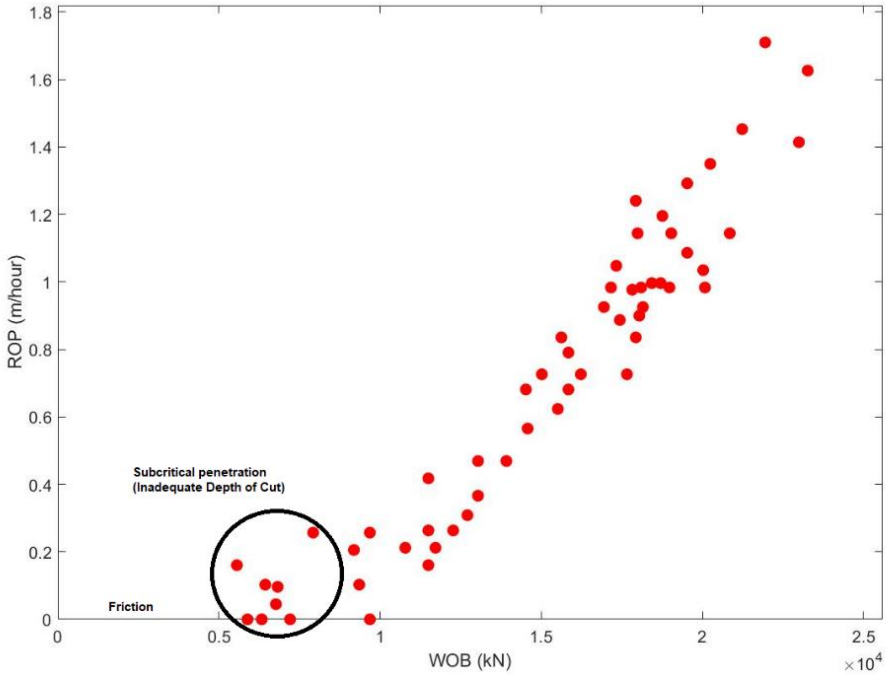

Figure 5-4 Representative curve of a TBM field performance test performed in very hard formation with 80 disc cutters.

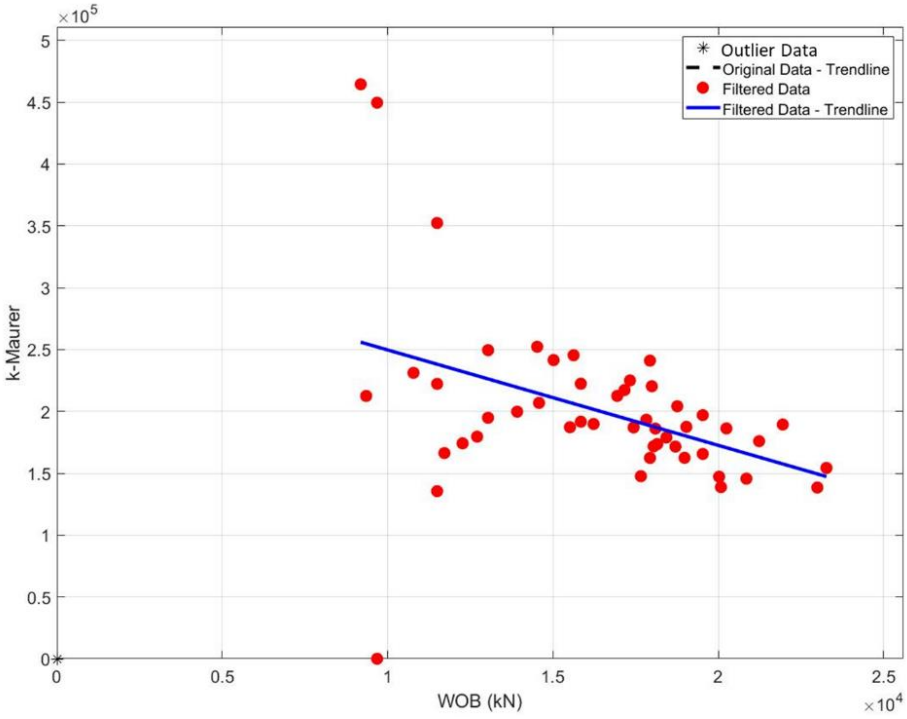

Figure 5-5 Drillability constant (Eqn. (5-5)) as a relation to the WOB for a TBM field performance test performed in very hard formation with 80 disc cutters.

Once the constants of Eqn. (5-7) are determined, the predicted values of the ROP can be calculated for the drilling data-set analyzed in this section. Figure 5-6 shows a comparison between

the real ROPs and the predicted ROPs by Eqn. (5-7). The closer the black solid line is to the red dashed line, the more accurate the prediction model. From the graph, the de Moura and Butt model presents high-accuracy ($\alpha = 0.9939$) and predicts the drilling performance with a low data dispersion ($R^2 = 0.9212$, $S_{y,x} = 0.136\ m/h$, and $RS_{y,x} = 16.92\%$).

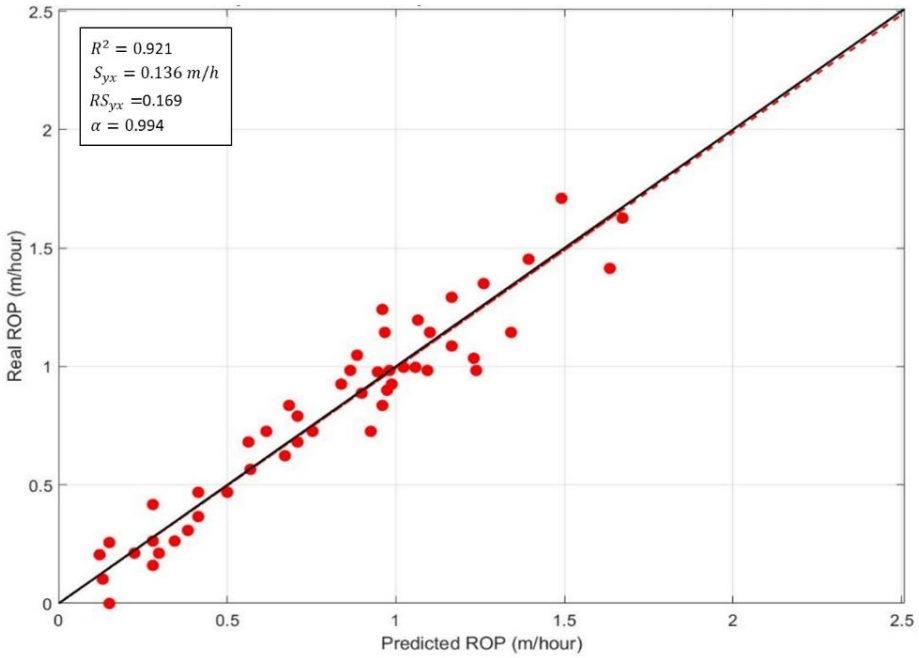

Figure 5-6 Comparison between the ROP of a TBM field performance test performed in very hard formation with 80 disc cutters and the ROP predicted by Eqn. (5-7).

5.5.2 Raise Boring Machine of 1.5 m Diameter in Hard Rock [10]

In 1996, Autio and Kirkkomäki based their work on three experimental full-scale deposition holes located at Research Tunnel in Olkiluoto, Finland. Three holes were drilled to 7.5 m depth and 1.5 m diameter with the rock's compressive strength value at 80 MPa. The drilling operation was divided into two stages: a) Pilot hole drilling of 12 ¼ inches; and b) Enlarge drilling of 1.5 m. In these operations, a raise boring machine of type Subterranean-005L-137 with maximum thrust force of 630 kN and maximum rotary speed of 98 rpm was used [10].

Figure 5-7 shows a representative curve of a 1.5 m diameter RBM in hard formation analyzed by Autio and Kirkkomäki (1996) during their research. In their paper, the WOB is called "total thrust" applied on the cutterhead and the ROP is called "advance".

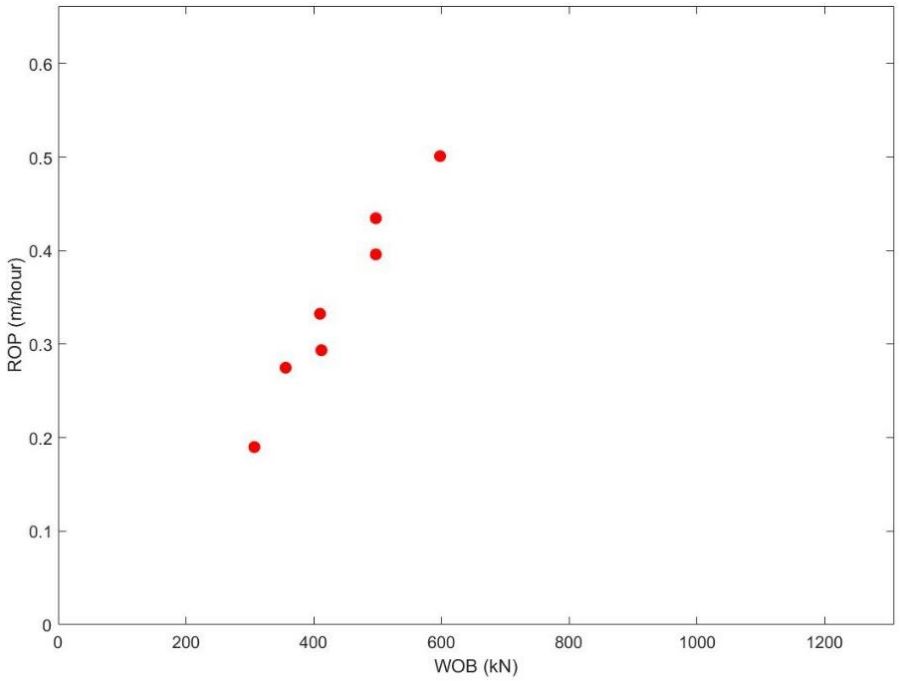

Figure 5-7 Representative curve of a field drilling test performed in hard formation with a 1.5 m diameter RBM.

Figure 5-8 shows that the "drillability constant" of the Maurer model also has a linear dependence on the WOB. Based on this relationship, the drillability coefficient and the drillability constant term can be defined by Eqn. (5-6).

Figure 5-9 shows a comparison between the real ROPs and the predicted ROPs by Eqn. (5-7). From the graph, the de Moura and Butt model presents high-accuracy ($\alpha = 0.9981$) and predicts the drilling performance with low data dispersion ($R^2 = 0.9861$, $S_{y,x} = 0.014$ m/h, and $RS_{y,x} = 2.98$ %).

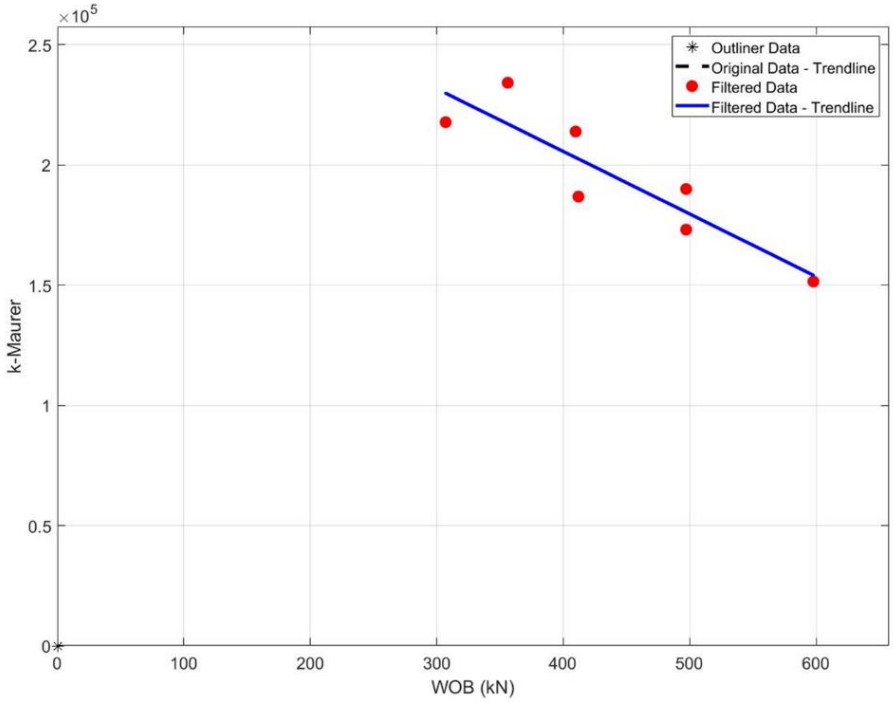

Figure 5-8 Drillability constant (Eqn. (5-5)) as a relation to the WOB for a field drilling test performed in hard formation with a 1.5 m diameter RBM.

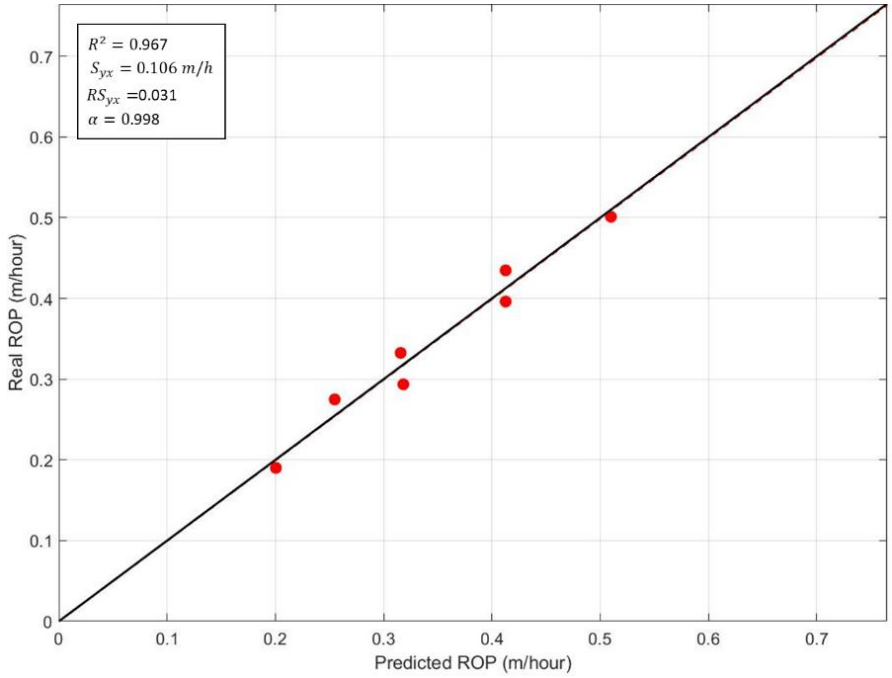

Figure 5-9 Comparison between the ROP of a field drilling test performed in hard formation with a 1.5 m diameter RBM and the ROP predicted by Eqn. (5-7).

5.5.3 Other Large Diameter Drilling Operations

Table 5-1 shows 19 distinct large diameter drilling operations that were analyzed to evaluate the de Moura and Butt model's accuracy including two scenarios analyzed in the previous sections. In this evaluation, RBM and TBM operations were analyzed with UCS varying between 81.60 and 224.10 MPa (different rock formations such as the shale, basalt, quartz, gneiss, and syenite).

Table 5-1 Comprehensiveness Evaluation of Eqn. (5-7).

Bit OD [mm]	**Mach.**	**Rock Type**	**UCS [MPa]**	R^2	**α**	$S_{y,x}$ **[m/h]**	$SR_{y,x}$ **[%]**	**Ref**
2600	RBM	Shale and basalt	84.57	0.2126	1.0261	1.318	84.07	[28]
1500	RBM	Quartz	175.00	0.9861	0.9990	0.014	2.97	[12]
1500	RBM	Quartz	175.00	0.9676	1.0262	0.016	2.95	[12]
1500	RBM	Quartz	175.00	0.9867	1.0018	0.046	6.76	[12]
1500	RBM	Quartz	175.00	0.9981	1.0007	0.024	4.91	[12]
1500	RBM	Quartz	175.00	0.9667	0.9981	0.011	3.06	[12]
1500	RBM	Quartz	175.00	0.9609	1.0067	0.076	15.06	[12]
1500	RBM	Quartz	175.00	0.9996	0.9999	0.003	0.49	[12]
1060	RBM	Granitic Gneiss	244.00	0.9944	0.9976	0.150	6.34	[29]
2134	RBM	Granodiorite	150.00	0.9985	0.9944	0.068	9.27	[29]
660	RBM	Syenite	150.00*	0.0683	1.0009	1.091	36.17	[29]
1524	RBM	-	224.10	0.0017	1.0000	0.231	18.83	[30]
2600	RBM	Basalt	81.60	0.1928	1.0162	1.397	88.06	[31]
10000*	TBM	Gneiss	122.00	0.9212	1.0051	0.136	16.92	[27]
10000*	TBM	Gneiss	122.00	0.8059	1.0262	0.251	27.66	[27]
10000*	TBM	Gneiss	122.00	0.8885	1.0077	0.195	17.48	[27]

10000*	TBM	Gneiss	122.00	0.9082	0.9857	0.046	4.38	[27]
10000*	TBM	Gneiss	122.00	0.6404	0.9998	0.263	16.08	[27]
10000*	TBM	Gneiss	122.00	0.7996	0.9994	0.138	9.31	[27]
			Mean	0.7525	1.0048	0.288	19.51	
			Standard Deviation	0.3411	0.0109	0.435	24.52	

* assumed value

A comprehensive evaluation of Eqn. (5-7) is very complex due to the reliability and accuracy of each drilling scenario available in the literature. However a global analysis of the results is a very good indication to the accuracy of Eqn. (5-7) to predict a drilling performance. Table 1 shows that Eqn. (5-7) has high accuracy in predicting the RBM and TBM drilling performance even in high-dispersion data-sets. In general terms, the de Moura and Butt model presented an average α of 1.0048 with a standard deviation of 0.0109 to predict the 19 large diameter drilling performances analyzed in this paper.

From Table 5-1, the highest data-set dispersion is shown in line 12 where $R^2 = 0.0017$, $S_{y,x} = 0.231\ m/h$, and $RS_{y,x} = 18.83\%$. In this case, despite the high dispersion of the data-set, Eqn. (5-7) presented a high accuracy in predicting the drilling performance ($\alpha = 1.000$). The lowest-accuracy use of Eqn. (5-7) to predict the drilling performance is shown in line 15 where $\alpha = 1.0262$ is associated with a relatively high data dispersion ($R^2 = 0.8059$, $S_{y,x} = 0.251\ m/h$, and $RS_{y,x} = 27.66\%$). Figure 5-10 and Figure 5-11 show a comparison between the real ROP and the predicted ROP by Eqn. (5-7) for both the drilling scenarios mentioned above, respectively.

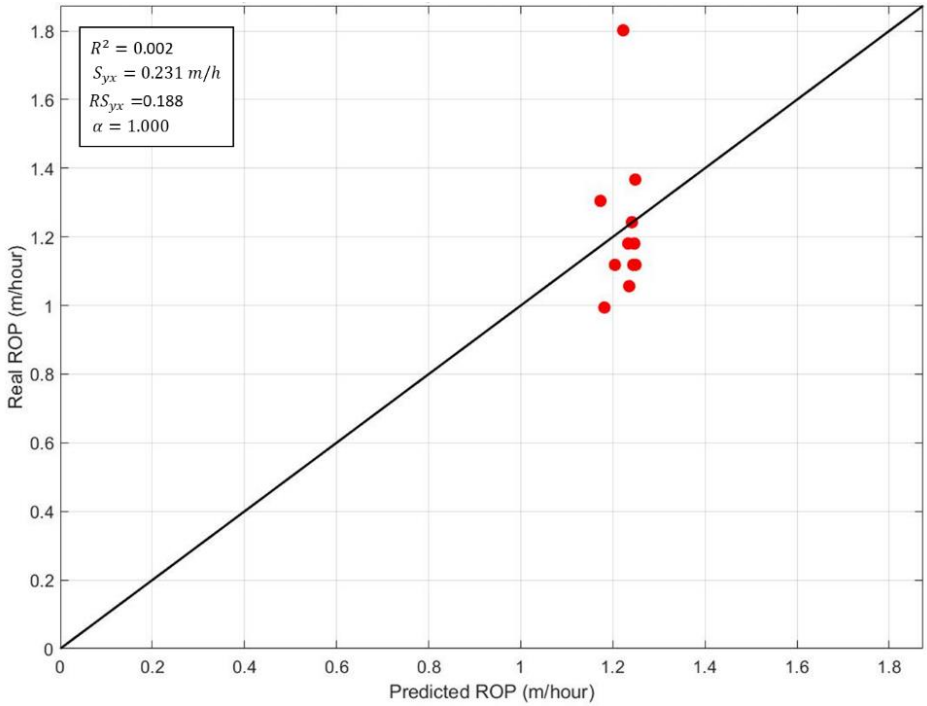

Figure 5-10 Comparison between the ROP of the drilling scenario on line 12 of Table 1 and the ROP predicted by Eqn. (5-7).

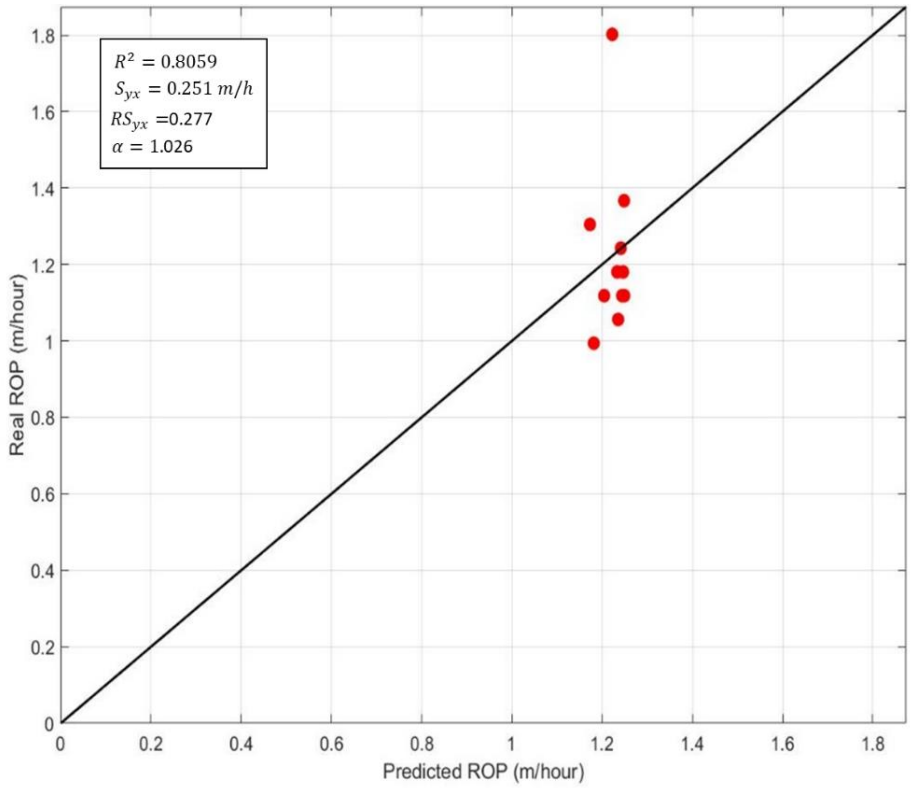

Figure 5-11 Comparison between the ROP of the drilling scenario on line 15 of Table 1 and the ROP predicted by Eqn. (5-7).

5.5.4 Comparative Analysis between the CSM, Gehring, and de Moura and Butt Model

As mentioned in Section 5.5.1, Wilfing *et al.* compared the CSM and Gehring models with real TBM performance data-sets. Based on their work and based on the assumptions and considerations mentioned in Section 5.5.1, a comparative analysis between these models and the de Moura and Butt model is possible.

Figure 5-12 shows the de Moura and Butt, CSM, and Gehring models applied to a real TBM performance in a very hard formation (UCS = 122 MPa) with friction of 3,805 kN, and the assumptions mentioned in Section 5.5.1. Both the real ROP and the predicted ROP by the CSM and Gehring models were presented by Wilfing *et al.* (details in [27]). From the graph, the CSM model underestimated and the Gehring model overestimated the ROP values for this specific TBM application, presenting low accuracy in predicting this scenario, while the de Moura and Butt model presented high accuracy.

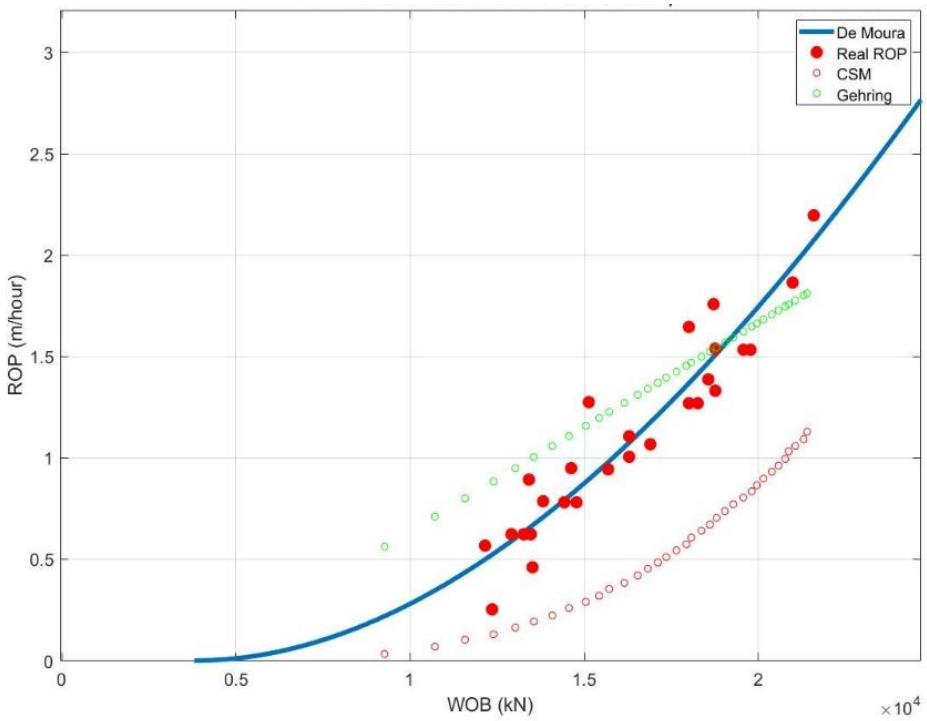

Figure 5-12 Comparison between the ROP of a TBM field performance test performed in a very hard formation with 80 disc cutters and a friction of 3,805 kN for CSM, Gehring and de Moura and Butt models.

Similarly, Figure 5-13 shows the de Moura and Butt, CSM, and Gehring models applied to a real TBM performance in a very hard formation (UCS = 122 MPa), with friction of 3,523 kN (details in [27]) and the assumptions mentioned in Section 5.5.1. From the graph, the CSM and Gehring models presented low accuracy in predicting this drilling performance, underestimating the ROP values, while the de Moura and Butt model presented high accuracy.

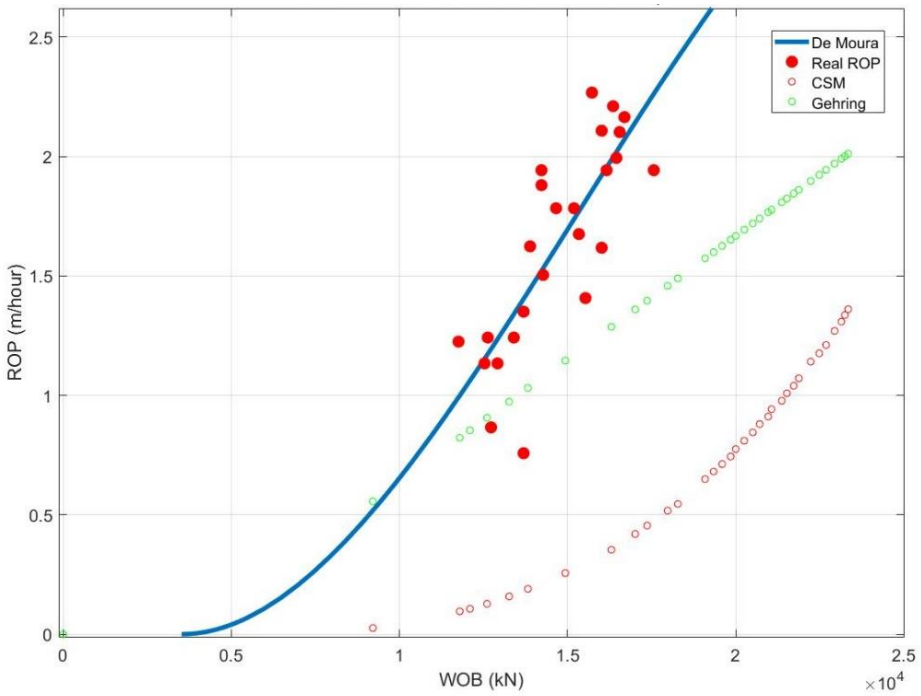

Figure 5-13 Comparison between the ROP of a TBM field performance test performed in a very hard formation with 80 disc cutters and a friction of 3,52 3 kN for CSM, Gehring and de Moura and Butt models.

5.5.5 The existence of the Founder Point in the Large Diameter Drilling Operations

In oil and gas drilling, the existence of the founding point is something known and explored despite the research scarcity on this topic. The founder point is a primordial factor for knowing the complete drilling performance curve and drilling process optimization. Additionally, the founder point permits a comparison between different drilling scenarios.

The existence of a founder point in large diameter drilling operations is an unexplored field because of the limitation imposed by excavation machines, disc cutters, or both. As the founder point is the local maximum point of the drilling performance curve, its location involves applying the highest thrust force possible for a specific drilling scenario, which is normally bigger than the equipment capacity involved in an excavation process.

Figure 5-14 and Figure 5-15 strongly suggest the founder point's existence in two distinct RBM drilling operations. Figure 5-14 refers to a RBM drilling operation in black shale and a submarine basalt complex formation (UCS = 84.57 MPa) with a cutterhead diameter of 2.6 m [28], and Figure 5-15 refers to another RBM drilling operation now in a syenite formation (UCS = 150 MPa) with a cutterhead diameter of 0.66 m [29].

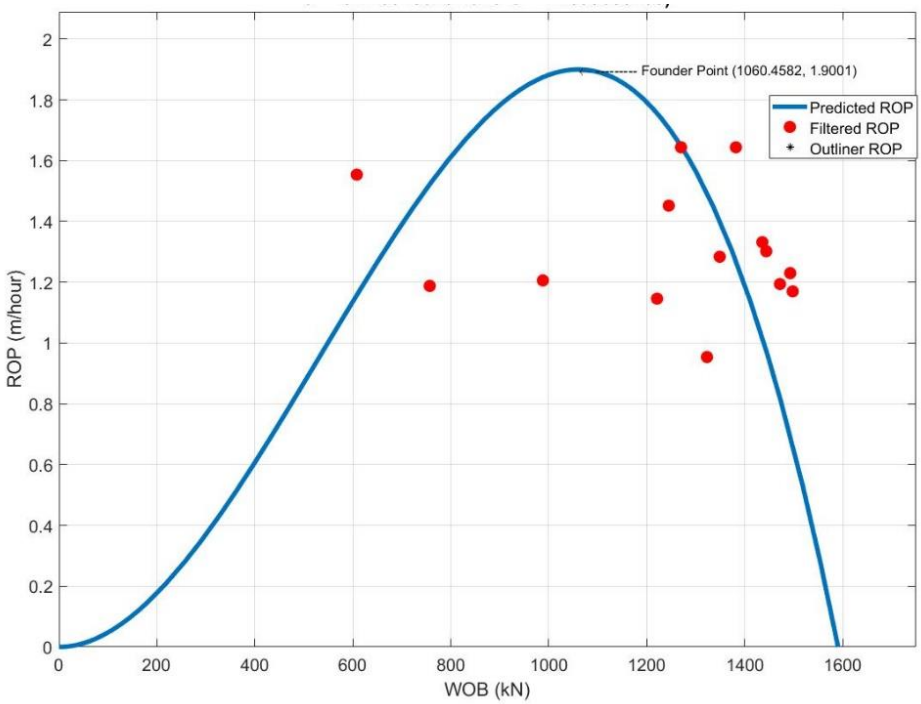

Figure 5-14 Comparison between the ROP of a RBM drilling operation of 2.6 m diameter and de Moura and Butt models including the founder point location.

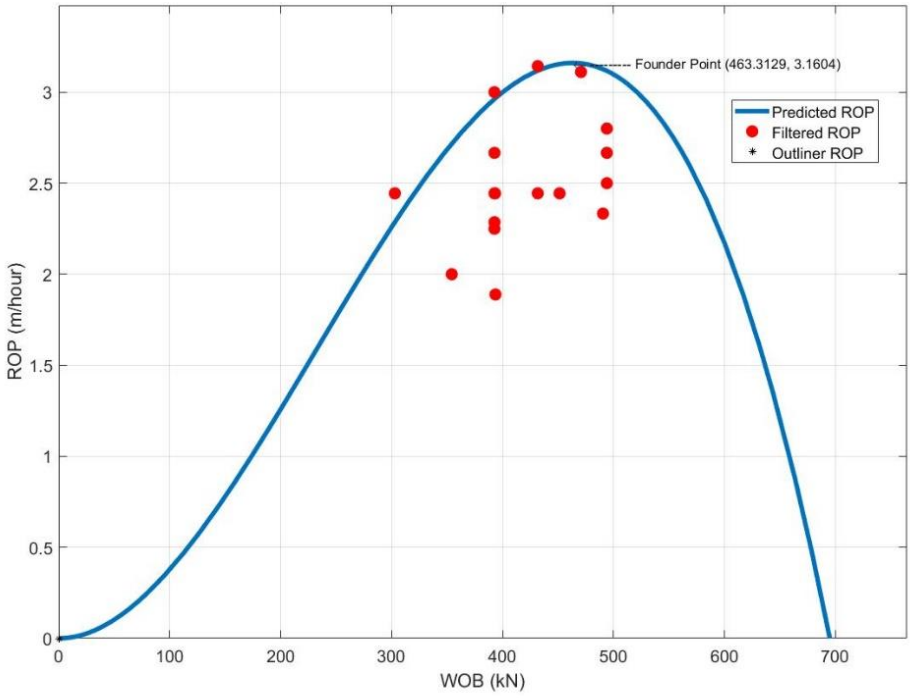

Figure 5-15 Comparison between the ROP of a RBM drilling operation of 0.66 m diameter and de Moura and Butt models including the founder point location.

5.6 Conclusion

In general terms, the comprehensiveness of the de Moura and Butt model for large diameter drilling operations proved to be effective in showing high accuracy (an average α of 1.0048 with a standard deviation of 0.0109) in predicting the drilling performance of 19 distinct RBM and TBM applications, even in the face of high data dispersion (an average R^2 of 0.7525 with a standard deviation of 0.3411, an average $S_{y,x}$ of 0.288 m/h with a standard deviation of 0.435 m/h, and an average $RS_{y,x}$ of 19.51% with a standard deviation of 24.52%). According to this paper's outcomes, the linear relationship between the "drillability constant" of the Maurer model and the WOB, observed by de Moura *et al.*[1], is present in a large diameter drilling context permitting successful application of the de Moura and Butt model for this drilling scenario. All peculiar characteristics

of large diameter drilling, such as rock mass properties, are absorbed by the drillability coefficient and drillability constant terms of the de Moura and Butt model.

During the analysis of a TBM performance with 80 disc cutters (17 inches diameter) in very hard rock formation, similarity to a typical oil and gas drilling performance curve, this TBM performance application was identified. Wilfing *et al.* highlighted the existence of a TBM performance curve region called the "subcritical penetration" where, in low ROPs, only a crushing process is present and a chipping process does not occur [27]. This region is related to the region called "inadequate depth of cut" in the oil and gas drilling context. In this region, the drilling mechanism is different than the other stages of the drilling process and needs to be disregarded during the application of a prediction model.

The de Moura and Butt model was compared to the CSM and Gehring models in two specific TBM applications [27]. In the first application, the CSM model underestimates and the Gehring model overestimates the ROP presenting a low accuracy, while the de Moura and Butt model demonstrates high accuracy to predict this TBM application. In the second one, the CSM and Gehring models also presented low-accuracy, underestimating ROP values, while the de Moura and Butt model kept its high accuracy.

In the last section of this paper the founder point's existence in large diameter drilling performance was discussed. According to both RBM applications shown, there is a strong indication of the existence of this point in large diameter drilling applications but its existence needs to be researched more.

5.7 Acknowledgments

The authors greatly thank the technical and financial support of Novamera Inc., Memorial University of Newfoundland, and MITACS through the Sustainable Mining by Drilling (SMD) project. Without their support, this paper could not have achieved its results.

5.8 Nomenclature

a	Drillability Coefficient
b	Drillability Constant Term
BI	Intact Rock Brittleness
BTS	Brazilian Tensile Strength, MPa
CSM	Colorado School of Mines
D	Drill Bit Diameter, mm
DOT	Drill-Off Test
FPI	Field Penetration Index
GSI	Geological Strength Index
k	Drillability Constant
K	Drillability Linear Equation
N	Rotary Speed, rpm
R	Rate of Penetration, m/h
RBM	Raise Boring Machine
RMR	Rock Mass Rating
ROP	Rate of Penetration, m/h

R^2	Coefficient of Determination
S	Rock Strength, MPa
$S_{y,x}$	Standard Error of Estimate, m/h
$SR_{y,x}$	Relative Standard Error of Estimate
TBM	Tunnel Boring Machine
UCS	Unconfined Compressive strength, MPa
W	Weight on Bit, kN
WOB	Weight on Bit, kN
W_0	Threshold WOB Before Cratering, kN
x	Predicted ROP, m/h
y	Real ROP, m/h
α	Slope of Least-Squares Linear Fit Curve with Origin Fixed at (0,0)
β	Constant Term of Least-Squares Linear Fit
γ	Constant Coefficient of Least-Squares Linear Fit

5.9 References

[1] J. de Moura, Y. Xiao, D. Ahmed, J. Yang and S. D. Butt, "Widening Drilling Operation: Performance Analysis on the Application of Fixed Cutter Drill Bits in Hard Rock Formation," in *ASME 39th International Conference on Ocean, Offshore and Arctic Engineering*, Virtual Conference-online, Aug. 2020, p. 10.

[2] A. Shaterpour-Mamaghani, H. Copur, E. Dogan, and T. Erdogan, "Development of new empirical models for performance estimation of a raise boring machine," *Tunnelling and*

Underground Space Technology, vol. 82, pp. 428–441, Dec. 2018, doi: 10.1016/j.tust.2018.08.056.

[3] Y. L. Zheng, Q. B. Zhang, and J. Zhao, "Challenges and opportunities of using tunnel boring machines in mining," *Tunnelling and Underground Space Technology*, vol. 57, pp. 287–299, Aug. 2016, doi: 10.1016/j.tust.2016.01.023.

[4] G. Barla and S. Pelizza, "TBM Tunnelling in Difficult Ground Conditions," presented at the ISRM International Symposium, Nov. 2000, Accessed: Dec. 08, 2020. [Online]. Available: https://www.onepetro.org/conference-paper/ISRM-IS-2000-037.

[5] P. C. Graham, "Rock Exploration for Machine Manufacturers," in *Exploration for Rock Engineering*, Johannesburg, 1976, p. 8.

[6] I. W. Farmer and N. H. Glossop, "Mechanics of disc cutter penetration," *International Journal of Rock Mechanics and Mining Sciences & Geomechanics Abstracts*, vol. 12, no. 6, pp. A123–A124, Jul. 1980, doi: 10.1016/0148-9062(80)90769-X.

[7] S. Yagiz, J. Rostami, and L. Ozdemir, "Colorado School of Mines Approaches For Predicting TBM Performance," presented at the ISRM International Symposium - EUROCK 2012, May 2012, Accessed: Dec. 06, 2020. [Online]. Available: https://www-onepetro-org.qe2a-proxy.mun.ca/conference-paper/ISRM-EUROCK-2012-047?sort=&start=0&q=Colorado+School+of+Mines+approaches+for+predicting+TBM+performance&from_year=&peer_reviewed=&published_between=&fromSearchResults=true&to_year=&rows=25#.

[8] L. Ozdemir, "Development of theoretical equations for predicting tunnel borability," PhD Thesis, Colorado School of Mines, Golden, CO, 1977.

[9] C. Hegde, H. Daigle, H. Millwater, and K. Gray, "Analysis of rate of penetration (ROP) prediction in drilling using physics-based and data-driven models," *Journal of Petroleum*

Science and Engineering, vol. 159, pp. 295–306, Nov. 2017, doi: 10.1016/j.petrol.2017.09.020.

[10] J. Autio and T. Kirkkomäki, *Boring of full scale deposition holes using a novel dry blind boring method*. Helsinki: Posiva, 1996.

[11] J. Rostami and L. Ozdemir, "A new model for performance prediction of hard rock TBMs," in *11th Rapid Excavation and Tunneling Conference*, Boston, MA, 1993, p. 18.

[12] S. Yagiz, "Development of rock fracture and brittleness indices to quantify the effects of rock mass features and toughness in the CSM model basic penetration for hard rock tunneling machines," Thesis, Colorado School of Mines, 2001.

[13] S. Yagiz, "A Model for prediction of tunnel boring machine performance," presented at the 10th congress of the International Association for Engineering Geology and the Environment, London, Nottingham, Sep. 2006.

[14] M. Ataei, R. KaKaie, M. Ghavidel, and O. Saeidi, "Drilling rate prediction of an open pit mine using the rock mass drillability index," *International Journal of Rock Mechanics and Mining Sciences*, vol. 73, pp. 130–138, Jan. 2015, doi: 10.1016/j.ijrmms.2014.08.006.

[15] A. S. Mamaghani, E. Avunduk, and N. Bilgin, "Rock mechanical aspects of excavation related to raise boring machine – A typical example from Asikoy underground mine, Kastamonu, Turkey," presented at the EUROCK 2015 & 64th Geomechanics Colloquium, Salzburg, Oct. 2015.

[16] J. Rostami, "Performance prediction of hard rock Tunnel Boring Machines (TBMs) in difficult ground," *Tunnelling and Underground Space Technology*, vol. 57, pp. 173–182, Aug. 2016, doi: 10.1016/j.tust.2016.01.009.

[17] G. Armetti, M. R. Migliazza, F. Ferrari, A. Berti, and P. Padovese, "Geological and mechanical rock mass conditions for TBM performance prediction. The case of 'La

Maddalena' exploratory tunnel, Chiomonte (Italy)," *Tunnelling and Underground Space Technology*, vol. 77, pp. 115–126, Jul. 2018, doi: 10.1016/j.tust.2018.02.012.

[18] M. H. Arbabsiar, M. A. Ebrahimi Farsangi, and H. Mansouri, "A new model for predicting the advance rate of a Tunnel Boring Machine (TBM) in hard rock conditions," *MGPB*, vol. 35, no. 2, pp. 57–74, 2020, doi: 10.17794/rgn.2020.2.6.

[19] M. Hedayatzadeh, K. Shahriar, and J. K. Hamidi, "An Artificial Neural Network model to predict the performance of hard rock TBM," in *ISRM International Symposium 2010 and 6th Asian Rock Mechanics Symposium - Advances in Rock Engineering*, New Delhi, India, Oct. 2010, p. 7.

[20] J. Hassanpour, J. Rostami, and J. Zhao, "A new hard rock TBM performance prediction model for project planning," *Tunnelling and Underground Space Technology*, vol. 26, no. 5, pp. 595–603, Sep. 2011, doi: 10.1016/j.tust.2011.04.004.

[21] Y. Ge, J. Wang, and K. Li, "Prediction of hard rock TBM penetration rate using least square support vector machine," *IFAC Proceedings Volumes*, vol. 46, no. 13, pp. 347–352, 2013, doi: 10.3182/20130708-3-CN-2036.00105.

[22] A. C. Adoko, C. Gokceoglu, and S. Yagiz, "Bayesian prediction of TBM penetration rate in rock mass," *Engineering Geology*, vol. 226, pp. 245–256, Aug. 2017, doi: 10.1016/j.enggeo.2017.06.014.

[23] A. Salimi, J. Rostami, C. Moormann, and J. Hassanpour, "Examining Feasibility of Developing a Rock Mass Classification for Hard Rock TBM Application Using Non-linear Regression, Regression Tree and Generic Programming," *Geotech Geol Eng*, Oct. 2017, doi: 10.1007/s10706-017-0380-z.

[24] M. Samaei, M. Ranjbarnia, V. Nourani, and M. Zare Naghadehi, "Performance prediction of tunnel boring machine through developing high accuracy equations: A case study in adverse

geological condition," *Measurement*, vol. 152, p. 107244, Feb. 2020, doi: 10.1016/j.measurement.2019.107244.

[25] X. Chen, J. Yang, and D. Gao, "Drilling Performance Optimization Based on Mechanical Specific Energy Technologies," in *Drilling*, A. Samsuri, Ed. InTech, 2018, pp. 133–162.

[26] H. Khorshidian, S. D. Butt, and F. Arvani, "Influence of high velocity jet on drilling performance of PDC bit under pressurized condition," presented at the 48th US Rock Mechanics/Geomechanics Symposium, Minneapolis, MN, Jun. 2014.

[27] L. Wilfing, H. Kasling, and K. Thuro, "Improvement of Penetration Prediction In TBM-Tunneling by Performing on-Site Penetration Tests," in *13th International Congrss of Rock Mechanics*, Montreal, Quebec, May 2015, p. 11.

[28] A. Shaterpour-Mamaghani, N. Bilgin, C. Balci, E. Avunduk, and C. Polat, "Predicting Performance of Raise Boring Machines Using Empirical Models," *Rock Mech Rock Eng*, vol. 49, no. 8, pp. 3377–3385, Aug. 2016, doi: 10.1007/s00603-015-0900-1.

[29] A. Lislerud and P. Vainionpää, "Application of raiseboring for excavating horizontal tunnels with Rhino machines," Posiva, Helsinki, Finland, Working Report 97–56e, 1997.

[30] W. K. Tony Seller, "Hard Rock Boring with Tungsten Carbide Insert Big Hole Cutters," presented at the The 12th U.S. Symposium on Rock Mechanics (USRMS), Jan. 1970, Accessed: Dec. 08, 2020. [Online]. Available: https://www.onepetro.org/conference-paper/ARMA-70-0961.

[31] A. Shaterpour-Mamaghani and N. Bilgin, "Some contributions on the estimation of performance and operational parameters of raise borers – A case study in Kure Copper Mine, Turkey," *Tunnelling and Underground Space Technology*, vol. 54, pp. 37–48, Apr. 2016, doi: 10.1016/j.tust.2016.01.027.

Chapter 6 Drillability Coefficient and Drillability Constant Term

6.1 Introduction

As mentioned in Chapters 3, 4, and 5, the de Moura and Butt model has high accuracy to predict the drilling performance for three distinct drilling scenarios: fixed cutter drill bits, roller-cone drill bits, and large drilling diameter. The relevance of this model is in its capability to unify the drilling performance prediction of three distinct drilling scenarios, which have a considerable difference between their drilling mechanics, in a unique model. The de Moura and Butt model, being a universal rotary drilling model, is a direct effect of the capability of its constants (drillability coefficient and the drillability constant term) to absorb the significant difference between these drilling scenarios. The general behavior analysis of these constants is disserted in the following sections based on the drilling scenarios analyzed in Chapters 3, 4, and 5. However, this analysis has a qualitative character, because when a specific parameter is analyzed, the other parameters are not kept constant, generating influence on each other. In other words, this chapter aims to present a qualitative analysis of the de Moura and Butt model constants and not a parametric analysis, due to the characteristics of the data-sets available.

6.2 General Behavior of the Constants of the de Moura and Butt Model

The drillability coefficient (a) and the drillability constant term (b) were determined for each drilling scenario presented in Chapters 3, 4, and 5. Figure 5-1 shows the values of a and b

determined to approximately 80 distinct drilling performance curves that were grouped in the three drilling scenarios: fixed cutter, roller-cone, and large diameter. From the graph, the association between the constants' behaviour and the drilling scenarios are easily identified.

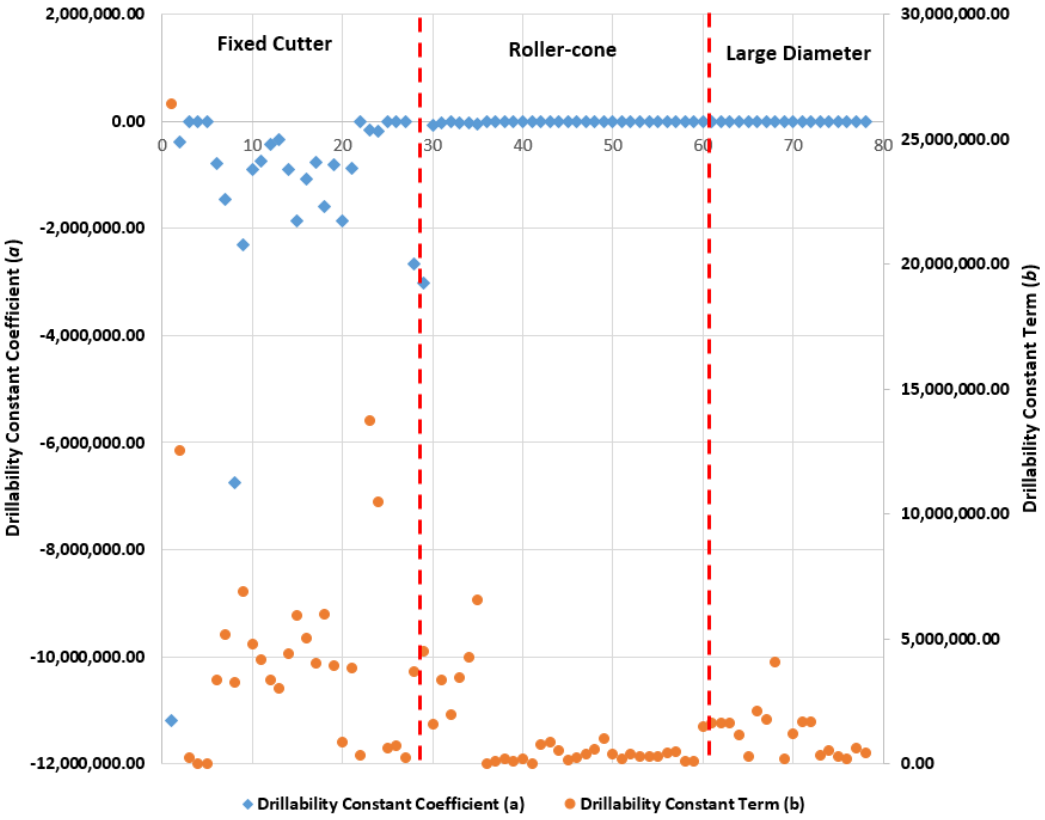

Figure 6-1 General behavior of the de Moura and Butt Model constants.

Figure 6-2 shows the same data of Figure 6-1 but now restricted to the roller-cone drill bits and large diameter drilling scenarios.

In following sections, the behavior of the de Moura and Butt Model constants for each specific drilling scenarios is discussed. To analyze the behavior of the de Moura and Butt model, its constants were plotted in relation to three drilling parameters: the unconfined compressive strength (UCS), bit diameter, and rotary speed.

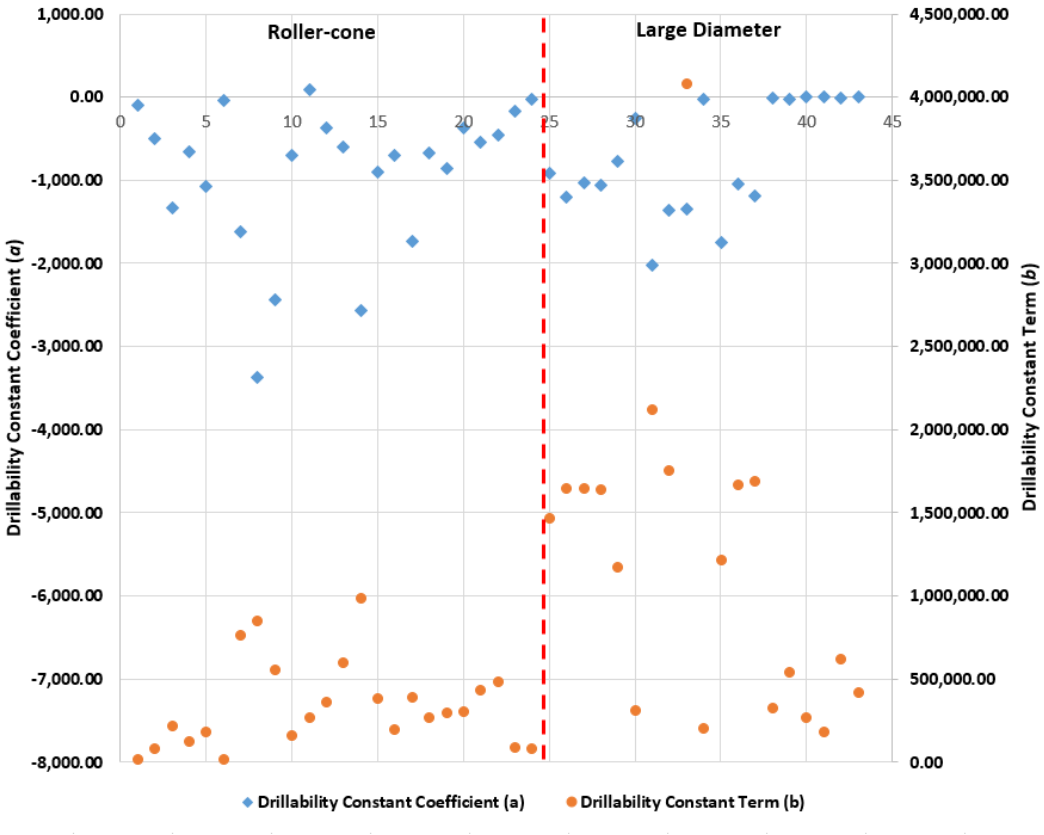

Figure 6-2 The general behavior of the de Moura and Butt Model constants in the face of the roller-cone drill bit, and large diameter drilling applications.

6.2.1 Fixed Cutter Drill Bits

Figure 6-3 shows the *a* and *b* values' behavior in relation to the UCS. From the graphic, there is no evident pattern in the constants behavior. This apparent random behavior can be explained based on the absorption of the drilling mechanics of the fixed cutter drill bits by the model constants. The same behavior of the values of a and b can be seen in Figure 6-4 and Figure 6-5.

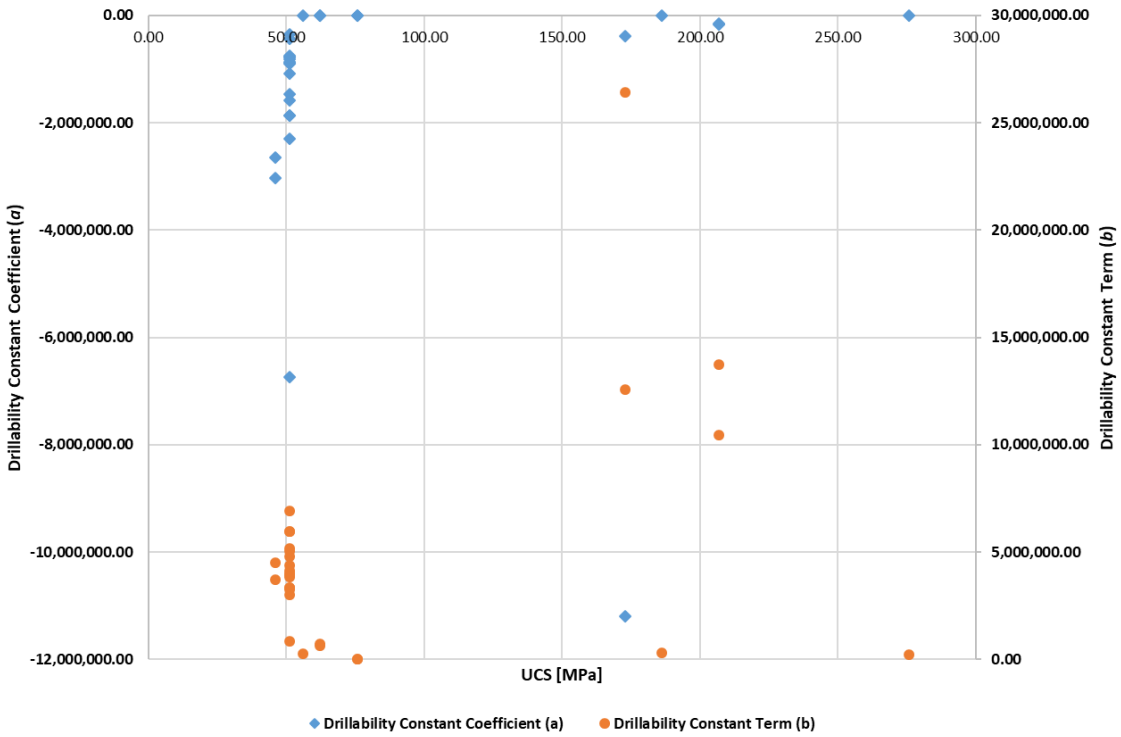

Figure 6-3 The behavior of the de Moura and Butt Model constants in the face of the UCS variation for fixed cut drills.

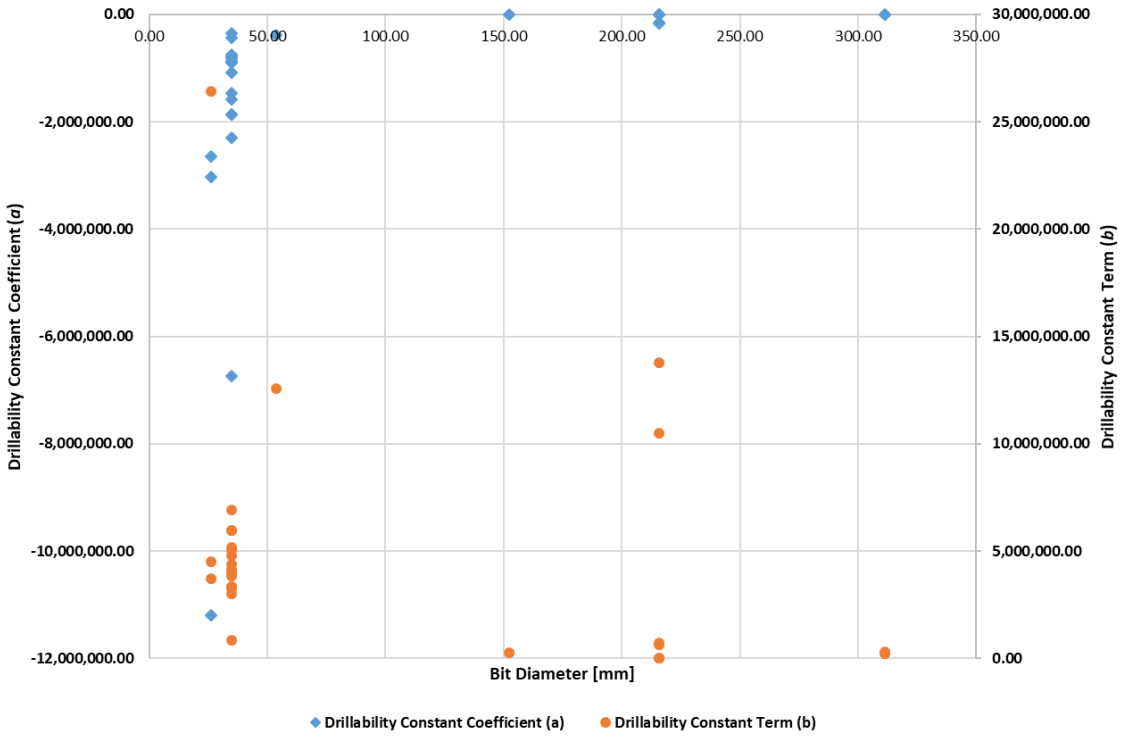

Figure 6-4 The behavior of the de Moura and Butt Model constants in the face of the bit diameter variation for fixed cut drills.

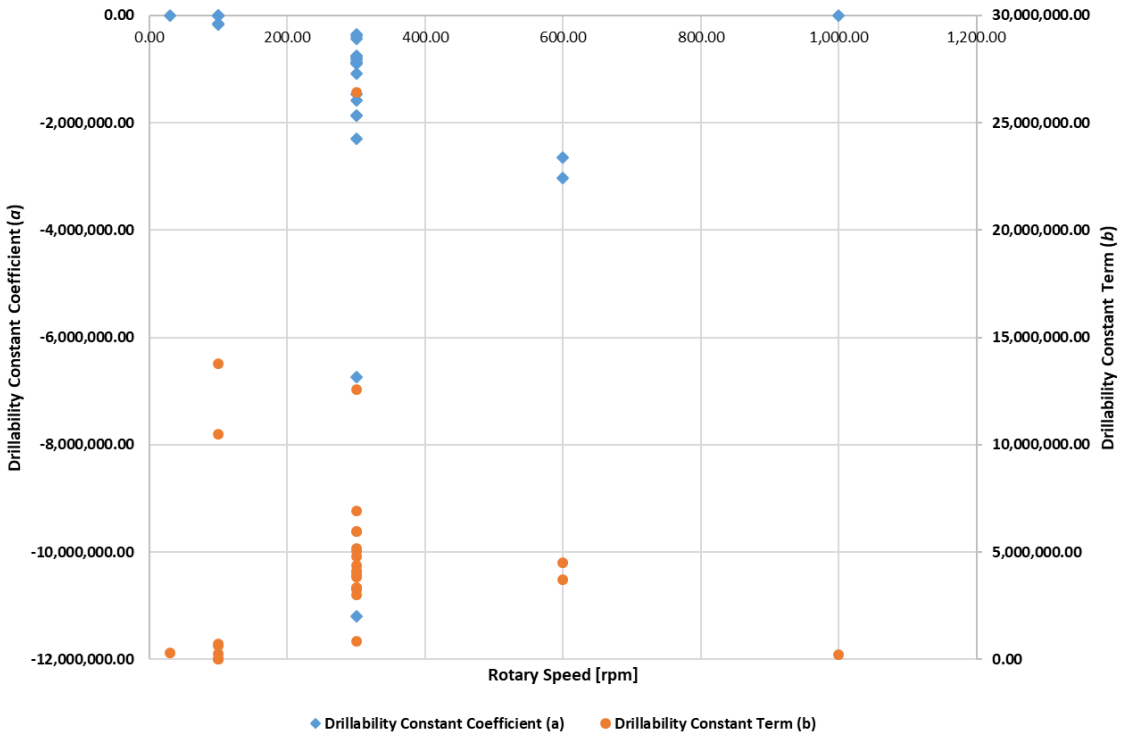

Figure 6-5 The behavior of the de Moura and Butt Model constants in the face of the rotary speed variation for fixed cut drills.

6.2.2 Roller-Cone Drill Bits

Figure 6-6 shows the behavior of the de Moura and Butt model constant in the face of the UCS variation for roller-cone drill bits drilling scenarios. In the graph, an expressive influence of this parameter in the values of *b* is observed but the same is not clearly observed in the values of *a*. When the UCS values increase, the *a* values increase as well indicating a possible direct proportion between the UCS and *a*. Due to this observation, there is a strong indication that the variations in the rock strength is absorbed by the drillability constant term of the de Moura and Butt model.

Figure 6-7 shows the behavior of the de Moura and Butt model constant in the face of the bit diameter variation. In the graph, an expressive influence of this parameter in the values of *a* and

b is observed and this influence acts in an inverse manner in the constants' values. When the bit diameter increases, there is a tendency of the values of *a* to increase and the values of *b* to decrease.

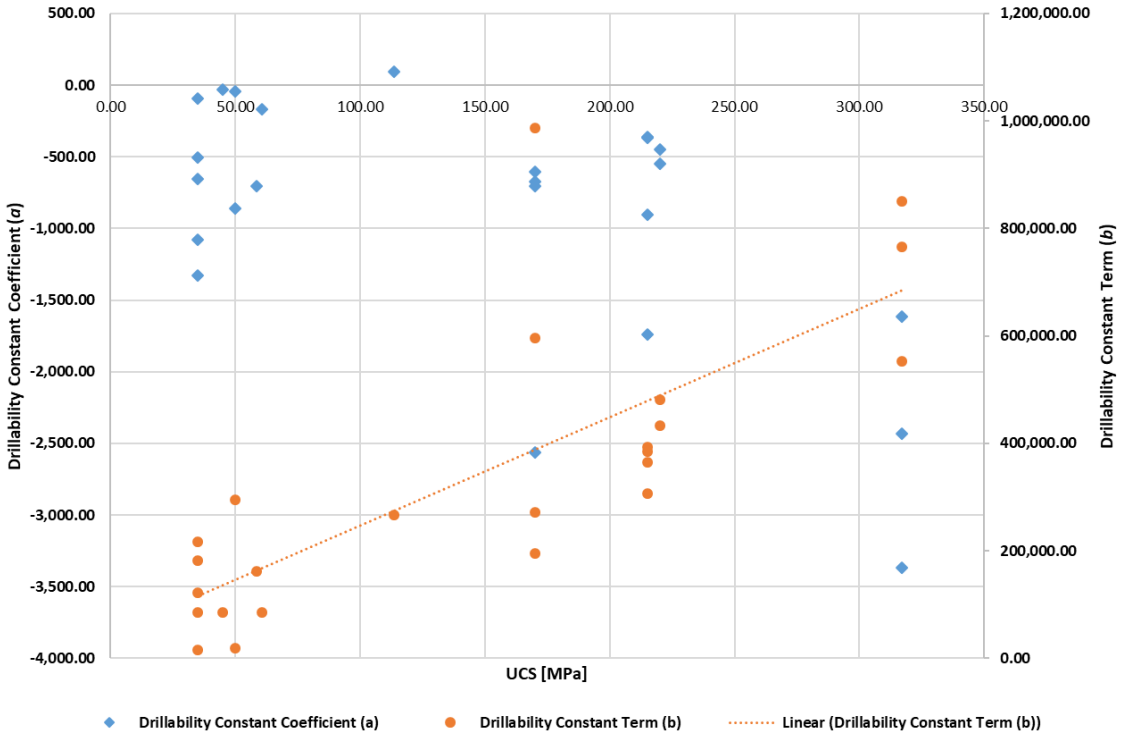

Figure 6-6 The behavior of the de Moura and Butt Model constants in the face of the UCS variation for roller-cone drill bits.

Figure 6-8 shows the behavior of the de Moura and Butt model constant in the face of the rotary speed variation. In the graph, despite the great data dispersion in the low rotary speeds, a suggestive influence of this parameter in the values of *a* and *b* is observed. Apparently, this influence indicates that when the rotary speed increases, the values of *a* decrease and the values of *b* increase.

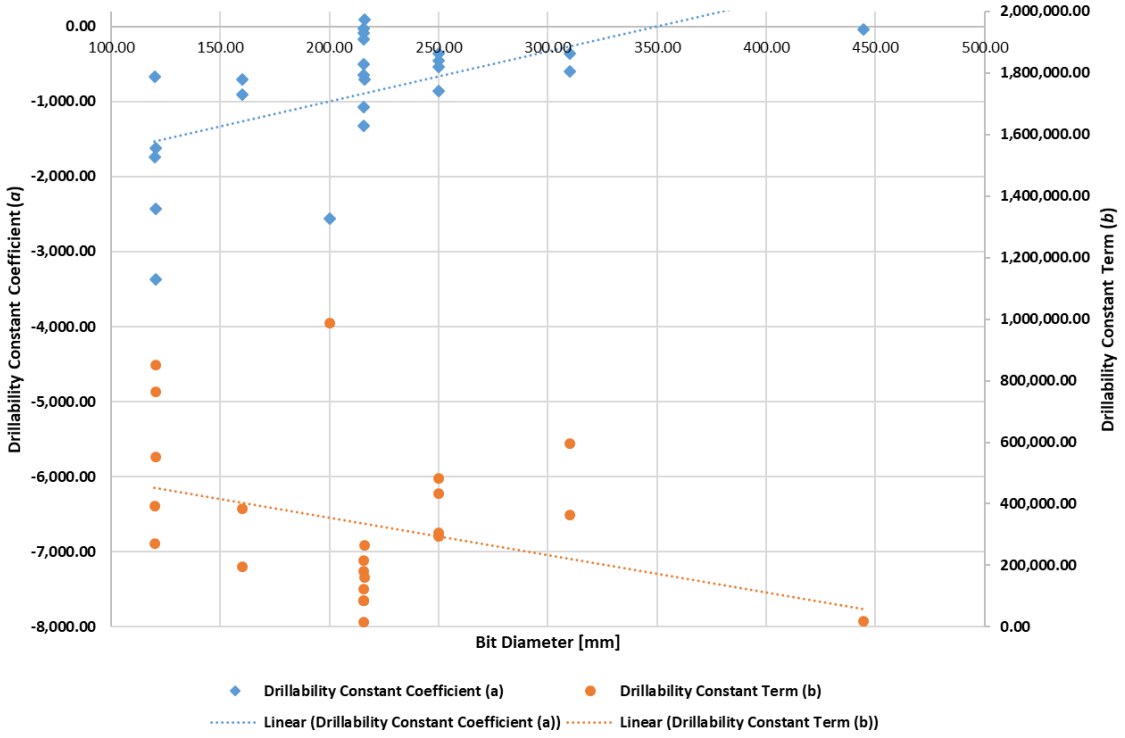

Figure 6-7 The behavior of the de Moura and Butt Model constants in the face of the bit diameter variation for roller-cone drill bits.

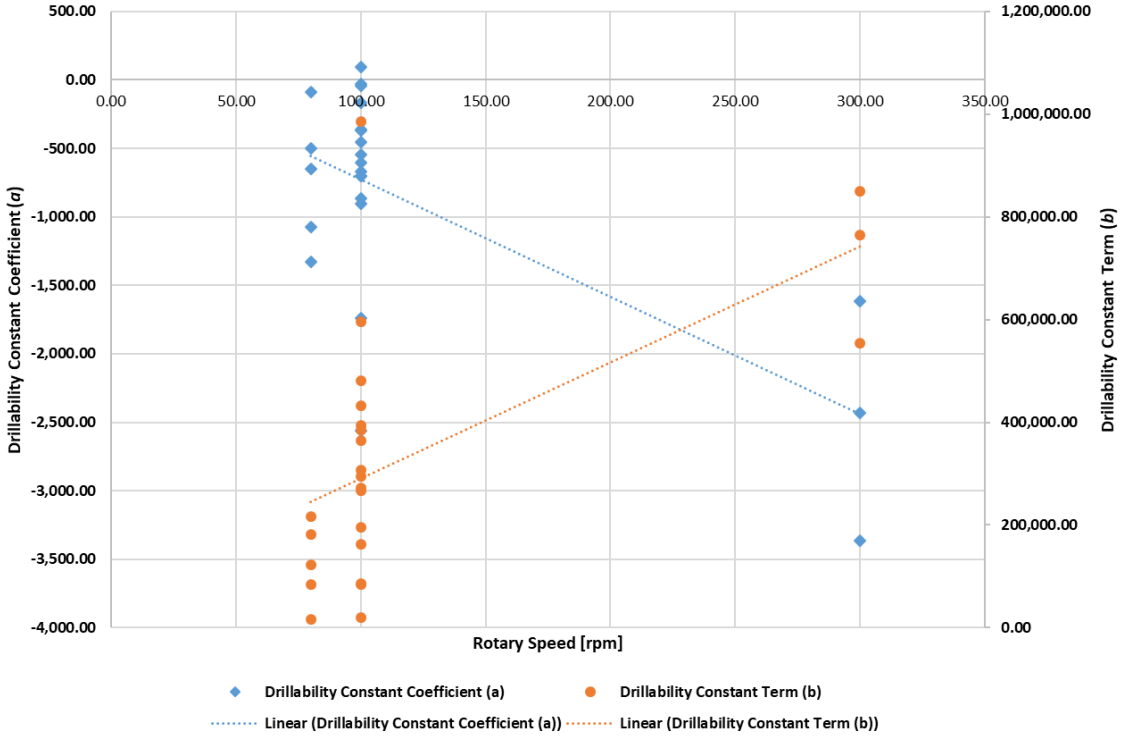

Figure 6-8 The behavior of the de Moura and Butt Model constants in the face of the rotary speed variation for roller-cone drill bits.

6.2.3 Large Diameter Drilling

Figure 6-9 shows the behavior of these constants in the face of the UCS variation. As can be seen, a pattern of behavior of the constants is not evident. This observation is plausible based on the influence of the rock discontinuities in the large diameter drilling performance. In other words, the constants absorb the rock mass characteristics, implying the increase of the complexity in the behavior of these constants when they are analyzed in relation to the UCS.

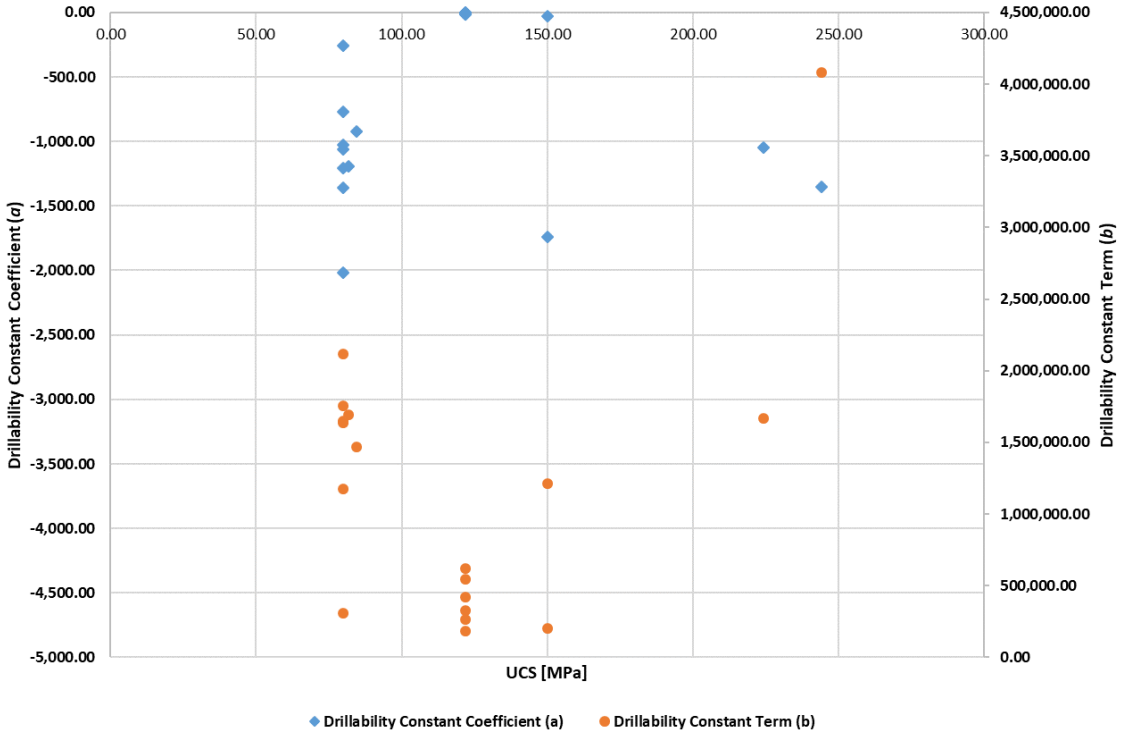

Figure 6-9 The behavior of the de Moura and Butt constants in the face of the UCS variation for large diameter drilling.

Figure 6-10 shows the behavior of the de Moura and Butt model constants in the face of the bit diameter variation. As expected in the large diameter drilling, the graph indicates a plausible influence of the bit diameter in the values of *a* and *b*.

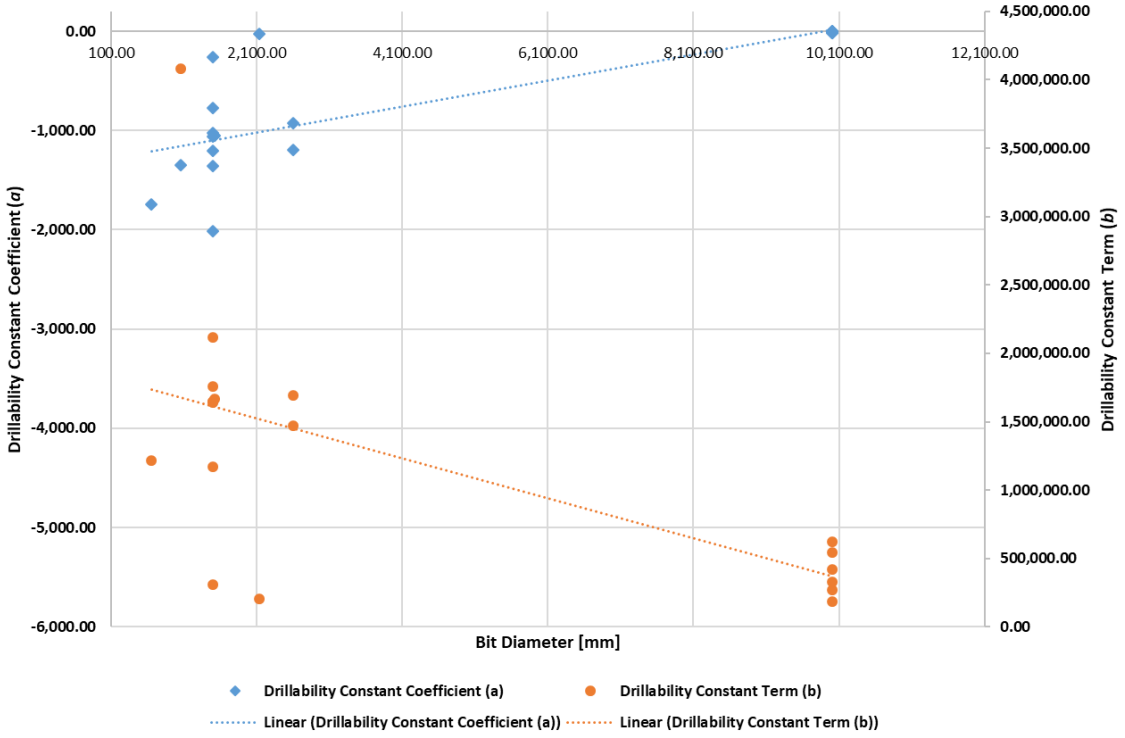

Figure 6-10 The behavior of the de Moura and Butt constants in the face of the bit diameter variation for large diameter drilling.

The same behavior that was previously mentioned is not observed when the constants' values are analyzed in relation to the rotary speed (see Figure 6-11). The high data dispersion and a lack of standard behavior of the de Moura and Butt model constants in this scenario is probably associated with the low velocity used in the large diameter drilling process. This observation is corroborated by the constants' behavior in the roller-cone drill bits in low velocity (see Figure 6-8).

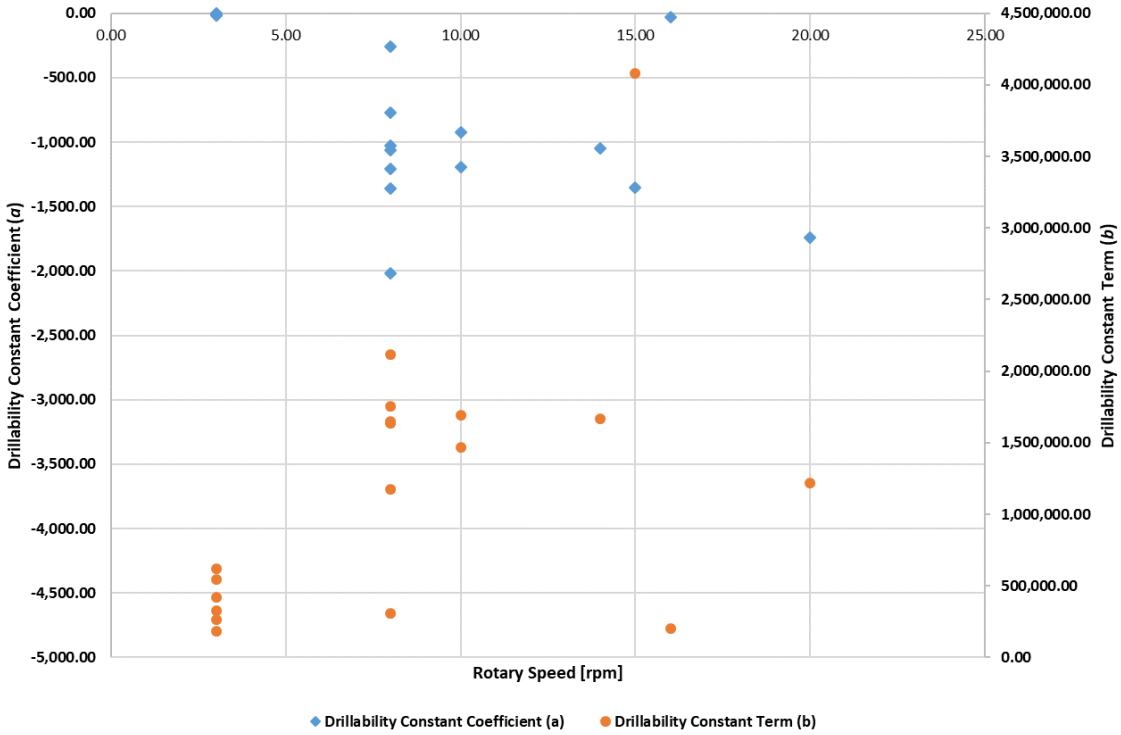

Figure 6-11 The behavior of the de Moura and Butt constants in the face of the rotary speed variation for large diameter drilling.

6.2.4 Conclusion

As mentioned in Chapter 2, there is a similarity between the fragmentation processes of the roller-cone drill bits and the large diameter drilling. This similarity is evident in Figure 6-1 where there is a border in the values of *a* between the fixed cutter drill bits and the union between the roller-cone drill bits and large diameter drilling. Based on this observation, the drillability coefficient is greatly influenced by the fragmentation process. The values of *b* carries the influence of the fragmentation process but this is not as latent as for the values of *a*.

From Figure 6-2, the difference between the drilling mechanics of the roller-cone drill bits and large diameter drilling is practically imperceptible in the values of *a* but pronounced in the

values of *b*. This observation suggests that the impact of the rock discontinuities (joints or other cracks) in the large drilling performance is more absorbed by the values of *b* than the values of *a*.

According to Chapter 3, the de Moura and Butt model was based on the linear dependence of the "drillability constant" of the Maurer model. The Maurer model was derived from rock cratering mechanisms and based on the roller-cone drill bit experiments. In its essence, the de Moura and Butt model is a model for roller-cone drill bit applications, but it showed high accuracy to predict the drilling performance for the fixed cutter drill bits (Chapter 3). This performance of the de Moura and Butt model for fixed cutter drill bits is explained by the capability of its constants to absorb the particularity of all drilling scenarios.

The apparently random behavior of the de Moura and Butt model constants when analyzed in the fixed cutter drill bits scenario can be explained based on the absorption of the drilling mechanics of this scenario by the model constants. In other words, the difference between the drilling mechanics of the fixed cutter drill bits and the roller-cone bits increases the complexity of the model constants.

A pattern of constants' behavior with low complexity is more evident for the roller-cone drill bits than for the fixed cutter drill bits because the de Moura and Butt model is based on the rock cratering mechanisms that are a strong characteristic of the roller-cone drill bits.

The last barrier for the de Moura and Butt model in rotary drilling is large diameter drilling. As mentioned in Chapter 1 and section 6.2, the similarity between the drilling mechanics of the roller-cone drill bits and large diameter drilling is strongly plausible (see Figure 6-1), but the

nuances of the large diameter drilling related to the rock discontinuities (joints or other cracks) suggests an influence in the behavior of the de Moura and Butt model constants.

In the large diameter drilling, the rock mass characteristics are absorbed by the de Moura and Butt model constants, which will imply an increase of the complexity in their behavior when they are analyzed in relation to the UCS. Possibly, the rock mass characteristics, that increased the complexity of the constant behavior in the previous scenario, conducted them to a pattern behavior when their values are analyzed in relation to the bit diameter. In conclusion, low velocity in the large diameter drilling process increases the complexity of the de Moura and Butt model constants.

Chapter 7 Concluding Remarks

7.1 Summary

In this research, the drilling performance was studied for three specific drilling scenarios: fixed cutter drill bits, roller-cone drill bits, and large diameter drilling. In the large diameter drilling study, RBM and TBM drilling operations were analyzed. The fundamental difference between these drilling scenarios is highlighted in their drilling mechanics. In fixed cutter drill bits, there is continuous contact between the cutter and the rock face; a parallel movement of the cutter is observed; and its fragmentation process is based on the shearing action. In the roller-cone drill bits, the drilling mechanisms happen through the chipping and crushing process, which is characterized by a tooth impact; crushed wedge formation; fracture creation and propagation; and debris ejection. In the large diameter drilling, specifically in raise boring machine (RBM) and tunnel boring machine (TBM) operations, the drilling mechanism is similar to the roller-cone drill bits' mechanism in the context of the fragmentation process. This is influenced by the rock discontinuities (joints or other natural cracks) due to the contact with a large area of rock. Because of the significant difference between the drilling mechanisms of these three drilling scenarios, this research was divided in three groups of analysis based on each type of drilling scenario. During the analysis of drilling data-sets, previously conducted in other studies and performed in the laboratory as part of the current study, a new model to predict the drilling performance curve that includes the founder point location was developed. This study is a comprehensive analysis of the drilling performance of the mentioned drilling scenario and shows to be a high precision tool to predict the

rate of penetration for both oil and gas drilling and for mining and construction applications. This model can be considered a universal prediction model for drilling.

The details of this research are provided in Chapters 3, 4, 5, and 6.

7.2 Concluding Remarks

Chapter 3 reports a study of the fixed cutter drill bit drilling performance and the development of a new model to predict the rate of penetration and the founder point location. This research aimed to provide a clear understanding of the development of the new model, including validation and applicability tests in several different fixed cutter drill bit scenarios. From the analysis on drilling data-sets, the "drillability constant" of the Maurer model was plotted as a relation to the Weight on Bit (WOB) and a linear relationship was observed. Based on this linear relationship, the cubic dependence between the Rate of Penetration (ROP) and WOB was proven. This cubic dependence provided the capacity of the new model to determine the founder point location that is a crucial parameter in the optimization of the drilling process. The comparative analysis between the new model and 27 different drilling data sets showed that the new model has high accuracy to predict the complete drilling performance curve for the fixed cutter drill bit drilling scenario. In these drilling scenarios, different bit types; bit diameter; rock formation; Unconfined Compressive Strength (UCS); flow rate; etc. were analyzed.

Chapter 4 reports a scope analysis of the new model that involves the roller-cone drill bit drilling performance. This analysis is not associated with the fixed cutter drill bits analysis (Chapter 3) because of significant differences between their drilling mechanisms and based on the inaccuracy normally present in drilling performance models developed for a specific drilling

scenario. Similar to Chapter 3, the new model was evaluated based on a comparative analysis with several distinct drilling scenarios. For roller-cone drill bit drilling, the new model showed high accuracy to predict the rate of penetration and locate the founder point. Additionally, equations to calculate the founder point location were introduced based on the fact that the founder point is the local maximum of the drilling performance curve.

Chapter 5 is the conclusion of the scope analysis of applicability and accuracy of the new model. In this chapter, the scope border of the new model was surpassed, including the large diameter drilling in its domain. Before this step, the new model was restricted to the inch-diameter bits, where rock mass properties - such as joints and cracks - have low or no impact in the drilling performance, and now its reach includes the meter-diameter bits. This chapter was an important step in the direction of a universal prediction model for rotary drilling. This study included the RBM and TBM drilling operations with diameters varying between 0.66 m to 10 m. The new model presented high accuracy to predict the drilling performance in 19 distinct RBM and TBM drilling scenarios. Additionally, a comparative analysis between the new model and the two more popular drilling performance prediction models (Colorado School of Mines (CSM) and Gehring model) was performed. In this analysis, the new model presented higher accuracy than the other two models. A discussion about the existence of the founder point in larger drilling operations was introduced. The existence of this point in the drilling performance curve is strongly suggested by two RBM applications, and its location can be determined by the new model.

Chapter 6 reports a qualitative analysis of the de Moura and Butt model constant for the three different drilling scenarios analyzed in this research: fixed cutter drill bits, roller-cone drill bits, and large diameter drilling. This analysis is conducted based on the behavior of the model

constants when they are analyzed in relation to the UCS, bit diameter, and rotary speed. As this analysis is qualitative, when a specific parameter is analyzed, the other parameters are not kept constant, influencing each other. In other words, the goal of this chapter is to present a qualitative analysis of the de Moura and Butt model constants and not a parametric analysis, because of the characteristic of the data-sets available. The similarity between the fragmentation processes of the roller-cone drill bits and the large diameter drilling is strongly evidenced in this chapter. The ability of the de Moura and Butt model to predict the drilling performance for fixed cutter drill bits with high accuracy is explained based on the capability of its constants to absorb the particularity of this drilling scenario. In other words, the difference between the drilling mechanics of the fixed cutter drill bits and the roller-cone bits increases the complexity of the model constants. The de Moura and Butt model constants presented lower complexity pattern in the roller-cone drill bits application than in the fixed cutter drill bits application because the model was developed based on the rock cratering mechanisms. In the large diameter drilling, the model constants presented an expected behavior when they were analyzed in relation to the UCS (high complexity), bit diameter (low complexity), and rotary speed (high complexity).

7.3 Dissertation Highlights and Contributions

7.3.1 Universal Rotary Drilling Performance Prediction Model

In this research, a universal rotary drilling performance prediction model was developed based on the linear relationship between the “drillability constant” of the Maurer model and the WOB. This model showed high accuracy to predict the drilling performance for three distinct scenarios: fixed cutter drill bits, roller-cone drill bits, and large diameter drilling that includes the RBM and TBM applications. The two constants present in this model, called drillability coefficient

and drillability constant term, show high capability to absorb the peculiarities of the drilling mechanics of each one of the drilling scenarios analyzed.

7.3.2 Founder Point Location

One relevant aspect of this research is the capability of the new model to determine the founder point location of a drilling performance curve. This point of the drilling performance curve is characterized by determining the maximum ROP present in this curve. This information is crucial in the comparative analysis between different drilling scenarios, including variation of a specific drilling method and the comparison between different drilling methods. Additionally, the founder point location is a powerful information in the drilling optimization process.

7.3.3 Adjustable Disc Cutter Mounting (ADCM) System

During this research, the necessity of more accurate drill-off tests (DOTs) for the large diameter drilling was identified and that the actual linear approach shows limitations compared to the circular real field application. Based on this observation, a new experimental setup approach was developed based on the circular movement of the disc cutter observed in real field drilling operations. This new experimental setup approach is called Adjustable Disc Cutter Mounting (ADCM) system. The ADCM system is designed to have three adjustment parameters: journal angle, offset angle, and radial adjustment. These three adjustment parameters will provide the ability to optimize the large diameter drilling based on the adjustment parameters normally used in roller-cone drill bit operation (see Appendix 1 for more details). Currently, the fabrication of the ADCM system is ongoing with deadline of January 2021.

7.4 Recommendations for Future Work

Based on this research, many knowledge gaps in the drilling performance prediction area were observed. Some of these knowledge gaps can be covered but not limited to future works listed below:

1. According to Chapter 6, there is a substantial indication of a pattern in the behavior of the de Moura and Butt model's constant when they are analyzed in relation to the UCS, bit diameter, and rotary speed. Based on this observation, a parametric analysis to understand this behavior is necessary including other drilling parameters such as flow rate, drilling fluid rheology, and rock mass properties. This parametric analysis can include drilling laboratory experiments and finite element analysis.
2. Due to the complexity to obtain an accurate DOT, an approach to predict the drillability constant coefficient and the drillability constant term of the de Moura and Butt model with reasonable accuracy is necessary.
3. According to Chapter 7, section 7.3.3, a validation of the ADCM system functionalities and a comprehensive analysis to associate the laboratory drilling experiment with ADCM and real large diameter drilling applications is necessary. This analysis includes, but is not limited to:
    a. Drilling performance Curve;
    b. Bit wear;
    c. Drilling vibration;
    d. Torque on bit;
    e. Drill string components fatigue;

f. Cutterhead design;

g. Drilling optimization;

h. Bit-rock interaction.

i. Rock fragmentation process.

4. Due to the clear and well-known influence of the rate of penetration in the torque on bit, the incorporation of the de Moura and Butt model in the torque on bit prediction is plausible and needs to be analyzed.
5. Due to the big impact of the optimization in the economic of a drilling project, a comprehensive analysis of the application of the de Moura and Butt model to predict the drilling performance with real-time update is necessary. This approach will permit the prediction of optimization opportunities during the drilling process.

Appendix 1 Adjustable Disc Cutter Mounted (ADCM) system

A.1 1 Introduction

Currently, the laboratory experiments for this drilling scenario are based on a linear approach where one huge machine, called the linear cutting machine, displaces a single disc cutter in a straight line on the rock face. Access to these machines is restricted and the drill-off tests (DOTs) are scarce.

During this research, the necessity of more accurate DOTs for the large diameter drilling and limitations that the actual linear approach shows compared to the circular real field application were identified (see Chapter 5). Based on this observation, a new experimental setup approach was developed based on the circular movement of the disc cutter observed in real field drilling operations. This new experimental setup approach is called Adjustable Disc Cutter Mounting (ADCM) system (see Figure A.1-1).

The development of the ADCM system is a cooperative work that involved the following group members including their respective activities:

- **Jeronimo de Moura Junior:** Identification of research topic, conceptual design, drawing review, finite element simulation review and group management.
- **Dipesh Maharjan**: Technical Support, drawing review and adjustment, and finite element simulation review and adjustment.

- **Andrew Joyce:** project management, mechanical design, and FE fatigue simulation.
- **Aarjan Poudel**: Mechanical design, assembly design, and FE stress analysis.
- **Tinotenda Mpofu**: Mechanical design, assembly design, and FE stress analysis.
- **Mohammad Monam**: Mechanical design, assembly design, and FE stress analysis.
- **Stephen D. Butt**: Technical support, conceptual design review, and group management.
- **Daiyan Ahmed**: Technical support.

A.1 2 ADCM System Conceptual Design

The ADCM system was designed to operate with two types of disc cutters: cylindrical and conical (see Figure A.1-2); and will be integrated with the Large Drilling System (LDS), a laboratory scale drilling simulator (see Figure A.1-3) that was designed and fabricated by Memorial University of Newfoundland.

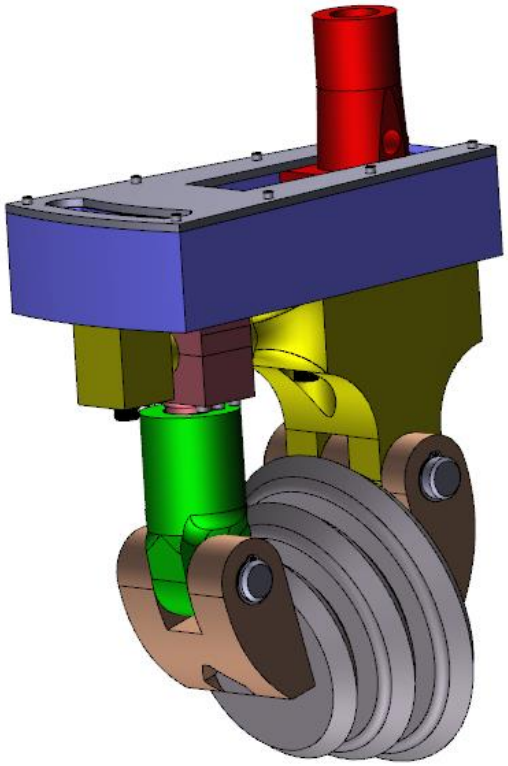

Figure A.1-1 Adjustable Disc Cutter Mounting (ADCM) system.

Figure A.1-2 Cylindrical disc cutter (left) and Conical disc cutter (right).

Figure A.1-3 shows the ADCM system mounted to the LDS.

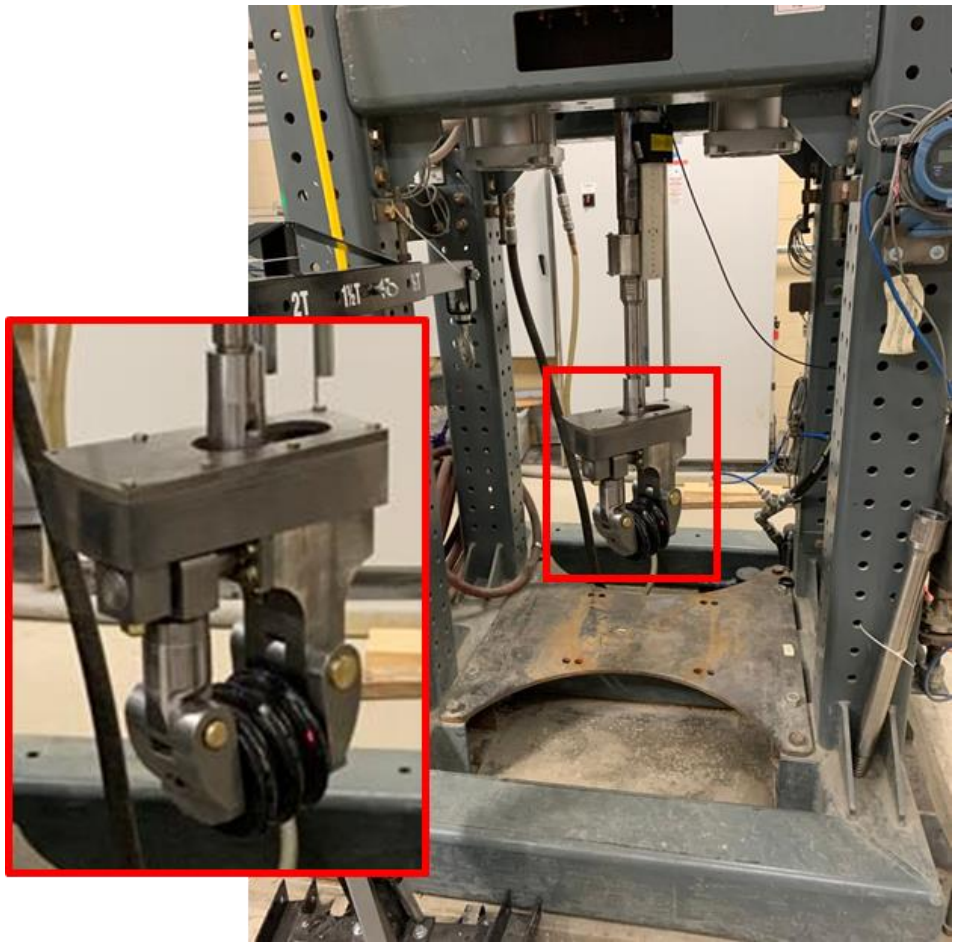

Figure A.1-3 the Large Drilling System (LDS).

The ADCM system is designed to have three adjustment parameters: journal angle, offset angle and radial adjustment (see Figure A.1-4). These three adjustment parameters will provide the ability to optimize the large diameter drilling based on the adjustment parameters normally used in roller-cone drill bit operations. Currently, the fabrication of the ADCM system is ongoing with a deadline of January 2021.

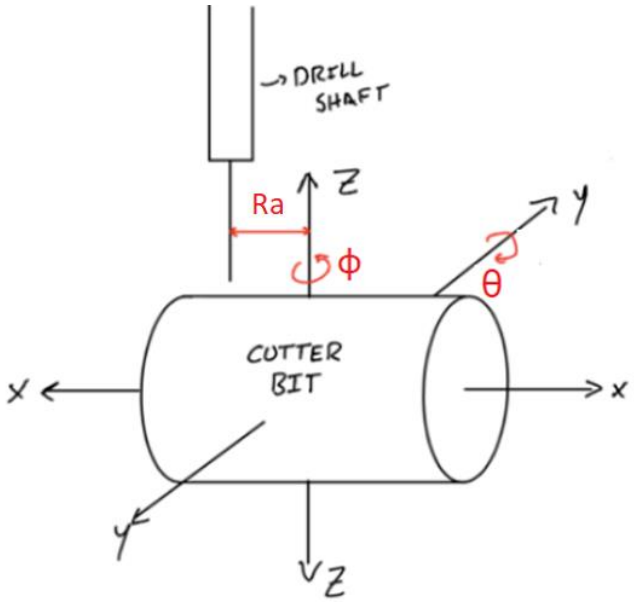

Figure A.1-4 ADM system adjustable parameters: journal angle (θ); offset angle (ϕ); radial adjustment (Ra)

Figure A.1-5 shows examples of ADCM system setups highlighting the variation of the three adjustment parameters.

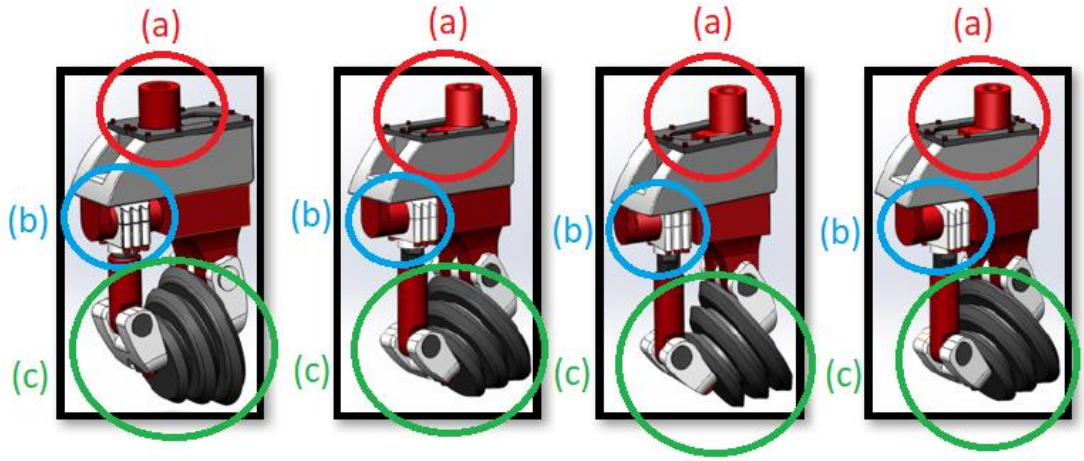

Figure A.1-5 ADM system setup: (a) radial adjustment variation, (b) journal angle variation, and (c) offset angle variation.

A.1 3 Conclusion

The ADCM system has potential to increase the accuracy of the laboratory drilling experiment related to the study of the drilling performance for the large diameter drilling applications because it simulates the real trajectory of a single disc cutter in real field operation, i.e., a circular trajectory. The circular trajectory decreases considerable the size of the rock specimen from meters (linear cutting approach) to centimeters and absorbs the nuances of this drilling scenario.

The possibility to adjust the journal angle, offset angle, and radial adjustment provides the flexibility necessary to optimize the drilling process of the large diameter drilling based on the known parameter used in the roller-cone drill bit optimization process.

A validation of the ADCM system functionalities and a comprehensive analysis to associate the laboratory drilling experiment with ADCM and real large diameter drilling application is necessary. This analysis includes, but is not limited to: drilling performance curve, bit wear, drilling

vibration, torque on bit, drill string components' fatigue, cutterhead design, and drilling optimization.

Currently, the fabrication of the ADCM system was concluded and the tuning and performance tests are ongoing with a deadline of May 2021.